FINAL REPORT

DIAGNOSIS AND REMEDIATION OF SUSTAINED CASING PRESSURE IN WELLS

Andrew K. Wojtanowicz, Somei Nishikawa, and Xu Rong
Louisiana State University

Submitted to:

US Department of Interior
Minerals Management Service
381 Elden Street
Herndon, Virginia 20170-4817

Baton Rouge, Louisiana
July 31, 2001

TABLE OF CONTENT

EXECUTIVE SUMMARY

Reported herein is a research project performed under TASK 2A - Remediation of Flow After Cementing of the project "Development of Improved Procedures for Detecting and Handling Underground Blowouts in a Marine Environment." The task has been added to the project program based upon modifications proposed by LSU in a letter to MMS, October 3, 1988, and approved by MMS on October 19, 1998.

This new task was intended to be a follow-up to Task 2, "Prevention of Flow After Cementing," and Task 11, "Study of Excessive Casing Pressures During Production Operations." A need for this new task arose from recent industry engagement in deep-water operations and the growing concern of MMS about sustained casing pressures (SCP). The overall objectives of this task were to identify theoretical principles and to conduct research into new technology for diagnosis and removal of SCP in producing wells.

The report on the first stage of this project, diagnosis and testing of SCP, presents the analysis of operator field testing procedures and the MMS guidelines for testing wells with SCP and includes data collected from field testing and monitoring SCP along with an analysis of typical recorded patterns of SCP buildup during the field tests.

The report on the theoretical stage of the project describes two mathematical models: pressure transient in a fully cemented annulus; and SCP buildup in a well with a mud column above the cement. The models were used to study the effects of well properties on SCP development patterns. Based upon the study, a computer-assisted method for SCP diagnosis was developed and validated using the field data; the software for this application is attached to the report. The report also includes examples for using the software.

The report on the experimental stage of the project addresses the most critical problem in remediation of SCP without using a drilling/workover rig: injection of high-density fluid into the affected annulus in order to kill SCP. The fluid is injected either at the surface directly into the casinghead (Bleed-and-Lube method) or through a flexible tubing inserted to a certain depth in the annulus (Casing Annulus Remediation System, CARS). Given the depth limitation of CARS, the two methods are similar in applying multi-cyclic injection of heavy liquid to kill SCP in the affected annulus. The objective of this portion of the study was to evaluate the efficiency of displacing annular fluid with injected fluid during cyclic injection.

A pilot-scale physical model of the well annulus was built and used for studying heavy fluid settling and displacement performance. The experimental matrix considered miscible and immiscible variants of the two fluids (displacing and annular) and included calcium carbonate brine, water-based mud, water, and white oil in various combinations.

The results showed that using brine with drilling mud may by entirely ineffective, particularly when high concentrations of clay occur in the mud. The brine flocculates the annular mud, which stops the displacement process. Good results may be obtained when the annular liquid is Newtonian, large number of injection cycles may be required to remove SCP. However, an immiscible combination of the two fluids provides the most desirable performance for cyclic injection. In this case the injected fluid would quickly displace the annular fluid and kill SCP.

The study indicates that assessment of compatibility is critical for matching an injected liquid with the annular fluid. Such an assessment could be done using the methodology and modified testing equipment developed in this work. Future work should focus on developing laboratory or pilot-size method and equipment for sampling and testing the synergy and performance of fluids used in mitigating the SCP problem by annular injection (Bleed-and-Lube) or circulation (CARS) methods.

1. BACKGROUND OF SCP DIAGNOSIS AND REMOVAL

The work reported herein is a follow-up to the recent report by Bourgoyne, et al. (Bourgoyne, 2000) that provided an overview of the problem of excessive and persistent casing pressures (sustained casing pressure, or SCP) in wells. The Minerals Management Service (MMS) defines SCP as a pressure measurable at the casinghead of a casing annulus that rebuilds when bled down and that is not due solely to temperature fluctuations and is not a pressure that has been deliberately applied. In contrast to SCP, an *unsustained casing pressure* determination is made if either the only casing pressure on a well is self-imposed (e.g., gas-lift pressure, gas- or water-injection pressure) or pressure is entirely thermally induced.

Typically, sustained casing pressure would result from late gas migration in one of the well's annuli and manifest itself at the wellhead as irreducible casing pressure. MMS statistics show that the problem of leaking wells in the GOM is massive, as 11,498 casing strings in 8122 wells exhibit sustained casing pressure. According to MMS, sustained casing pressure represents a potential risk of losing hydrocarbon reserves and polluting the water column with leaking hydrocarbons. Although 90% of sustained casing pressures are small and can be contained by casing strength, it is still potentially risky to produce or, more importantly, to abandon such wells without eliminating the pressure.

Risk of SCP depends upon the type of affected casing annulus and the source of migrating gas. Most serious problems have resulted from tubing leaks. A tubing leak would exhibit SCP at the production casing. A failure of the production casing may result in an underground blowout that, in turn, could cause damage to the offshore platform, loss of production, and/or widespread pollution. Catastrophic outcomes of SCP on production casing have been documented in several case histories (Bourgoyne, et al., 2000). Consequences of SCP on casings other than the production casing are less dramatic but equally serious. SCP on these casings usually represents gas migration originating from an unknown gas formation. As the gas migration continues, casing pressure may increase to the point at which either the casing or casing shoe fails, which allows the migrating gas to leak into the annulus of the next (and weaker) casing string. As a result, the gas would not be contained by any of the well's casings and would come to the surface outside the well. Eventually, the process could result in destabilization of the seafloor around the well, loss of the platform, and pollution of the water column and surrounding area.

Diagnostic methods are used to determine the source of the SCP and the severity of the leak. Most of these methods use data (such as fluid sample analysis, well logs, fluid levels, or wellhead/casing pressure testing) obtained from routine production monitoring performed by operators. In addition, MMS has specified a standardized diagnostic test procedure to assist in this analysis when SCP is detected. These tests include pressure bleed-down and pressure build-up. In the bleed-down test, MMS requires recording the casing pressure once per hour or using a data acquisition system or chart recorder. Also, the pressure on the tubing and the pressure on all casing strings are to be recorded during the test to provide maximum information. The recorded data are used to see how much of the initial pressure can be bled down during the test. Also, the recorded pressures from other annuli would indicate whether there is communication between different casings in the well. However, no analytical method to analyze these tests quantitatively has previously been developed.

A similar situation exists for pressure build-up tests. MMS requires the pressure build-up period to be monitored for 24 hours after bleeding off SCP. The pressure build-up test is especially important when the SCP cannot be bled to zero through a 0.5-in. needle valve. The

rate of pressure build-up could provide additional information about the size and possibly the location of the leak. However, no method for interpreting the test has previously been developed. Therefore, one of the recommendations of the recent SCP report (Bourgoyne, et al., 2000) was to conduct additional research and develop analysis procedures for diagnostic test for wells with SCP.

Remedial treatments of wells that have SCP are inherently difficult because of the lack of access to the affected annuli. Since there is no rig at the typical producing well, the costs and logistics involved in removal of SCP are frequently equivalent to a conventional workover. Moreover, there are additional casing strings between the accessible wellbore and the affected annulus. Methods for SCP removal can be divided into two categories: rig and rig-less methods.

The rig method involves moving in a drilling rig, workover rig or, in some cases, a coiled tubing unit and performing some kind of cement bridge or cut-and-squeeze operations in the well. Generally, this method is most effective when SCP affects the production casing string. However, the rig method is inherently expensive due to the moving and daily rig costs.

When the SCP affects outer casing strings, the rig method usually involves squeezing cement. These procedures involve perforating or cutting the affected casing string and injecting cement to plug the channel or micro-annulus. Both block and circulation squeezes have been attempted. The success rate of this type of operation is low (less than 50%) due to the difficulty in establishing injection from the wellbore to the annular space of the casing with SCP and getting complete circumferential coverage by the cement. As a last resort, the rig method may involve cutting and pulling the casing. This complication generates additional expense due to the time it takes to recover the casing, since it often must be pulled in small segments.

The rig-less technology involves external treatment of the casing annulus using a combination of bleeding off pressure and injecting a sealing/killing fluid either at the wellhead (Bleed-and Lube) or at depth through flexible tubing inserted into the annulus (CARS). A limited number of case histories report the Bleed-and-Lube method as partially successful (Hemrick and Landry, 1996). However, completion of the job would have required months, or years, of pressure "cycling" application since the volumes injected at each cycle were extremely small. Other operators also observed incomplete reduction in surface casing pressures when this method was employed. In one report, the field data indicates that pressures can increase while applying this method (Bourgoyne et al, 2000).

A search continues for techniques that would eliminate very expensive and unreliable workovers involving rigs. The Bleed-and-Lube technology has already proved feasible but not consistently effective for a variety of reasons. Therefore this project was designed to provide improvements in two areas: testing SCP; and investigating the Bleed-and Lube remediation method.

2.   CURRENT PROCEDURES FOR SCP TESTING

The concept of departure from the rig intervention required by 30 CFR 250.517 is based on the understanding that small and non-persistent pressure induces the least risk. However, technical criteria, which are based on the ratio of casing pressure to its strength and the ability to bleed to the zero pressure, are arbitrary to some degree.

MMS has developed guidelines under which the offshore operator could self-approve a departure from 30 CFR 250.517. Departure approval is automatic as long as the SCP is less than 20% of the minimum internal yield pressure and will bleed down to zero through a 0.5-in. needle

valve in less than 24 hours. Diagnostic testing of all casing strings in the well is required if SCP is seen on any casing string.

Records of each diagnostic test must be maintained for each casing annulus with SCP. The diagnostic tests must be repeated whenever the pressure is observed to increase (above the value that triggered the previous test) by more than 100 psi on the conductor or surface casing or 200 psi on the intermediate or production casing. Well operations such as acid stimulation, shifting of sliding sleeves, and replacement of gas lift valves also require the diagnostic tests to be repeated. If at any time the casing pressure is observed to exceed 20% of the minimum internal yield pressure of the affected casing, or if the diagnostic test shows that the casing will not bleed to zero pressure through a 0.5-in. needle valve over a 24 hour period, the operator is expected to repair the well under regulations stated in 30 CFR 250.517.

The recent report on the SCP problem (OTC 11029, Bourgoyne et al., 1999) shows the technical complexity of the SCP mechanism and provides recommendations for changing the criteria used in the SCP risk evaluation. It suggests that the flow rates of gas and liquid causing the SCP should be included. Also, the well should be regularly shut in and tested for casing pressure buildup behavior.

Recently, MMS proposed a modified procedure for diagnostic testing (MMS Draft NTL, January 2000). Under this guideline, operators must address all casing pressure diagnostics and departures on a whole well basis. This means that when any annulus on a well needs a diagnostics test, operators must diagnose all casings with SCP at the same time, unless TAOS Section specifically directs otherwise. During a diagnostic test, operators must record all initial pressure and both bleed-down and buildup pressure, using either graphs or tables, in at least 1-hour increments for each casing annulus in the well bore. Operators must bleed down and build up separately. Also operators must record the rate of buildup of each annulus for the 24-hour period immediately following the bleed-down. If fluid is recovered during bleed-down, operators must record the type and amount. Operators should conduct bleed-down to minimize the removal of liquid from the annulus.

For subsea wells, where only the production annulus can be monitored, operators must conduct diagnostics as indicated, except that results for the adjacent annulus will be restricted to monitoring tubing pressure response.

3. FIELD DATA ANALYSIS

3.1 SCP Data Bank
Appendix A contains SCP data that were developed from field data. The data are made up of casing pressure records provided by various operators from 23 wells and are contained in Microsoft Excel (.xls) files. Each file has a worksheet of raw data. Usually, charts include only the casing strings that have SCP problems, and chart names are the outer diameters of those strings. In some cases, if the string has more than one continuous buildup, each period has a separate chart.

3.2 Statistical Analysis
3.2.1 SCP Occurrence
We analyzed casing pressure data from 26 wells. Among those, 22 wells, 85% of the total, have SCP problems (Table 1). As indicated by the table, the following trends may be observed:
- About 30.8% of the casing strings exhibiting SCP are production casing.

- About 65.4% of the casing strings exhibiting SCP are intermediate casing strings.
- About 34.6% of the casing strings exhibiting SCP are surface casing strings.
- About 15.4 % of the casing strings exhibiting SCP are conductor casing strings.

3.2.2 SCP Magnitude by Casing String

Shown in Figure 1 is a cumulative frequency plot of the occurrence and magnitude of SCP in psi units for the various types of casing strings. About 50 percent of the production casings and 35 percent of the intermediate casings have SCP of less than 1000 psi. For the other casing strings, about 90 to 100 percent of the strings have SCP of less than 500 psi.

Table 1 - SCP OCCURRENCE IN VARIOUS CASING STRINGS

Count #	Well #	Production Casing			Intermediate Casing			Surface Casing			Conductor Casing	
		6 5/8"	7"	7 5/8"	8 5/8"	9 5/8"	10 3/4"	11 3/4"	13 3/8"	16"	16"	20"
1	MUA1		NA			NA			Y			N
2	MUA2		Y			N			Y			Y
3	MUA3		Y			Y			Y			N
4	MUA4		Y			Y			N			N
5	MUA5		Y			Y			N			N
6	MUA6		NA			NA					N	N
7	MUA7		N			N			N			N
8	MUA8		Y			Y			Y			N
9	MUA9		Y			Y			Y			Y
10	MUA10		Y			Y			Y			N
11	MUA11	N			N			Y				Y
12	MUA12		Y			Y			Y			N
13	MUA13		N			N			N			N
14	MUA15		N			Y			N			N
15	MUA16		N			N			N			N
16	APTA19		NA				Y	NA			NA	
17	APTA30		NA				NA	NA			Y	
18	APTA31		NA				Y	NA			NA	
19	APTL9		NA				Y	NA			NA	
20	BPTB6		NA				Y	NA			NA	
21	PTCA25C		NA				Y	NA			NA	
22	PTCA7D		NA				NA		Y		NA	
23	B7		N				Y			N	N	
24	HIA1			N			Y				N	
25	HIA2			N			Y				N	
26	HIA3			N			Y				N	
Total		0	8	0	0	8	9	1	8	0	1	3
P$_{SCP}$ %		30.8			65.4			34.6			15.4	

Y- SCP problem;   N- no SCP problem;   NA - data not available.

7
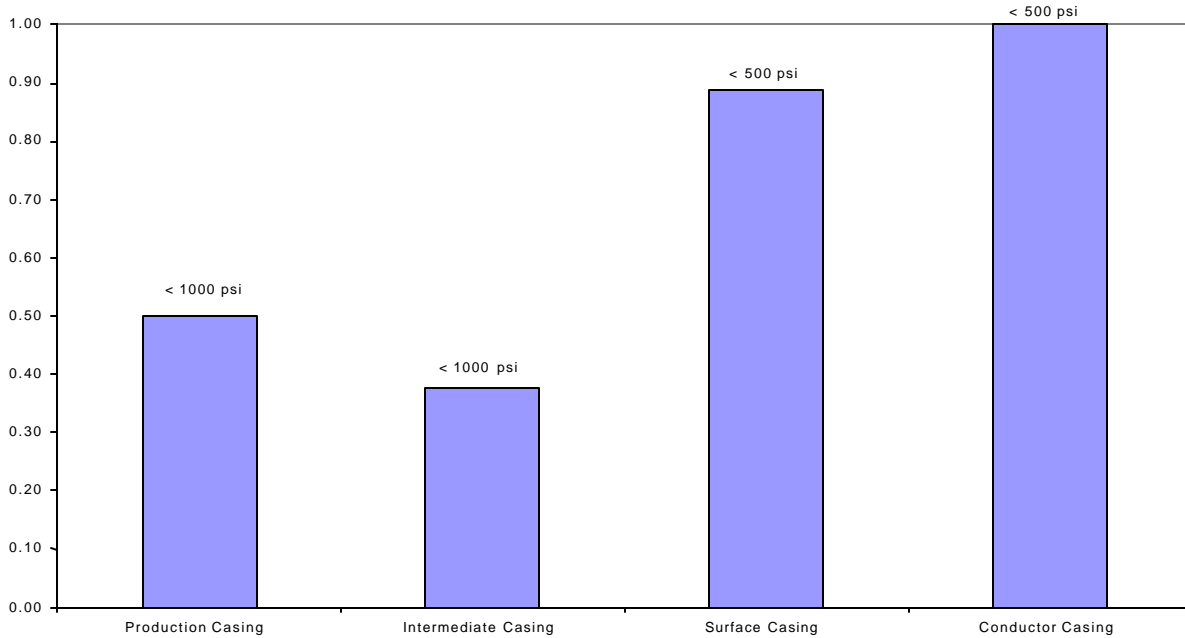
Figure 1. Frequency of SCP for different casings.

3.3   Patterns of SCP Buildup Plots

3.3.1   Typical Patterns

Figure 2 shows the typical casing pressure buildup behavior in a well with a SCP problem. The casing pressure will rise quickly after the bleed down and will stabilize at a certain level. The pressure stabilization is affected by mud weight and formation pressure. Transient time depends on the magnitude of gas migration in the cement and mud column.
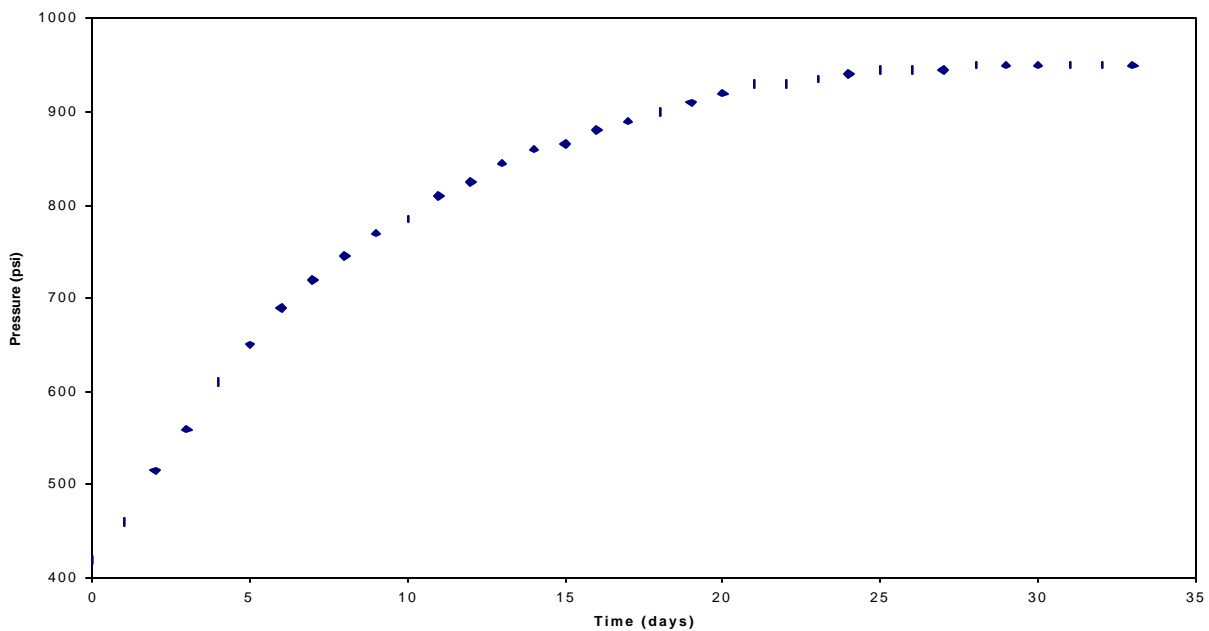
Figure 2. Typical pattern of SCP buildup plot.

3.3.2 Anomalous Patterns

Figure 3 shows an abnormal case of SCP response. The well was shut in at about 500 days. The casing pressure fluctuated significantly in response to frequent bleeding off of the wellhead pressure. Pressure monitoring was not frequent enough to show the pattern of pressure buildups. On the other hand, bleed-downs were too frequent, so a full pattern of pressure recovery did not develop. The plots do give a clue to the point at which the pressure would stabilize. Discerning buildup patterns from this plot would be very difficult.
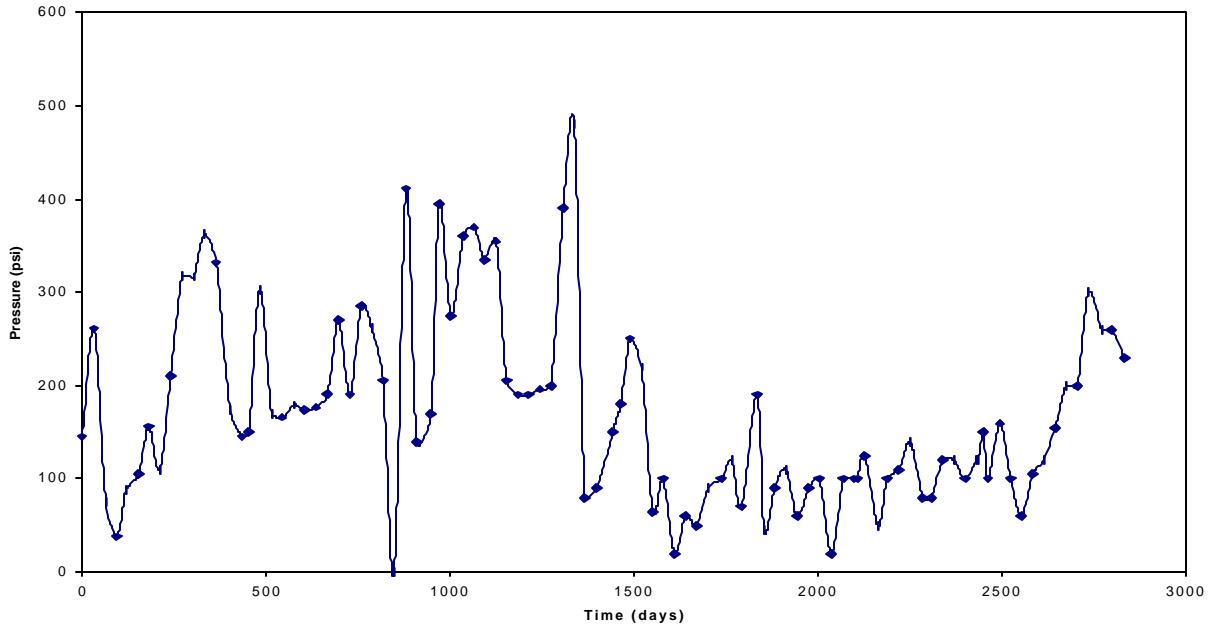
Figure 3. Abnormal casing pressure buildup behavior.
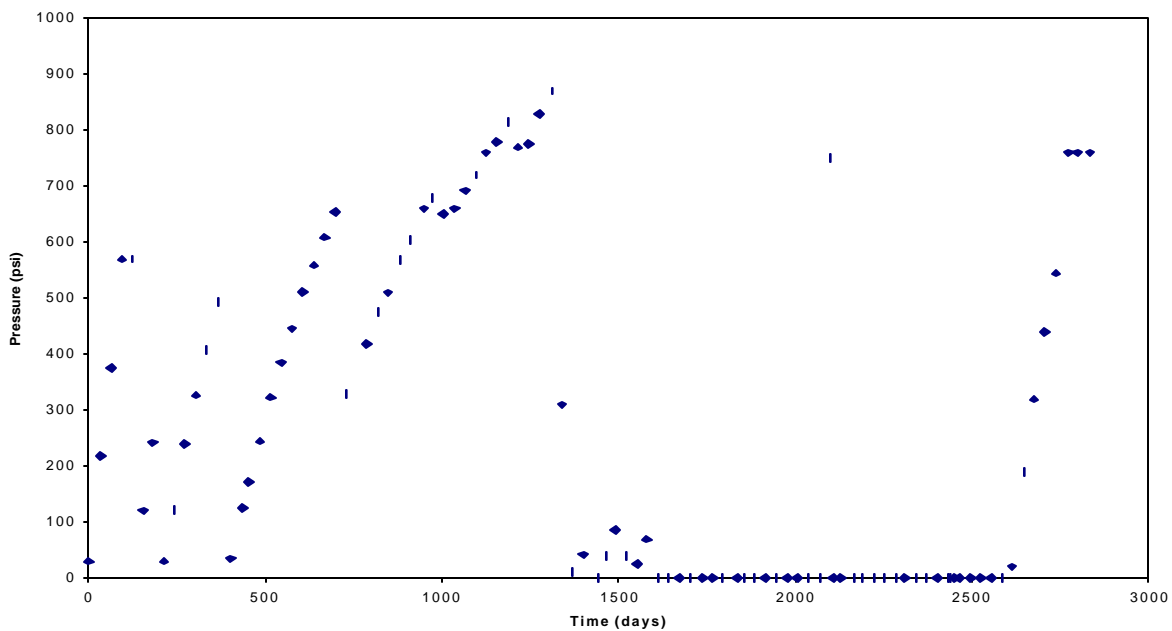
Figure 4. Undeveloped patterns of pressure build-up due frequent bleed-downs.

9

4. ANALYSIS OF SCP PRESSURE TESTING MECHANISM

In the Outer Continental Shelf (OCS) of GOM, weak marine formations contain pockets of over-pressured sand with gas or water. Intrusion of gas to the cement column may occur early, after cement placement, or late, when the cement sheath is fully set. In the latter case, the migration of gas is enabled by residual conductivity of the cemented annulus, as illustrated in Figure 5. This residual conductivity may cause zonal isolation loss and failure of the cement to seal the annulus. Two physical mechanisms, matrix permeability and interfacial channeling, may contribute to the development of annular conductivity. Matrix permeability refers to flow within the body of the cement column. Interfacial channeling, on the other hand, refers to a micro-annulus between the cement column and the casing or rock.

Interfacial channeling is a mechanical discontinuity that forms a micro-annulus at the contact surface of the cement column. At the cement-rock surface a micro-annulus could result from poor removal of the mud cake. At the casing-cement contact, a micro-annulus is caused by thermal or hydraulic stresses after cement placement (pressure testing, completion fluid replacement, stimulation treatment, wellbore cooling or heating). A very small micro-annulus may provide a flow path for slow gas migration, resulting in SCP.
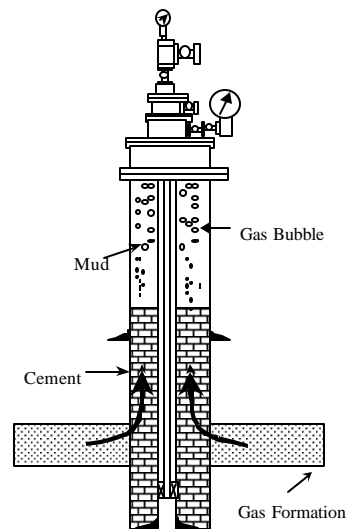
Figure 5. SCP buildup mechanism.

After the cement is in place, the cement column may develop some secondary porosity and permeability. One mechanism of gas flow through the cement matrix is matrix channeling. After hydrostatic pressure in the cement slurry column drops below the value of the formation pore pressure, gas enters the slurry matrix either as a slug or dispersed fluid. The slug of gas migrates upwards and creates a channel. Gas channels of up to about 1/4 inch in the cement matrix have been documented in experiments. It seems unlikely, however, that such channels may provide flow paths for SCP. Their conductivity is too large to explain the small rate of SCP buildup.

Another mechanism of gas flow through cement relates to the development of secondary permeability in the cement matrix. The mechanism can be explained as follows: After the

hydrostatic pressure decrease to the formation pressure, cement hydration causes an absolute volume reduction of the cement matrix. Chemical shrinkage is responsible for the creation of secondary porosity. Interstitial water in the cement matrix is trapped in the pores by capillary forces. The trapped water is consumed in the hydration reaction, thus creating a void that results in pore pressure reduction and a "suction effect." When combined with pressure underbalance, the suction effect may become a major mechanism for developing matrix permeability to gas.

The suction effect has been observed and described by several researchers (Levine et al.,1979; Tinsley et al., 1979; and Appleby, et. al, 1996). Laboratory measurements have shown that a well-cured cement typically has a permeability on the order of 0.001 md, with a pore size below 2 μ and a porosity around 35%. However, when gas is allowed to migrate within the slurry before complete curing, the pore structure is partially destroyed and gas generates a network of tubular pores that can reach 0.1 mm in diameter and lead to permeability as high as 1 to 5 md (Schlumberger, 1989). Matrix permeability is another likely mechanism of gas flow causing SCP.

Two possible configurations of the cement column in the annulus are common: cement top extending to the surface or a mud column above it. In wells cemented to the surface, gas migration can be considered a one-dimensional flow through a medium having some conductivity (Nishikawa, 1999). After bleed-down at a constant rate, the casing pressure increase is analogous to the pressure transient buildup, as shown in Figure 6. The buildup behavior is controlled by cement properties, such as permeability and porosity, and by gas formation pressure.
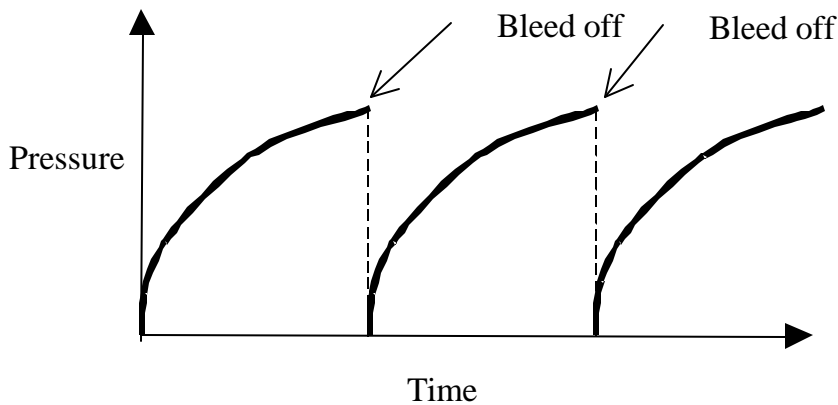
Figure 6. Conceptual patterns of consecutive SCP buildups.

If a mud column extends above the cement column, gas migration occurs in two stages. In the cement column, the gas flow follows Darcy's Law; while in the mud column, gas bubbles rise through stagnant non-Newtonian drilling fluids. Not only will the gas migration be affected by the characteristics of the mud, such as mud compressibility and density, but it will also be affected by the top gas cap at the wellhead where migrating gas accumulates. We believe that the PVT behavior in this gas cap can be explained by the Real Gas Law. Therefore, the lower the mud compressibility, the faster the gas bubbles rise, and the faster the pressure increases. Eventually, if not bled off, pressure at the wellhead would stabilize at a value equal to the gas formation pressure.

5. MATHEMETICAL MODELS OF SCP BUILDUP

5.1 Analytical Model of SCP Transient in Annulus Cemented to Surface

In this model, we assumed that the cement top is at the surface (Nishikawa, 1999). A diagram of gas migration in a cement column is shown in Figure 7. To develop a mathematical model of gas migration, the following assumptions were made:
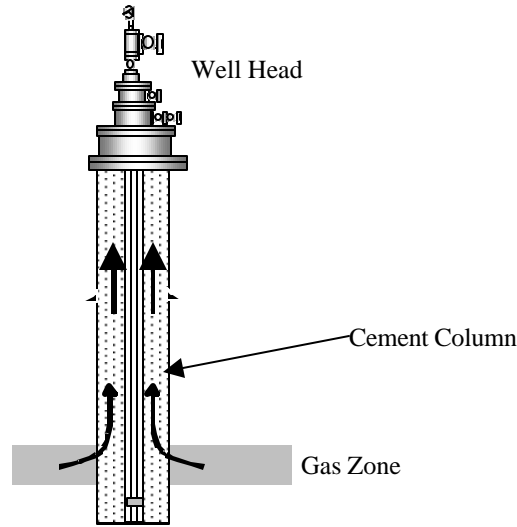
Figure 7. Gas migration in an annulus cemented to the surface.

- The gas formation pressure is constant, because permeability of the gas zone is much higher than that of the cement column.
- The pseudo gas pressure concept is used.
- At the end of bleed down, gas is vented out from the well at a small constant rate.
- The well is cemented to the surface.

The flow of gas in the cement is described by the equation,

$$\frac{\partial^2 m}{\partial x^2} = \frac{\phi \mu c_t}{0.0002637 k} \frac{\partial m}{\partial t} \tag{1}$$

where,

k = average (equivalent) permeability of the annulus
μ = viscosity of gas
m = gas pseudo pressure
N = cement porosity
t = time
x = vertical distance from bottom

The solution to the flow equation is presented in Appendix B, and the analytical model is,

$$m(t) = m(P_e) - \sum_{n=1}^{\infty} \frac{316.05}{L} \frac{qP_{sc}T}{T_{sc}AK} \frac{(-1)^{n+1}}{a^2} \cdot e^{-c^2 a^2 t}. \tag{2}$$

12

5.2   Numerical Model of SCP Buildup in Cemented Annulus with Mud Column

In this model, we assumed that a column of mud is above the cement top (Xu and Wojtanowicz, 2001). Gas migration in the cement and mud columns is shown in Figure 8.

$P_t(t)$

Gas cap	L_t

Gas-cut mud

$\mathbf{r}=const$

$P_c(t)$

L_f

L_c

Gas flow in cement

$P_f=$ constant
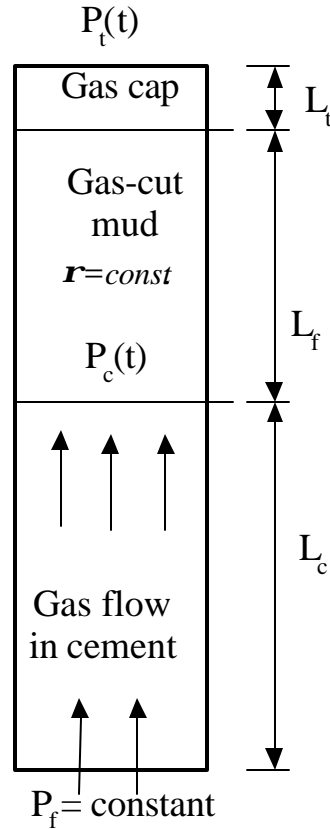
Figure 8. Conceptual diagram of SCP buildup in a cemented annulus with a mud column.

The following assumptions have been made in the derivation of this model:

- Formation pressure does not change, i.e., $p_f = const$.
- There is a steady-state flow of gas through the cement ($0 < z \le L_c$) at each time step in response to changing pressure at the cement top, p_c.
- Gas density is neglected in the cement column.
- The gas law deviation factor does not change, i.e., Z = constant.
- The gas cut mud column is compressible.
- Temperatures on top of the cement and mud (T_{wb} and T_{wh}) are different.
- Mud density is known and constant throughout the process, a pressure-averaged density of the gas-cut mud.
- The rising velocity of bubbles v_{sg} is constant, and it controls the time step.

Based on those assumptions, we derived an iterative procedure for step-by-step calculation of pressure buildup that is shown in detail in Appendix C. In the procedure, at the nth time step, pressure at the wellhead, p_t, is

$$p_t^n = \frac{1}{2}\left(p_t^{n-1} - \frac{V_t^{n-1}}{c_m V_m^{n-1}} + \sqrt{\left(p_t^{n-1} - \frac{V_t^{n-1}}{c_m V_m^{n-1}} \right)^2 + \frac{4T_{wh}\sum_{k=1}^{n} p_c^k q_c^k \Delta t}{c_m V_m^{n-1} T_{wb}}} \right) \tag{3}$$

and, pressure at the top of the cement column, p_c, is

$$p_c^n = p_t^{n-1} + 0.052\, r_m L_f^{n-1} + 0.052\frac{p_t^{n-1} M}{ZR'T_{wh}} L_t^{n-1} \tag{4}$$

All symbols used in these formulas are defined in Appendix C.

6. EFFECT OF WELL PARAMETERS ON CASINGHEAD PRESSURE BUILDUP

6.1 Wellhead Pressure Transient Behavior in a Fully Cemented Annulus
For wells cemented to the surface pressure transient is the mechanism of SCP buildup described by the analytical model in Section 5.1. The top of the well is shut in after being open to atmospheric pressure. Pressure buildup follows and its pattern is controlled by conductivity of annulus (in the model, cement permeability). Other parameters such as porosity, temperature and gas specific gravity may also play a role.

Effect of Cement Porosity
Input data are shown in Table 2. Casing pressure buildups are shown in Figure 9. The results indicate that the effects of cement porosity variations are small, of the order of 10 percent pressure value.

Table 2. Input Data for Fully Cemented Well Study

Outer CSG ID & OH Size	(in)	=	19
Inner CSG OD	(in)	=	13.375
CMT Permeability	(md)	=	1
Porosity		=	0.25-0.35
CMT column Length	(ft)	=	4000
Viscosity	(cp)	=	0.02
Reservoir Pressure	(psi)	=	2300
Total Compressibility	psi-1	=	0.0003
Psc	(psia)	=	14.7
Tsc	(°F)	=	60
Temperature @ TOC	(°F)	=	90-110
Temperature @ BOC	(°F)	=	130
Flow Rate	(scf/day)	=	0.010
Gas SG		=	0.7-0.9
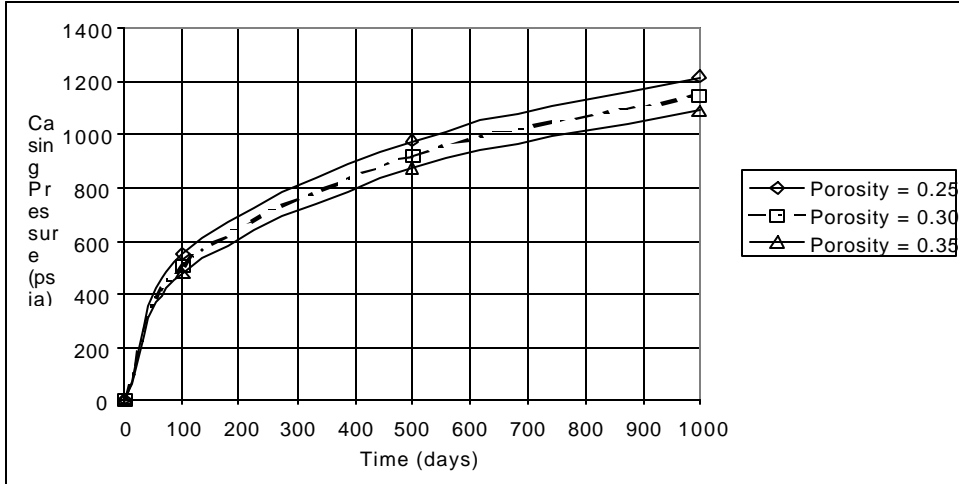
Figure 9. Effect of cement porosity on casing head pressure buildup.

Effect of Temperature

The input data are shown in Table 2. Casing pressure buildups are shown in Figure 10. The results indicate that the temperature effect is small; increased temperature would give smaller pressure buildup.
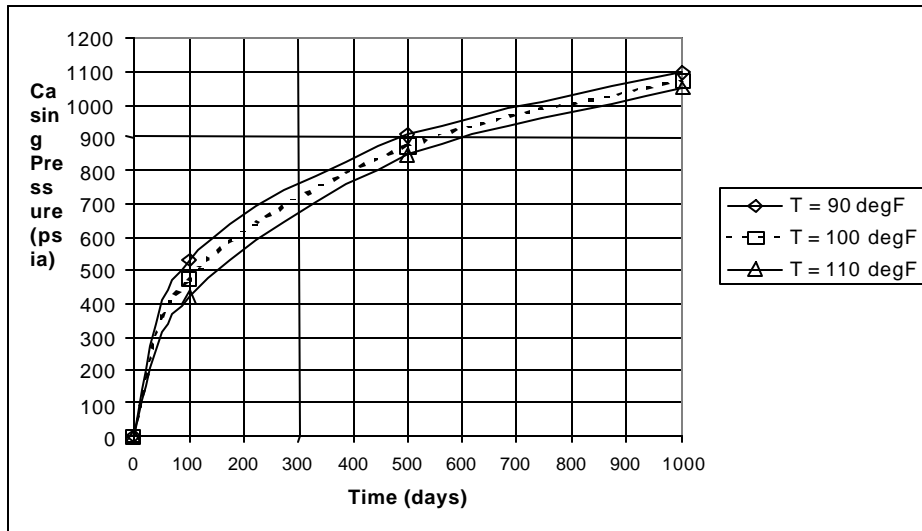
Figure 10. Effect of temperature on casing head pressure buildup.

Effect of Gas Specific Gravity

The input data are shown in Table 2. Casing pressure buildups are shown in Figure 11. Again, the effect of gas gravity is insignificant.
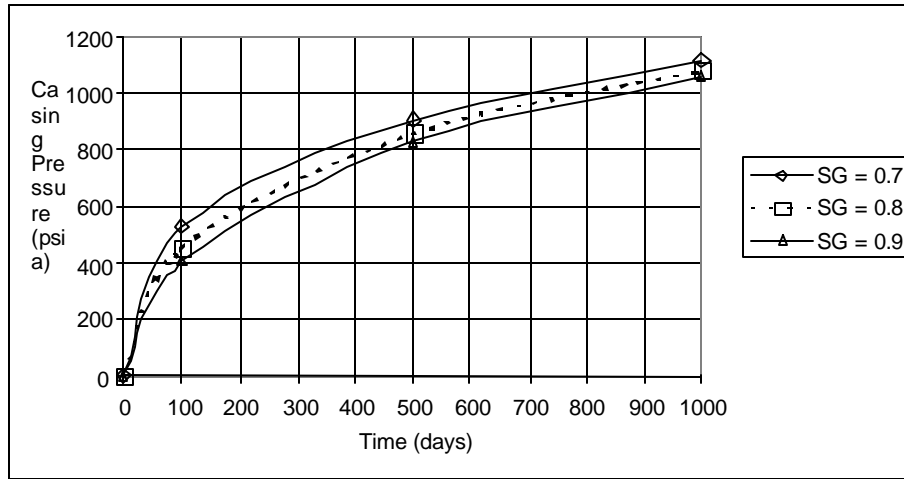
Figure 11. Effect of gas gravity on casing head pressure buildup.

6.2   Pressure Buildup in Cemented Annulus with Mud Column

When a column of mud sits on top of the cement, the mechanism of pressure buildup is different than that for fully-cemented well and described by the numerical model in Section 5.2. After the annulus is shut-in, initial pressure at the cement top is high and controlled by hydrostatic pressure of the mud column. Thus, the initial pressure drawdown across the cement column is much smaller than that in the case of a fully cemented well. Also, during the process of gas flow, a gas cap at the casing head is formed and controls the gas flow and pressure buildup. Thus, new parameters should be added to the list of factors controlling the process: mud characteristics in addition to cement and formation properties.

Effect of Gas Cut Cap

Here, the cap represents the void between the top of the mud column and the well head. Usually, this cap is filled with gas or gas-cut mud with a high gas concentration. In our study, we found this cap functions as a "stabilizer." The larger the gap, the slower the casing pressure will reach to the stable pressure (See Figure 12).

16
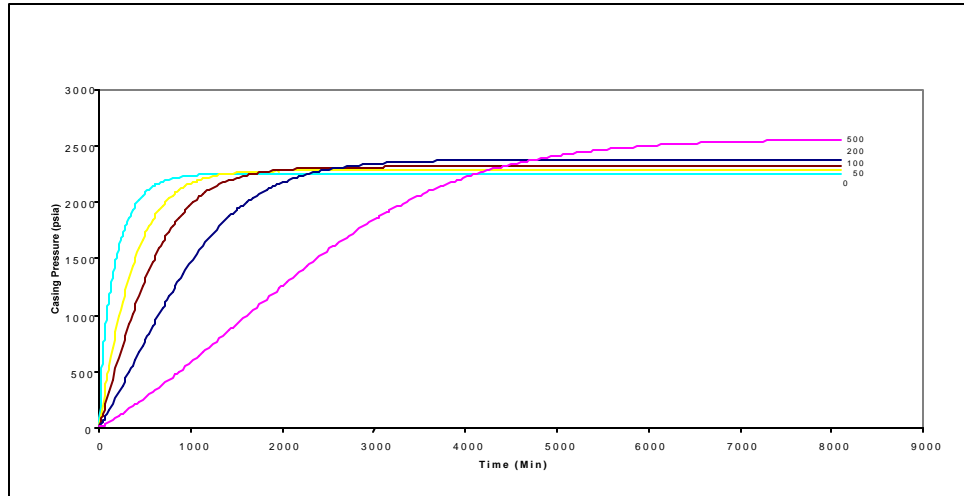
Figure 12. Effect of gas cap size (length).

Effect of Mud Compressibility

In this model, we also considered mud compressibility. Figure 13 shows the effect of compressibility very clearly. The higher the compressibility, the slower the casing pressure buildup.
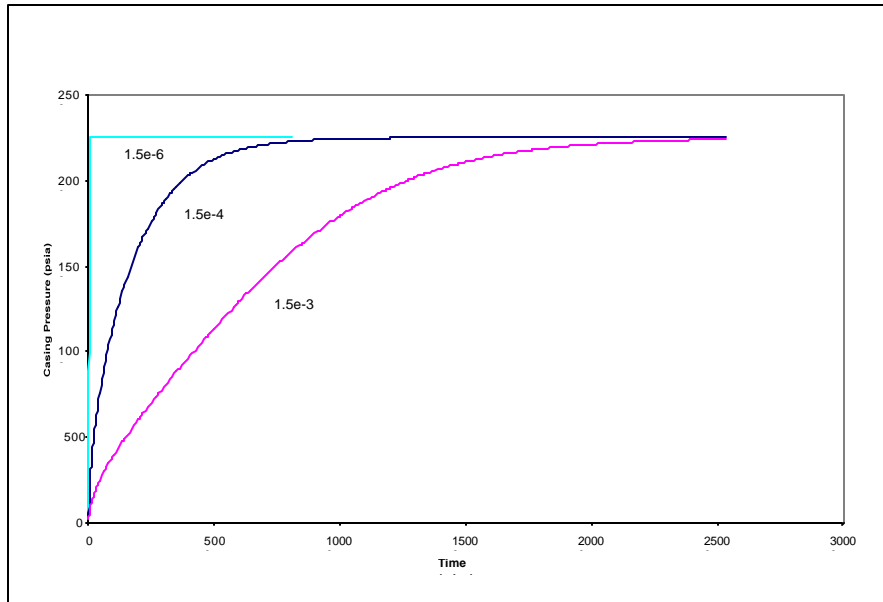
Figure 13. Effect of mud compressibility.

Effect of Cement Permeability

In this model, we assume that conductivity of the cemented section of the annulus, whether caused by micro-channeling or matrix permeability, is represented by a "cement permeability" property. The effect of cement permeability is opposite to that of the mud compressibility, i.e., the more permeable the cement, the faster the casing pressure increases (See Figure 14).

17
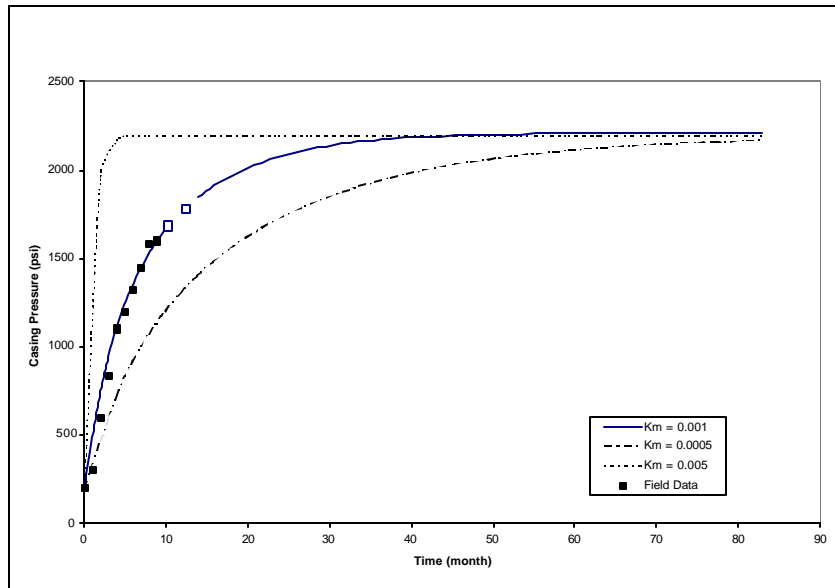
Figure 14. Effect of cement permeability.

Effect of Formation Pressure
In the model, the formation pressure is assumed constant throughout the whole process of pressure buildup. Its magnitude will affect the equilibrium pressure at the casing head after a long time. Obviously, the higher the formation pressure is, the higher the equilibrium pressure and the longer the need for pressure stabilization (See Figure 15).
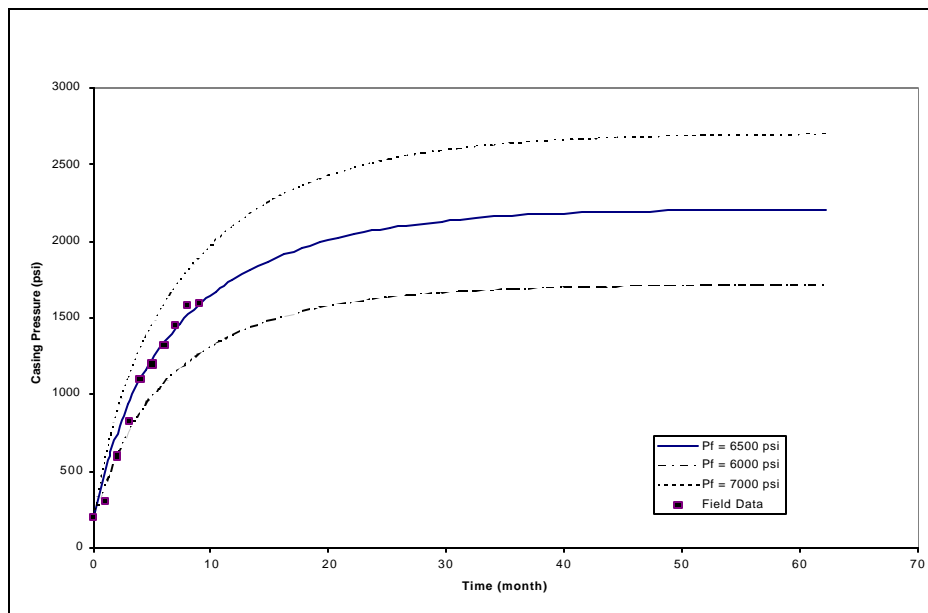
Figure 15. Effect of formation pressure.

Effect of Gas Slip Velocity in Mud
As shown in MMS statistics, most SCP problems happened in the intermediate casing where the mud column in the casing is relatively short compared to the whole length of the casing, so the travel time of the gas across the mud column to the wellhead is relatively short. Furthermore,

18

according to some studies, gas will rise faster in viscous mud than in water because of the size of the equilibrium slug (A. B. Johnson, et al). Therefore, we simplified the model by assuming that the gas travel time in the mud is in the range of the time step used in the model, which means that all the gas generated at the cement top is transferred to the gas cap in one step.

7. METHOD FOR SCP DIAGNOSIS

Based upon the theory and numerical model presented above, we have developed a method, software, and procedure for analyzing casing head pressures qualified as SCP. Qualification is not part of the method since, by the MMS definition, this method has been based upon recurrence and source of pressure buildup rather than the pattern of pressure behavior in time. The diagnostic method enables determination of well parameters that control SCP but are usually unknown, such as severe channeling in the cement, depth of the pressure source formation, and gas pressure gradient.

7.1   Validation of Numerical Model with Field Data

Matching the field and theoretical data allows the numerical model to be used to determine the two most uncertain parameters affecting SCP: the formation pressure and cementing quality. The matched data are shown in Table 3.

Table 3. Results of Matching Field Data

		Case I	Case II
k	md	0.001*	0.0028*
T_{wb}	R	575	552
T	R	630	584
T_{wh}	R	520	520
D_1	ft	0.829	0.829
D_2	ft	0.583	0.635
L_c	ft	1821	2783
Initial L_f	ft	8273	3650
Initial L_t	ft	27	0
m_g	cp	0.02	0.015
P_f	psia	6515*	4029*
P_{sc}	psia	14.7	14.7
c_m	psi^{-1}	4.0e-6	1.2e-6
Δt	day	15	2
ρ_m	ppg	10	10
Z		0.86	0.92

* Matched parameters

7.1.1   Case 1: Partial SCP Buildup Data

A schematic of gas production Well A is shown in Fig. 16. The well is located offshore in GOM. SCP has developed in the annulus of the $10^3/_4$-inch intermediate casing of the well. Casing head pressure rose from 200 psi to 1600 psi and was still increasing after 9 months of buildup, as shown in Fig. 17.
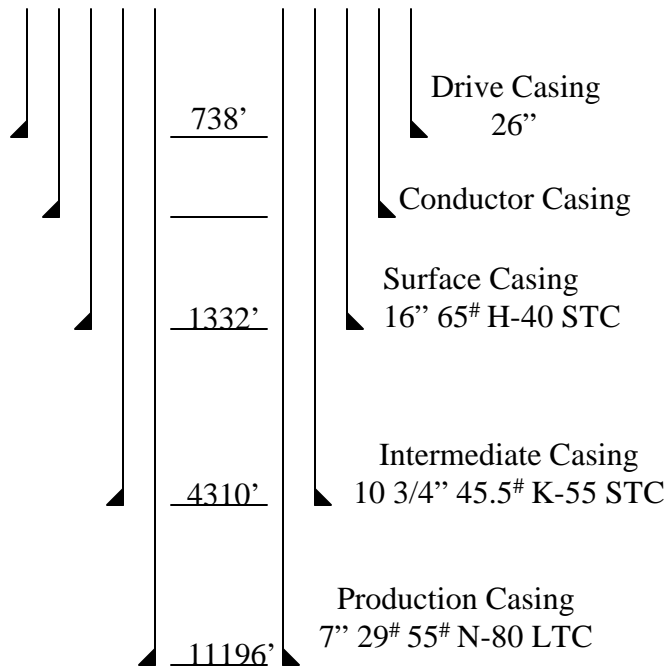
Figure 16. Schematic of Well A, offshore GOM.

Using the numerical model, we matched the pressure data and found out that the casing pressure would stabilize at about 2200 psi in 30 months, as also shown in Fig. 17. In this case, the operator was not sure about two sets of data: cement permeability and formation pressure. The matched value for permeability, 0.001md, was very small. However, laboratory measurements (discussed above) have shown similar values for well-cured cements. Therefore, the matched cement permeability was realistic to some degree.
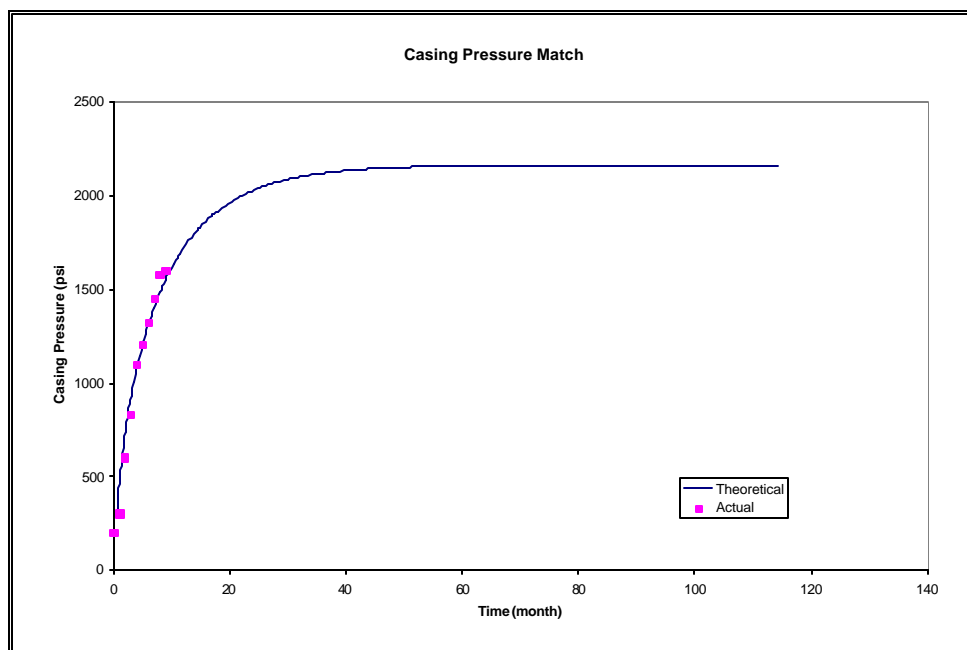
Figure 17. SCP buildup match and extrapolation for Well A.

The formation pressure controls the stabilized value that the buildup pressure can reach. Only for pressures around 6500 psi can the top casing pressure reach 1600 psi in 9 months. In this case, the method helped the operator to determine formation pressure and cementing quality.

7.1.2 Case 2: Complete SCP Buildup Data
In Case 2, Well B, shown in Fig. 18, exhibited SCP in the intermediate casing. Before the casing pressure buildup, shown in Fig. 19, was recorded, the well had been frequently bled down. After each bleed-down, heavier mud would be pumped into the $10^3/_4$-inch intermediate casing annulus. The operator would record the volume and weight of the bled and pumped muds. After one month of buildup, the casing pressure stabilized at about 1000 psia.

Drive Pipe
26"

582'

Conductor Casing
20" 94$^{\#}$ H-40

1061'

Surface Casing
16" 75$^{\#}$ K-55

4776'

Intermediate Casing
10 3/4" 45.5$^{\#}$ L-80

6433'

Production Casing
7 5/8" 33$^{\#}$ N-80

9084'
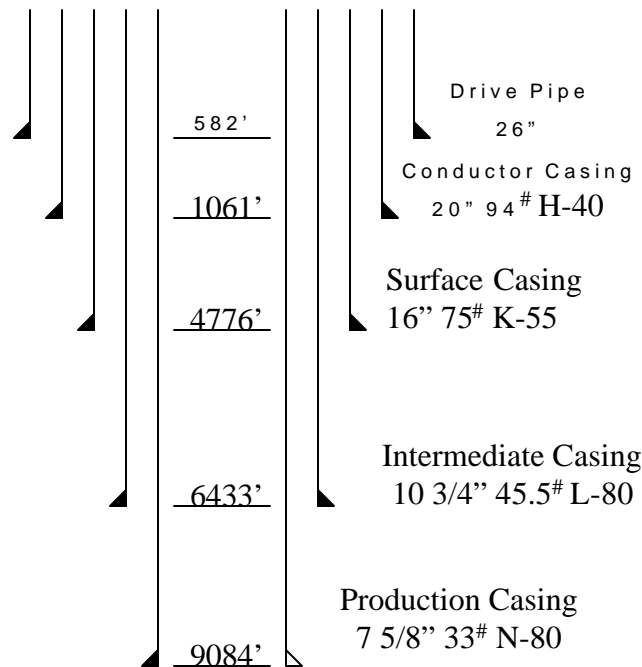
Figure 18. Schematic of Well B, offshore GOM.

The pressure match in Figure 19 is not as perfect as in the previous case due to the following reasons: First, it was very difficult to estimate mud density due to frequent bleed-downs and lack of original mud density records. (We assumed that the mud in the annulus should be heavier than the bled out mud in the last bleed down.) Secondly, no data on mud compressibility was available. In this case, the method helped the operator to determine the degree of channeling in the cemented annulus. (The matched cement permeability was 0.0028md.) Interestingly, the gas formation pressure gradient (at the $10^3/_4$-in. casing shoe) was found to be normal, 0.46 psi/ft.
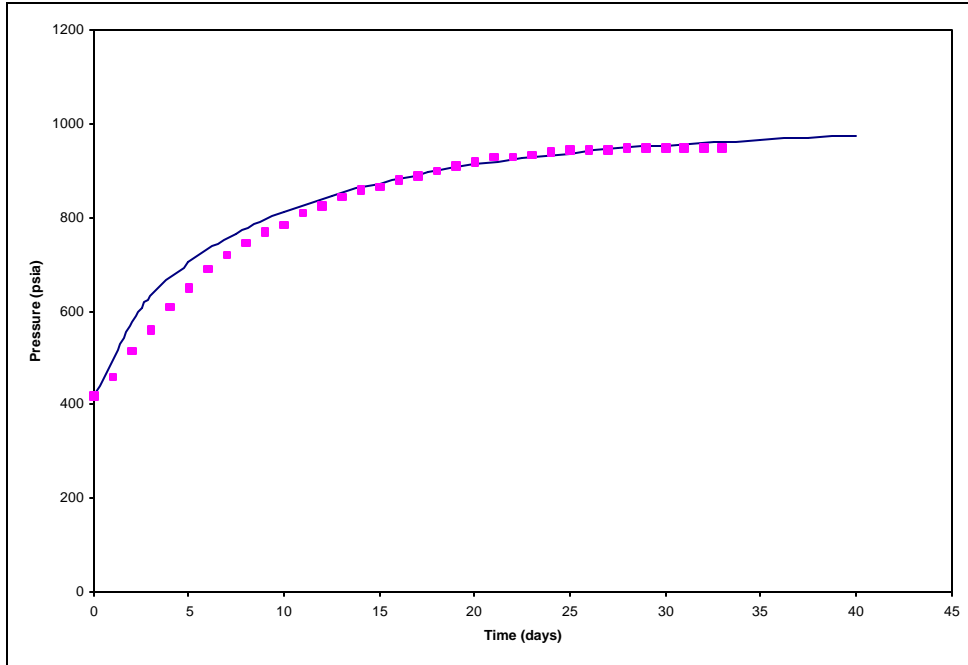
Figure 19. SCP buildup match for Well B.

7.2 Diagnostic Software and Applications

Using the numerical model, a spreadsheet-based computer program NumMdl.xls. has been developed. A worksheet called "General Instructions" gives general description of the software. A worksheet called HistData is used to input pressure data. Also, a sheet called TheoData is used for entering property parameters of the mud, cement, and rock. By pushing the button "Calculate SCP Buildup" predicted pressure buildup vs. time is computed. The resulting data is stored in a new sheet called "SCPBuildup" from which a plot can also be made.

Users can find the most uncertain parameters by trial-and-error; The values of parameter are changed, until the recorded SCP buildup is matched by the calculated one.

Input Data Format and Units:

$c_m = $ mud compressibility, psi^{-1}

$D_1 = $ outer diameter of the annulus, ft

$D_2 = $ inner diameter of the annulus, ft

$k = $ cement permeability, md

$\rho_f = $ Equivalent formation pressure density, Equivalent ppg

$TD = $ true depth, ft

$L_t = $ length of gas chamber, ft

$L_f = $ length of mud column, ft

$T = $ reservoir condition temperature, $^\circ R$

$T_{wb} = \dfrac{1}{2}(T + T_{wh}) = $ average wellbore temperature, $^\circ R$

22

T_{wh} = wellhead temperature, $°R$ (usually $520°R$)

Z = gas-law deviation factor, dimensionless

$\boldsymbol{m_g}$ = gas viscosity, cp

$\boldsymbol{r_m}$ = density of mud in wellbore, ppg

Calculated Parameters:

$A = \dfrac{\boldsymbol{p}}{4}(D_1^2 - D_2^2) =$ wellbore area, sq ft

$L_c = $ TD-L_f -L_t = length of cement column, ft

$p_f = 14.7 + 0.052 * TD * \rho_f$ = reservoir pressure (constant), psia

$V_t = A * L_t$ = volume of gas-cut cap, cu ft

V_m = volume of mud column, cu ft

p_c = pressure on the top of the cement, psia

p_t = pressure on surface, psia

q_c = flow rate on the top of the cement, SCF/D

Matching Hints:

Two strings of SCP buildup data, P_t, recorded and calculated is stored in the sheet called "SCPBuildup". Also the difference between the data is listed in the sheet. Pushing the "OK" button in the message box, gives a comparison plot of the two pressure buildups. The plot is stored in the sheet, "MatchingPlot". By visually inspecting the plot a user can assess quality of the match. If the match is poor, the user would change input data in the "TheoData" sheet, run the program again, and repeat the procedure until satisfactory match is achieved.

The following are hints on how to change input data:

- If the calculated value of stabilized P_t is too high, the assumed value of the formation pressure equivalent density, ρ_f , may be too large, or the formation is shallower than assumed. Therefore, one of the two parameters (the most uncertain one), pore pressure or depth, should be decreased within acceptable limits.
- If P_t increases faster than the actual data, cement conductivity k should be reduced (or, mud compressibility c_m increased) step-wise until a matching trend is obtained.

8.   SCP DIAGNOSIS: CONCLUSIONS AND RECOMMENDATIONS

Conclusions:

- Statistical analysis of casing pressure in a single oilfield shows similar trends to those reported by MMS for the whole GOM. Thus, we conclude that the SCP problem is widespread and independent from conditions of specific oilfield in the GOM. Also, the analysis method validated for one oilfield should work anywhere in the GOM.
- SCP buildup pattern is controlled by parameters of cement, mud and gas invasion zone. Using the mathematical model, we theoretically analyzed the effects of those parameters and found out as follows:

- Large casing gas cap prolongs the SCP buildup cycle and would complicate buildup analysis by reducing the buildup plot resolution. Operators should keep this cap as small as possible by filling up the well after the bleed-off.
- Mud compressibility controls the early stage of SCP buildup. Thin drilling mud having low tendency for gas cutting would considerably improve the analysis of SCP buildup by removing the compressibility effect.
- Cement permeability parameter represents the quality of cementing. It controls early stage of SCP buildup. Thus, SCP buildup rate analysis may become an overall measure of the annular seal performance of the well.
- Formation pressure controls the maximum value of stabilized SCP, with high formation pressure resulting in high stabilized SCP value. Potentially, a combined analysis of the stabilized SCP value, mud density, top cement depth and formation pressure gradients may identify the gas invasion zone. In case when maximum value of SCP is not attainable (too high) from the field data, the mathematical model presented here could extrapolate the value.

- Field validation of the model, presented here, gives acceptable estimates of the gas-source formation pressure, cement conductivity, and expected maximum casing pressure value. Ambiguity of the analysis can be significantly reduced by reducing the number of unknown parameters to two: cement conductivity and formation pressure. Early stage of SCP buildup is controlled by cement conductivity; while stabilized pressure is determined by formation pressure. If data collected could exclude the effects of other parameters, the test analysis would be very straightforward.
- The model has been simplified by disregarding effects of gas migration in the mud and gas cutting of the mud. The two parameters may have strong effects on the rate of SCP buildup. Future study should address SCP buildup analysis including the effect of gas migration in non-Newtonian fluids.
- Measuring the bleed rate is as important as the pressure record when determining the potential hazard posed by sustained casing pressure.
- Gas flow through the unset cement matrix seems to be a major cause of sustained casing pressure; the matched values of cement permeability support this conclusion.
- The analytical model provided a basic analysis of specific SCP buildup in an annulus cemented to the surface.
- The numerical model seems more feasible for prediction and diagnosis of casing pressure buildup behavior because it considers the effect of a mud column above the cement.
- There are two major limitations of this study: mathematical modeling was simplified; and, no testing procedure combining bleed-down and buildup pressures was developed.
-

Recommendations:

In addition to pressure and flow rate records, annular mud, cement, and formation information is critical for proper diagnosis of SCP. Also, the configurations of each well, such as cement depth and fluid (mud) level, are important for obtaining a good match. Therefore, sampling and monitoring procedures should be modified in the future.

In view of this work, we recommend continuing this research program to develop criteria for the SCP risk evaluation. As stated above, flow rates of gas and liquids causing the SCP should be included in the risk evaluation procedures. In the procedure, the affected annuli should be produced (or vented out) under controlled conditions. The venting rate should be measured

and controlled by a choke smaller than 1/8 inch. Also, the well should be regularly shut-in and tested for ability to rebuild the casing pressure. Also, there is a need for supporting the modified criteria with engineering science.

Additional research should be conducted to develop improved diagnostic test procedures for wells with SCP. The main objective of such research would be to provide theoretical support for the criteria, standards, and procedures to be used in identifying wells with SCP, assessing the severity of the problem, and defining the level of tolerance to the problem. Also, the program should develop field-deployable procedures for multi-rate testing that would include the bleed-down and buildup procedure and analysis method.

9. CURRENT STATUS OF SCP REMOVAL: CYCLIC INJECTION

In the recent review of SCP problems, Bourgoyne, et al. (Bourgoyne, 2000) discusses various methods, both with and without using a drilling rig, of SCP removal. In principle, the rig-less methods involve injecting high-density fluid into the affected annulus in order to kill SCP. The fluid is injected either at the surface directly into the casing head (Bleed-and-Lube method) or through a flexible tubing inserted to a certain depth in the annulus (Casing Annulus Remediation System, CARS). The concept of these two methods is to replace the gas and liquids produced during the pressure bleed-off process with high-density brine, such as Zinc Bromide. The goal of these techniques is to gradually increase the hydrostatic pressure in the annulus.

The lube-and-bleed procedure involves bleeding small amounts of lightweight mixtures of gas and fluid from the annulus and lubricating in Zinc Bromide brine over several treatment cycles. A limited number of case histories reported the lube-and-bleed method as partially successful. In one of these cases, SCP in the 13-3/8"casing was reduced from 4,500 psi to 3,000 psi. The operation took over a year with numerous cyclic injections, during which 118 bbls of 19.2 ppg Zinc Bromide brine replaced 152 bbls of the annular fluid (a gas-cut water-based mud having density of 7.4-9.5 ppg) (Hamrick and Landry, 1996).

Other operators also observed incomplete reduction in surface casing pressures after using this method. In one field application the brine was pumped into the SCP affected wells through the casing valves on top of the closed-ended annuli, and the operator estimated that the volumes that could be pumped (or lubricated) during a given cycle were as small as a quart per one cycle. On the other hand, the required volume of heavy fluid necessary to overbalance the casing pressure was usually from as low as 5 barrels to as high as 80 barrels. Thus, completion of the job would have required months, or years, of application. Additionally, surface pump pressures would reach relatively high levels. In some cases, several iterations of pressuring up to high levels and bleeding off (or pressure "cycling") has been proven to worsen the casing pressure problem, probably due to opening a micro-annulus in the cement or breaking down previously competent cement.

Field observations indicate that pressures can increase while applying this method (Bourgoyne et al., 2000). The hypothesis has been proposed that this occurs when a new "gas bubble" migrates to the surface. After trying the lube-and-bleed method for several years in several wells, the field results have not been as promising as first indicated.

The CARS system is similar to the lube-and-bleed process in that it is designed to place heavy fluids into the casing annulus without using a workover rig or perforating. The fluids are introduced by inserting a small diameter flexible hose into the casing annulus through the casing valve. After placing the hose at a certain depth, heavy fluids can be circulated through the hose,

as opposed to the lube-and-bleed process, in which fluids are squeezed into the closed annulus system from the top of the annulus.

Although the CARS system has been used successfully in many wells and the CARS equipment functioned satisfactorily during the jobs, it is still too early to make conclusions as to the effectiveness of using the system to satisfy MMS regulations. To date, field experience with CARS showed that the maximum injection depth could not exceed 1000 feet, while in most wells the injection depth was less than 300 feet and could not be increased. Thus, injection depth has become one of the major barriers for widespread use of CARS.

10. EXPERIMENTAL ASSESSMENT OF CYCLIC INJECTION

Given the depth limitation of CARS, the two methods (Bleed-and-Lube, and CARS) would require multi-cyclic injection of heavy liquid to kill SCP in the affected annulus. The objective of this study was to evaluate the performance of cyclic injection in view of the efficiency of displacing annular fluid with injected fluid (Nishikawa,1999; Nishikawa, Wojtanowicz and Smith, 2001)

Several factors may affect displacement efficiency. For example, a small clearance in the annulus would restrict a downward movement of the injected (kill) liquid. Using brine as a kill liquid brings about a miscibility problem. High miscibility would not contribute to weighting up the fluid in the whole annulus, only in the top sections. Thus, cyclic injection may not be effective for killing SCP because most of the injected fluid would return when bled off.

In this work, we identified and studied several mechanisms of displacement in the cyclic-injection process. Using a pilot-scale physical model of annulus and brine ($CaCl_2$) as a primary kill liquid, we investigated efficiencies of cyclic injection for different rheology and miscibility. An annular fluid containing gas was not considered in this study.

10.1   Experimental Design

10.1.1 Physical Model

To investigate the cyclic-injection method, a physical model of casing annulus was designed and fabricated as shown in Fig. 20. A 3-in. clear PVC (ID 3 in./OD 3.5 in.) pipe was installed inside a 6-in. clear PVC pipe (ID 6 3/8 in./6 5/8 in. OD) to construct the annulus. This 3-in. pipe was opened at both ends and welded to a 6-in. plastic flange. A 3/8-in. inlet was installed on the 6-in. flange to pump a kill liquid into the annulus. At the top of the 6-in. pipe, a 3/4-in. outlet was installed just below the flange, and a 3/4-in. valve was attached to this outlet. This valve represented a needle valve used in field operations. At the bottom of the apparatus, a 3/4-in. outlet with two valves was installed. A pressure gauge was installed between the valves to simulate the location of the cement top in the annulus.
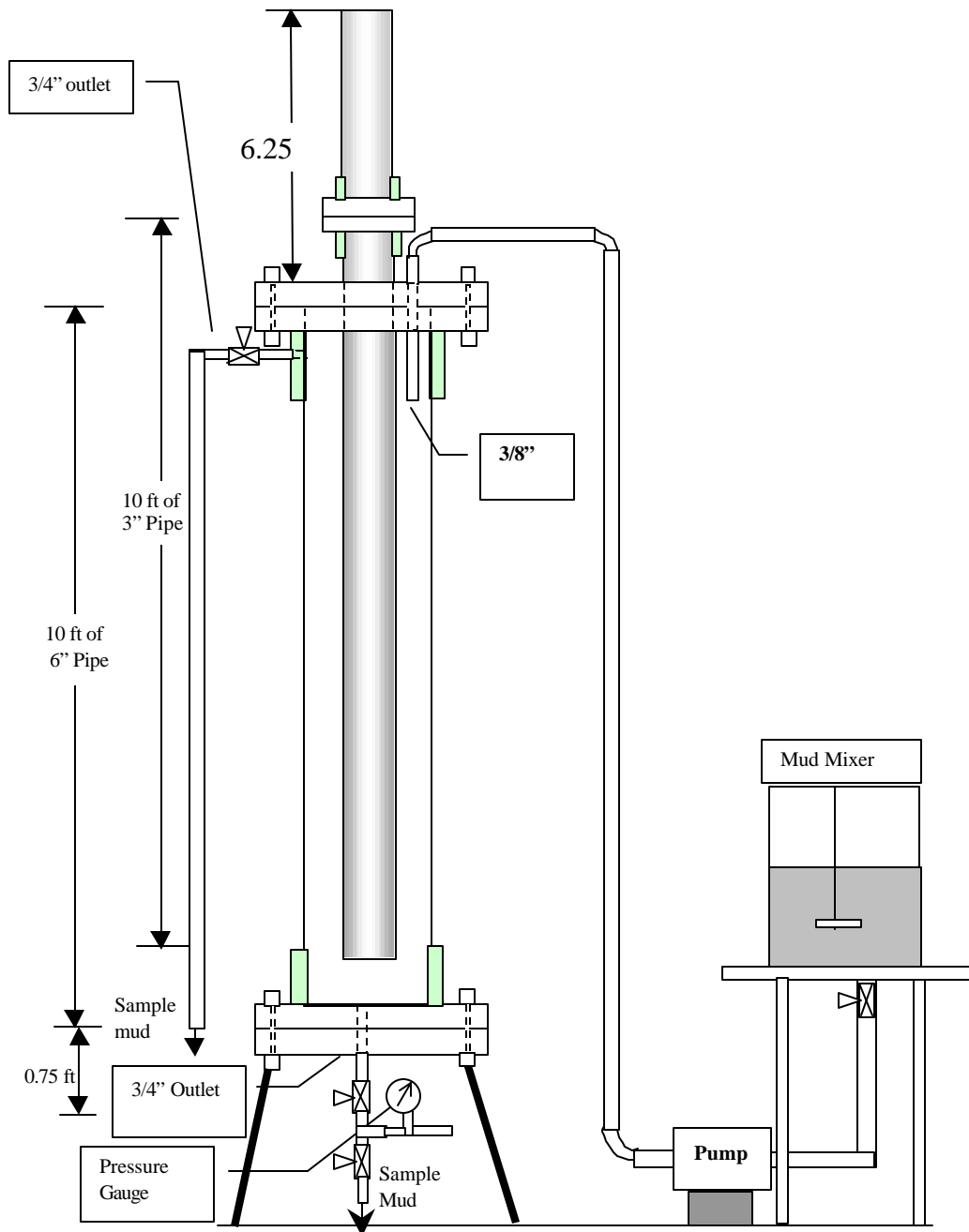
Figure 20. Physical model of a well annulus.

In field operations, after a needle valve is installed, a kill liquid is injected ("Injection" in Fig. 21). Then the system of the annulus is shut-in ("shut-in" in Fig. 21). After a certain time of shut-in to settle the kill liquid, the needle valve is opened again. The kill liquid returns mixed with the annular fluid through the needle valve, because a compressed annular fluid flows backward to release the injection pressure.

This operation would be difficult to simulate experimentally by designing an apparatus because of the high working pressure. However, to investigate cyclic injection, an experiment

must simulate only the cyclic procedure of injection, shut-in, and bleed-off at any pressure. It is conceivable that if the method worked at low pressure, it would also work at high pressure.
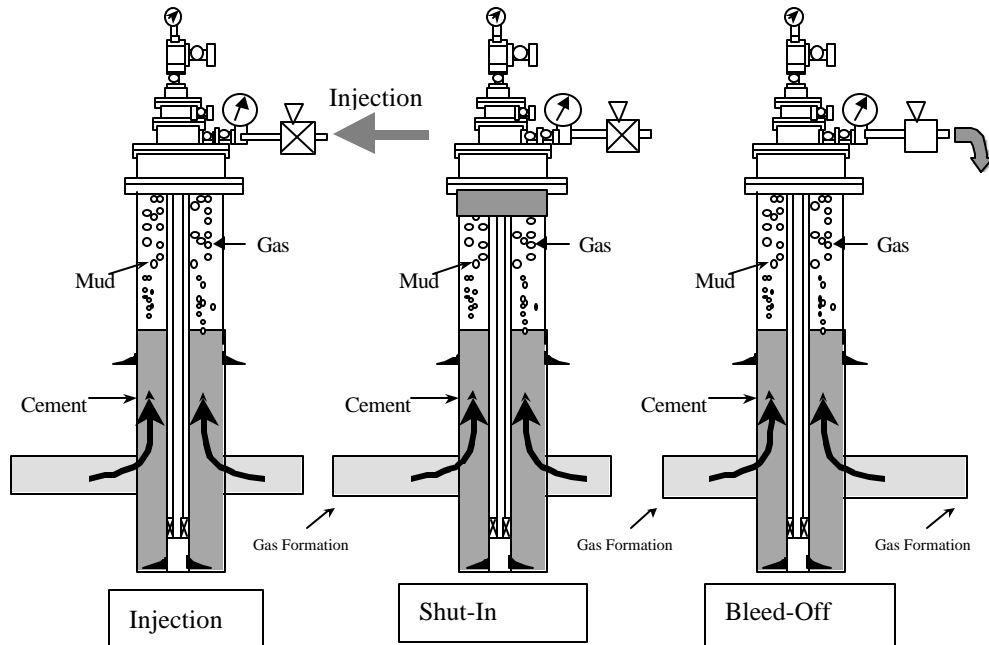
Figure 21.   Cyclic injection procedure.
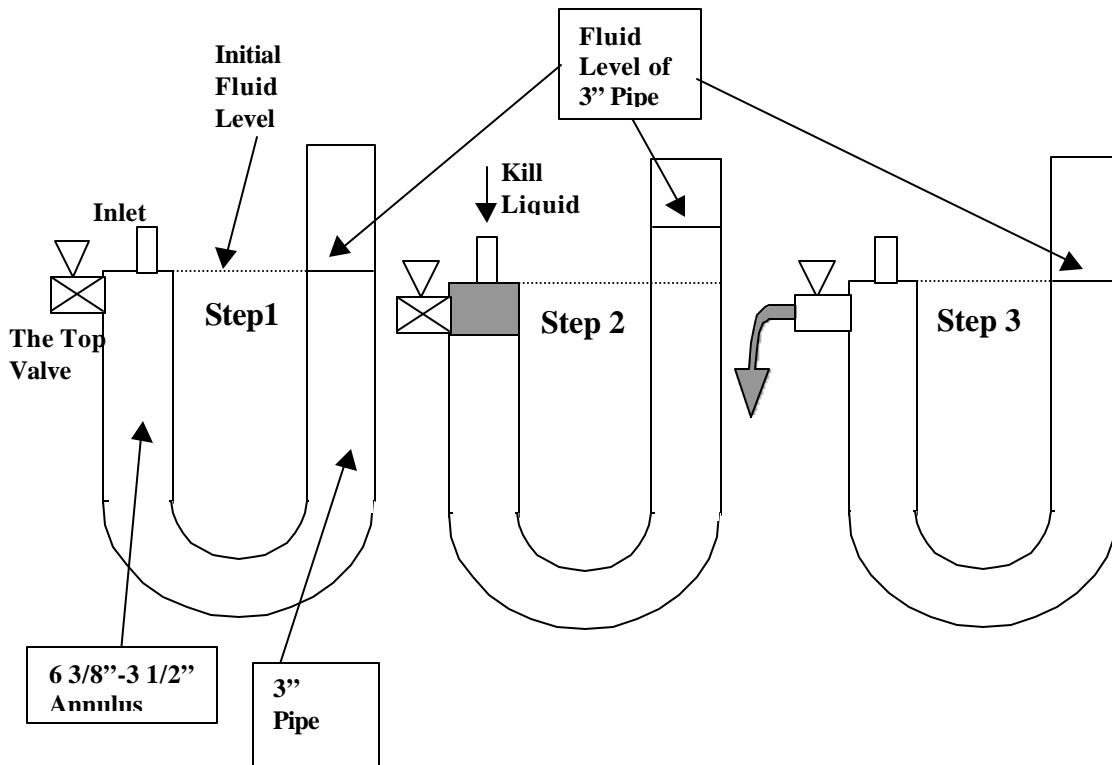
Figure 22. Simulation of a single injection cycle in experiments.

To simulate killing SCP, we applied a U-tube effect instead of fluid compressibility in the annulus (Fig. 21 and Fig. 22). Initially, fluid levels were the same between the 6 3/8-in. and 3 1/2-in. annulus and the 3-in. pipe (Condition 1 shown in Fig. 22). The kill liquid was injected into the annulus through the top flange with a closed position of the top valve (Condition 2 shown in Fig. 22). The top valve represented a needle valve for field operations. The liquid level increased inside the 3-in. plastic pipe in response to the volume of the injected kill liquid (Condition 2 in Fig. 22). When the top valve was opened, the fluid returned from the top outlet to keep the balance of hydrostatic pressure (Condition 3 shown in Fig. 22). If the annular density were not changed, the fluid levels would be equal. If the annular density increased, a fluid level in the 3-in. pipe would be higher than the level in the annulus.

The capacity of the apparatus is shown in Fig. 23. The annular volume was 10.2 gal; the 3-in pipe volume was 3.3 gal. There was 1.7 gal below the 3-in. pipe. Thus, an injected volume in one cycle was below 1.7 gal in all the experiments.

Capacity of 3" Pipe = **3.3 gal**

Annular capacity:
6" pipe (6.625" OD, 6.375" ID) and 3" pipe (OD 3.5", ID 3.0"),
= **10.2 gal**

Sump volume below 3" Pipe = **1.7 gal**

Pressure Gauge
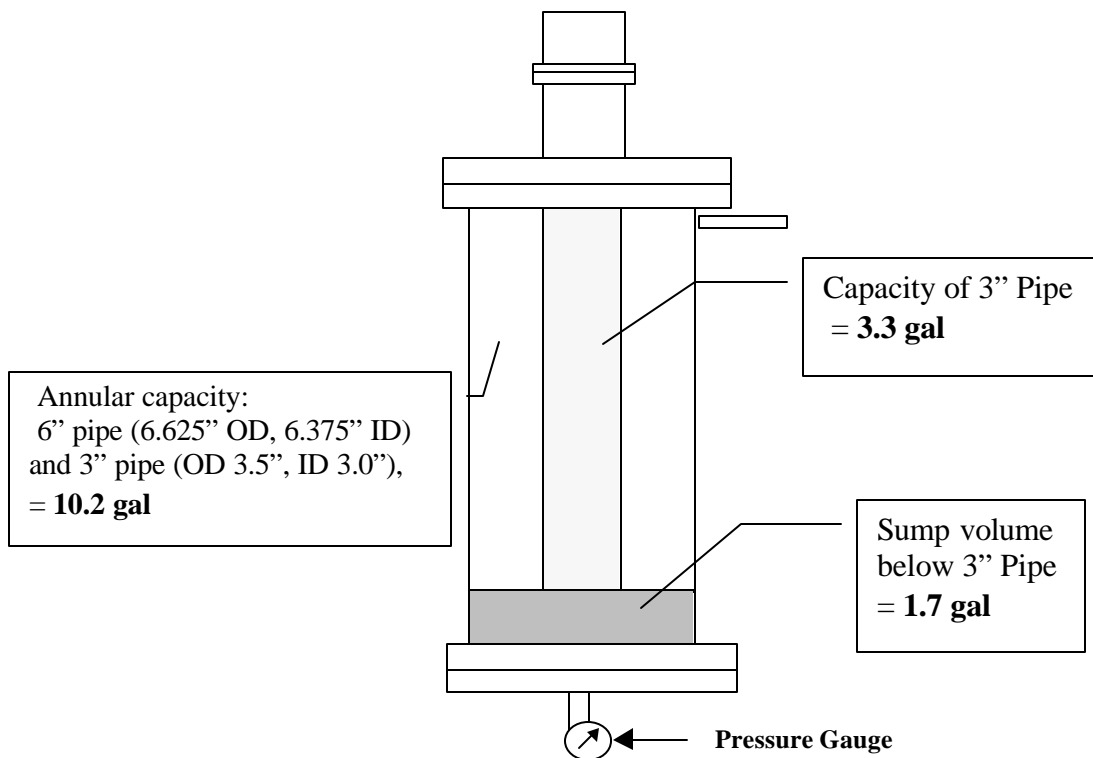
Figure 23. Volumetric capacity of physical model.

10.1.2 Data Analysis Method

To evaluate the performance of cyclic injection, a method was developed based upon the following concepts: Typically, an annular fluid above the top of the cement is a Bingham Plastic fluid with some gas content. In this study, we considered combinations of the annular fluid with various types of displacement liquids, such as Newtonian-miscible fluid (brine), Bingham-miscible fluid (drilling mud), and Newtonian-immiscible fluid (oil base mud). In addition to fluid

properties, the following patterns of mixing and displacement were considered, as shown in Fig. 24.

Case A: Kill liquid moves downwards and settles without mixing with the annular fluid.
Case B: There is some liquid settling and mixing at the bottom of the annulus.
Case C: Kill liquid mixes perfectly with the annular fluid.
Case D: There is some mixing in the top section of annulus with little settling.
Case F: Kill liquid stays at the wellhead on top of an annular fluid—no mixing, no settling.

When a mixed pattern was observed, we applied a two-letter category. For example, if a kill liquid showed Case B at early time, followed by Case A, we recorded the kill fluid pattern as Case B-to-Case A.
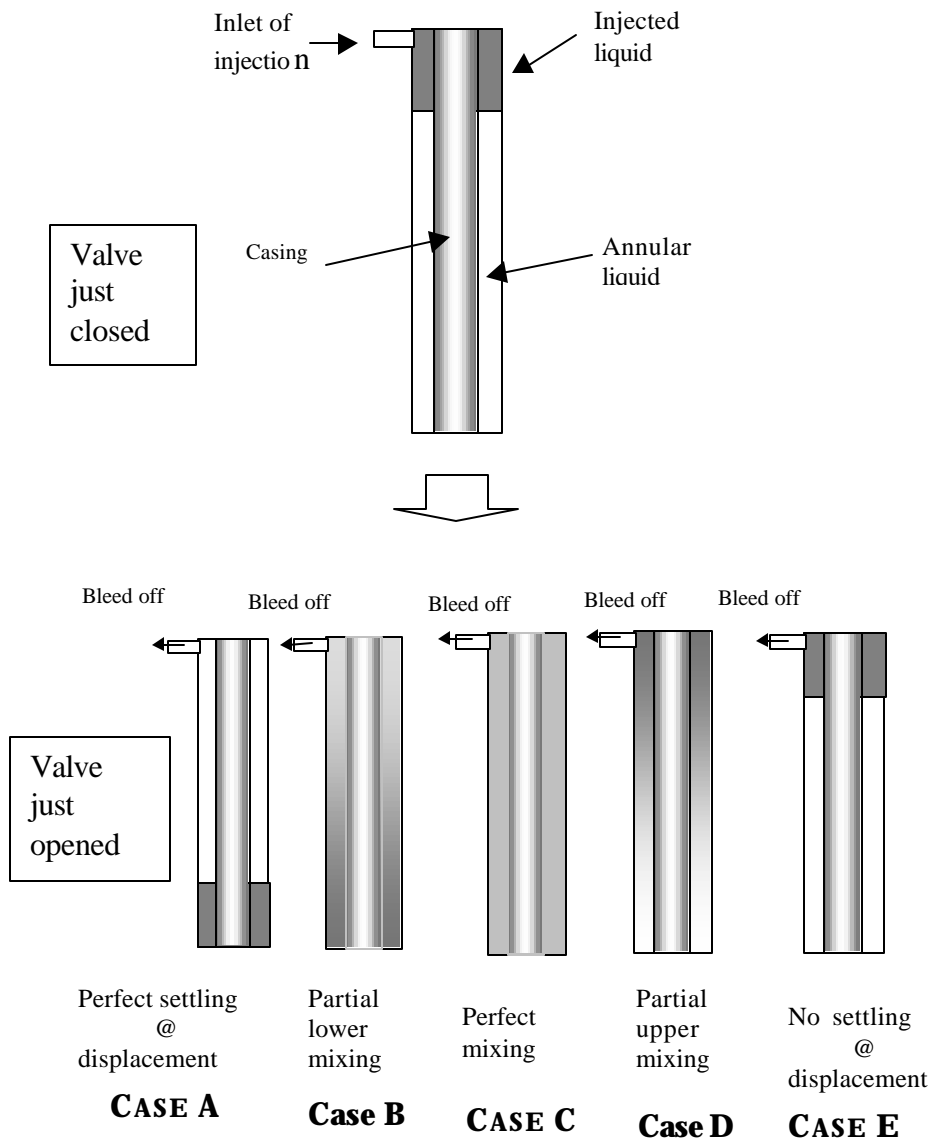
Figure 24. Displacement performance patterns.

In typical field operations, the working pressure of the well equipment and the fracture pressure below the cement top limit the maximum volume injected at each cycle. If injection is effective, the hydrostatic pressure at the cement top must increase in a step-wise fashion, as shown in Fig. 25. Fig. 25 shows that the hydrostatic pressure increases during injection and then decreases during bleed-off. However, hydrostatic pressure would not go down to its previous value if the density in the annulus increases.
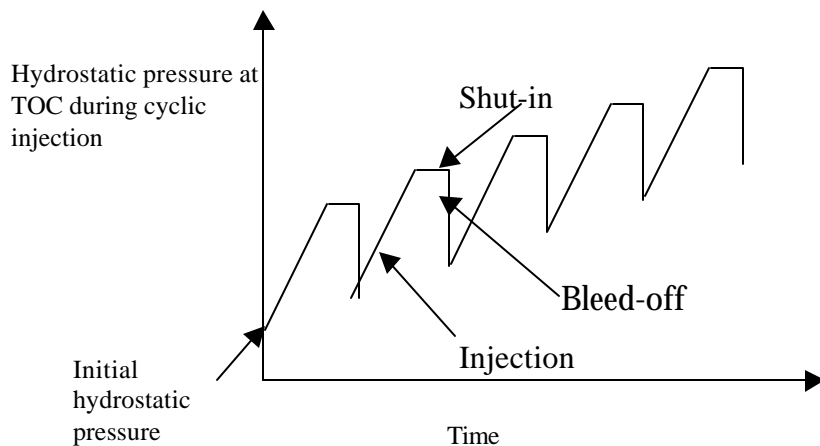
Figure 25. Bottom-hole pressure increase during cyclic injection.
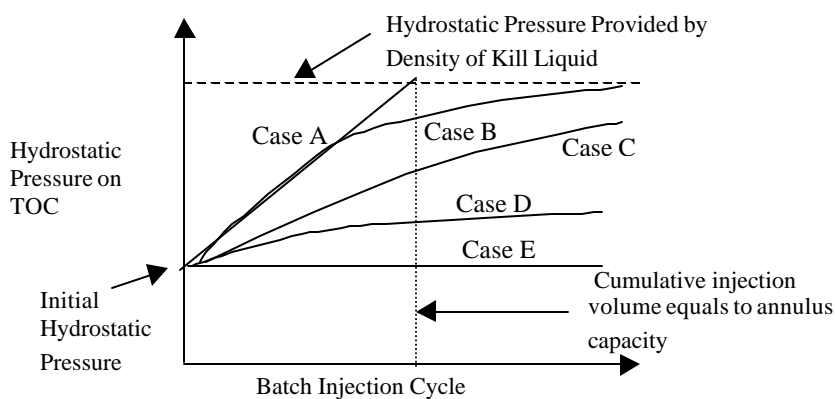
Figure 26. Bottom-hole pressure increase for various cases.

Conceptual patterns of the increases in hydrostatic pressure at the cement top are shown in Fig. 26. The plots correspond to the injection patterns from Fig. 24. For Case A, after just one cycle, hydrostatic pressure would become equal to the hydrostatic head of the kill liquid. In Cases B, C, and D, more than one annular volume is needed to reach the hydrostatic head of the kill liquid.

31

Finally, we needed a criterion to evaluate the process quantitatively. We could predict the hydrostatic pressure for Cases A and E. However, we could not estimate how much pressure would increase in other cases, except for Case C. For Case C, we developed a mathematical model as follows:

The mixture density after one injection is

$$\boldsymbol{r}_1 = \frac{\boldsymbol{r}_o V_o + \boldsymbol{r}_k V_k}{V_o + V_k},\tag{5}$$

where,
ρ_o = initial density in the annulus (ppg),
ρ_k = density of the kill liquid (ppg),
ρ_1 = density in the annulus for the first injection (ppg),
V_o = initial annular volume (gal),
V_k = one-cycle volume of the injecting kill liquid (gal).

If we inject the same volumes into the annulus several times, the mixing densities will increase in the following manner. The second injection, following Eq. (5), gives the annular density,

$$\boldsymbol{r}_2 = \frac{\left(\dfrac{\boldsymbol{r}_o V_o + \boldsymbol{r}_k V_k}{V_o + V_k}\right)V_o + \boldsymbol{r}_k V_k}{V_o + V_k} = \frac{\boldsymbol{r}_o V_o + \boldsymbol{r}_k V_k}{(V_o + V_k)^2}V_o + \frac{\boldsymbol{r}_k V_k}{(V_o + V_k)}.\tag{6}$$

The third injection gives

$$\boldsymbol{r}_3 = \frac{\left(\dfrac{\boldsymbol{r}_o V_o + \boldsymbol{r}_k V_k}{(V_o + V_k)^2}V_o + \dfrac{\boldsymbol{r}_k V_k}{(V_o + V_k)}\right)V_o + \boldsymbol{r}_k V_k}{V_o + V_k} =$$

$$= \frac{\boldsymbol{r}_o V_o^3}{(V_o + V_k)^3} + \frac{\boldsymbol{r}_k V_k}{(V_o + V_k)^3}V_o^2 + \frac{\boldsymbol{r}_k V_k}{(V_o + V_k)^2}V_o + \frac{\boldsymbol{r}_k V_k}{(V_o + V_k)}\tag{7}$$

At n time injection, the density in the annulus gives

$$\boldsymbol{r}_n = \frac{\boldsymbol{r}_o V_o^n}{(V_o + V_k)^n} + \boldsymbol{r}_k V_k\left(\frac{V_o^{n-1}}{(V_o + V_k)^n} + \frac{V_o^{n-2}}{(V_o + V_k)^{n-1}} + \frac{V_o^{n-3}}{(V_o + V_k)^{n-2}} + \cdots\cdots + \frac{1}{(V_o + V_k)}\right)\tag{8}$$

where,
ρ_n = density in the annulus (ppg)

Substituting, $[r = \dfrac{V_o}{V_o + V_k}]$ gives,

$$\boldsymbol{r}_n = r^n \boldsymbol{r}_o + \frac{\boldsymbol{r}_k V_k}{V_o}\left(r^n + r^{n-1} + r^{n-2} + \cdots\cdots r^2 + r\right).\tag{9}$$

Multiplying both sides by r gives,

$$r\boldsymbol{r}_n = r^{n+1} \boldsymbol{r}_o + \frac{\boldsymbol{r}_k V_k}{V_o}\left(r^{n+1} + r^n + r^n + \cdots\cdots r^3 + r^2\right).\tag{10}$$

Subtracting Eq. (9) from Eq. (10) gives,

$$(1-r)\boldsymbol{r}_n = \boldsymbol{r}_o r^n (1-r) + \frac{\boldsymbol{r}_k V_k}{V_o} \cdot r(1-r^n)$$

Thus, density after the nth injection cycle is,

$$\boldsymbol{r}_n = \boldsymbol{r}_o r^n + \frac{\boldsymbol{r}_k V_k}{V_o} \cdot \frac{r(1-r^n)}{1-r} . \tag{11}$$

For $r < 1$; $\lim\limits_{n \to \infty} r^n = 0$

$$\lim\limits_{n \to \infty} \boldsymbol{r}_n = \boldsymbol{r}_o r^n + \frac{\boldsymbol{r}_k V_k}{V_o} \cdot \frac{r(1-r^n)}{1-r} = \frac{\boldsymbol{r}_k V_k}{V_o} \cdot \frac{r}{1-r} = \frac{\boldsymbol{r}_k V_k}{V_o} \cdot \frac{V_o}{V_o + V_k - V_o} = \boldsymbol{r}_k \tag{12}$$

$$\lim\limits_{n \to \infty} \boldsymbol{r}_n = \boldsymbol{r}_k \tag{13}$$

where,

$$r = \frac{V_o}{V_o + V_k} ,$$

n = number of injection cycles.

Formula (13) implies that the density in the annulus approaches the density of the kill liquid for a large number of injection cycles.

This mathematical model provides a criterion for evaluation of the experiments. As a reference level, we used Case C in Fig. 24 as the "criterion of perfect mixing (CPM)." If, after several injection cycles, hydrostatic pressure increased at a rate greater than that for Case C in Fig. 24, we designated displacement performance as "good." Otherwise, the performance was designated as "poor."

10.1.3 Selection of Displacing Fluids
One of the main purposes in this experimental research was to investigate brine as a kill liquid. This section presents a selection of brines.

Density Range
Table 4 shows the approximate density range of solid-free salt solutions. Potassium chloride brines provide densities up to about 9.7 lb/gal at 85°F. Sodium chloride brines provide densities up to 9.8 lb/gal. Sodium-chloride/Calcium-chloride mixtures can provide densities from 10.0 to 11.0 lb/gal. Calcium chloride can be used for weights up to 11.7 lb/gal. Formulations of calcium chloride and calcium bromide can provide solid-free densities up to 15.0 lb/gal. Use of Zinc Bromide can increase the solids-free fluid density up to 19.2 lb/gal.

Table 4 Density Range of Salt Solution

Density (lb/gal)	Salt solutions
8.3-9.7	Potassium Chloride
8.3-9.8	Sodium Chloride
9.8-11.0	Sodium Chloride-Calcium Chloride
11.0-11.7	Calcium Chloride
11.7-15.0	Calcium Chloride-Calcium Bromide
15.2-19.2	Calcium Chloride-Calcium Bromide, Zinc Bromide

Corrosiveness, Toxicity, and Safety

When mixing high concentrations of $CaCl_2$, $CaBr_2$, or $ZnBr_2$, precautions should be taken to keep the dry chemical dust out of the eyes and lungs. Rubber protective clothing should be worn to prevent skin damage. Considerable heat may be generated; thus, precautions should be taken to prevent burns. $CaCl_2$-$CaBr_2$ brine toxicity is low enough to allow use of these solutions in marine waters. $ZnBr_2$ can be toxic to fish, which limits its use in offshore areas. Onshore, precaution must be taken to avoid contamination of water supplies. $CaCl_2$-$CaBr_2$ brines are alkaline, whereas $ZnBr_2$ brines are slightly acidic and therefore more corrosive.

Cost

Heavy brines are expensive. 15.0-lb/gal $CaCl_2$-$CaBr_2$ brine costs about 25 times more than 10.0-lb/gal $CaCl_2$ brine. Eighteen-lb/gal $CaCl_2$-$CaBr_2$-$ZnBr_2$ brines cost over 80 times more than 10.0-lb/gal $CaCl_2$ brine.

10.1.4 Testing Procedure

Combinations of all fluids considered for this study are shown in Table 5. Table 6 is the actual matrix of our experiments. All results are shown in Appendix D.

Table 5. All Possible Combinations of Displacing and Annular Fluids

Case	Kill Liquid	Annular Fluid	Miscibility	Remarks
1	Brine	Water	Miscible-Miscible	Newtonian-Newtonian
2	Brine	Drilling Fluids	Miscible-Miscible	Newtonian-Bingham
3	Drilling Fluids	Water	Miscible-Miscible	Bingham-Newtonian
4	Brine	Oil	Miscible-Immiscible	Newtonian-Newtonian
5	Drilling Fluids	Oil	Miscible-Immiscible	Bingham-Newtonian

Table 6. Experimental Matrix

Experiment	Kill Liquid	Annular Fluid
1	Brine (CaCl$_2$, 11.0 ppg)	Water
2	Brine (CaCl$_2$, 11.0 ppg)	Water
3	Brine (CaCl$_2$, 11.3 ppg)	Brine (CaCl$_2$, 10.35 ppg)
4	Brine (CaCl$_2$, 10.15 ppg)	Bentonite (3 wt %, 8.48 ppg)
5	Brine (CaCl$_2$, 11.0 ppg)	Bentonite (6 wt %, 8.66 pgg)
6	Bentonite (11.0 ppg by Barite)	Water
7*	Brine	Oil
8*	Bentonite	Oil

*Data from Experiments 7 and 8 are not included in Appendix D

A testing procedure was designed to investigate the performance of each experimental run compared to CPM. The procedure was as follows:
1. Fill the annulus through the inside pipe up to the level of the top valve.
2. Close the top valve and read pressure.
3. Inject fixed volume of kill liquid and stop pumping.
4. Record the value of a bottom pressure.
5. Wait three to five minutes (shut-in).
6. Take a minimum volume sample of a fluid from the bottom valve and measure a density (rheology by Fann 35 viscometer, if necessary).
7. Open the top valve to bleed off the pressure.
8. Record value of the bottom pressure.
9. Take a sample from the top valve and measure its density (rheology by Fann 35 Viscometer, if necessary).
10. Close the top valve.
11. Repeat steps 3 to 8 until there is no significant change of the bottom pressure.

10.2   Results and Analysis

10.2.1 Miscible Displacement Experiments

Brine (CaCl$_2$) into Water
First, we conducted an experiment using a single-cycle injection of brine (CaCl$_2$) into water. The 11.0-ppg brine (CaCl$_2$) was pumped into the annulus until a total volume of 1.6 gal was reached. We stopped pumping at 7 min. We sampled the fluid from the bottom valve and recorded the density every minute for 10 min. After 60 min, we bled off and sampled from both the bottom and top valves. The result is shown in Experiment 1 of Appendix D and Fig. 27.

Second, we conducted Experiment 2 using multi-cyclic injections. We injected 1.4 gal of 11-ppg brine (CaCl$_2$) into an annulus filled with water, then shut-in 3 minutes, and bled-off. We repeated this procedure 9 times. The results are shown in Fig. 28 and Appendix D. The results show that the hydrostatic pressure increases with injections, and the same density comes from the top and bottom in every injection. However, we did not see a stabilized hydrostatic pressure by the kill liquid.

Finally, we conducted Experiment 3 to find out the final condition that the hydrostatic pressure achieved with this kill liquid, as shown in Fig. 30. We injected 11.3 ppg brine (CaCl$_2$) into an annulus filled with 10.3 ppg brine (CaCl$_2$). The injections were repeated until the hydrostatic pressure stabilized. It took 18 cycles to reach the maximum pressure with the 11.3-

ppg brine. In addition, every sample from the top and bottom valves indicated the same density, as shown in Fig. 31.

Results from Experiment 1 showed the density increasing with pumping up to a value of 8.69 ppg. This density matches the density calculated by Eq. (5.1). Moreover, the densities from the top valve and that of the bottom valve were the same when we sampled them 60 minutes after the injections started. Thus, this single-cycle injection was evaluated as CPM.

In addition, we compared Experiment 2 with the calculated values from Eq. (11). The comparison is shown in Fig. 32. The results matched CPM. We also compared a calculation from Eq. (11) with results from Experiment 3, as shown in Fig. 33.

From these comparisons, we concluded that the cyclic injection of brine into an annulus filled with water could be classified as CPM (Case C shown in Fig. 24). In other words, this combination will work in the field. If we inject a large amount of the kill liquid, we will reach a desirable hydrostatic pressure eventually.
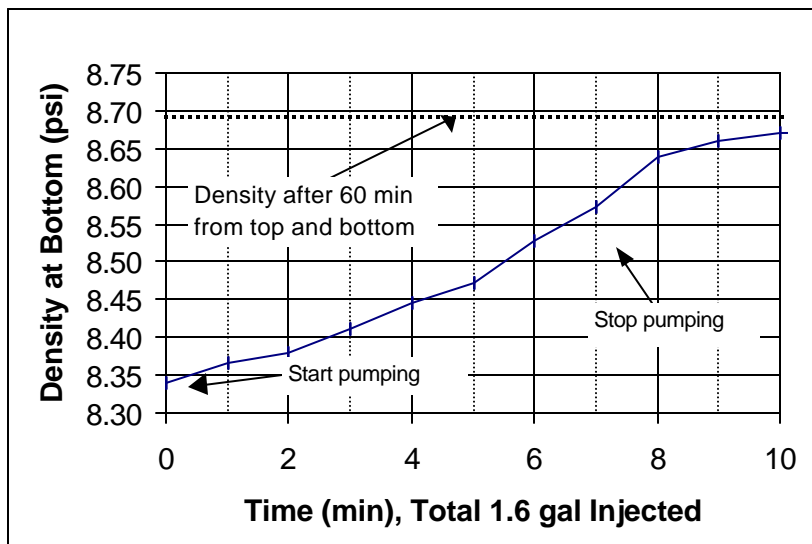
Figure 27. Results of Experiment 1.
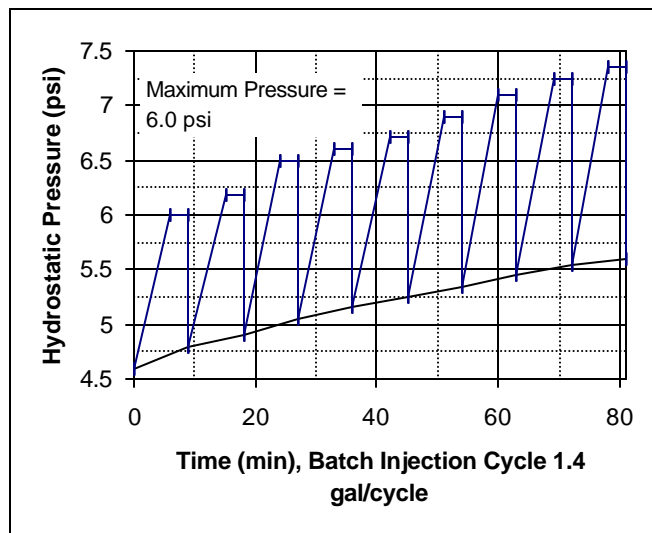
Figure 28. Results of Experiment 2.
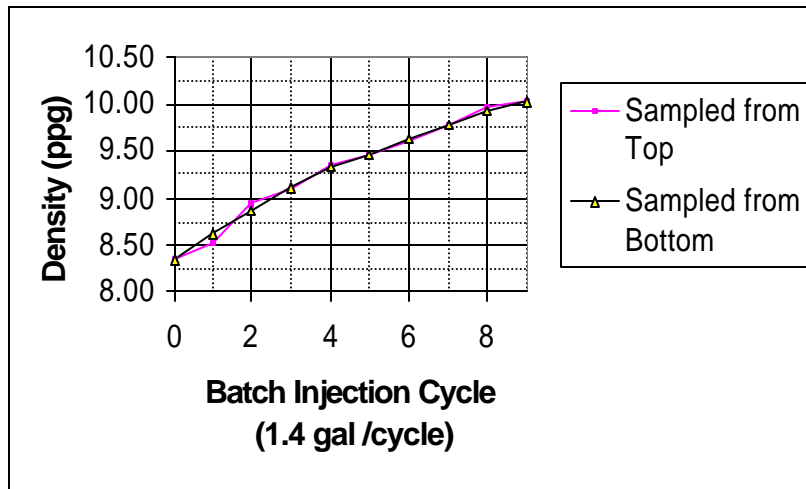
Figure 29. Results of density in Experiment 2.
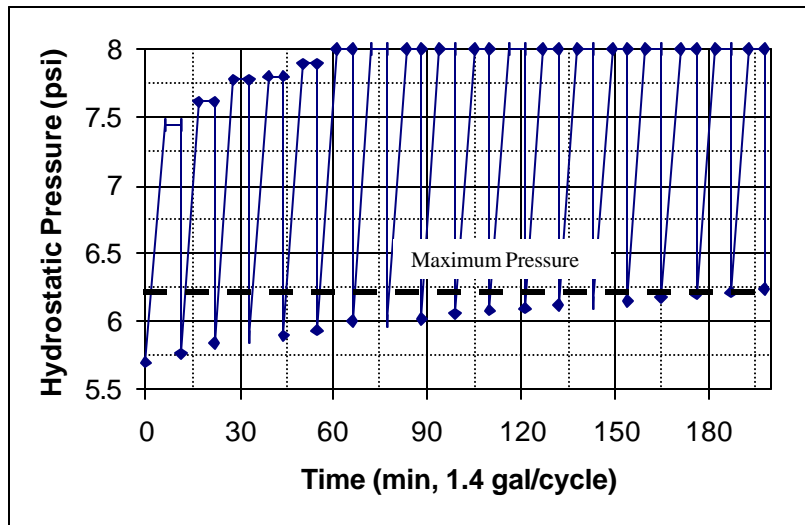
Figure 30. Results of Experiment 3.
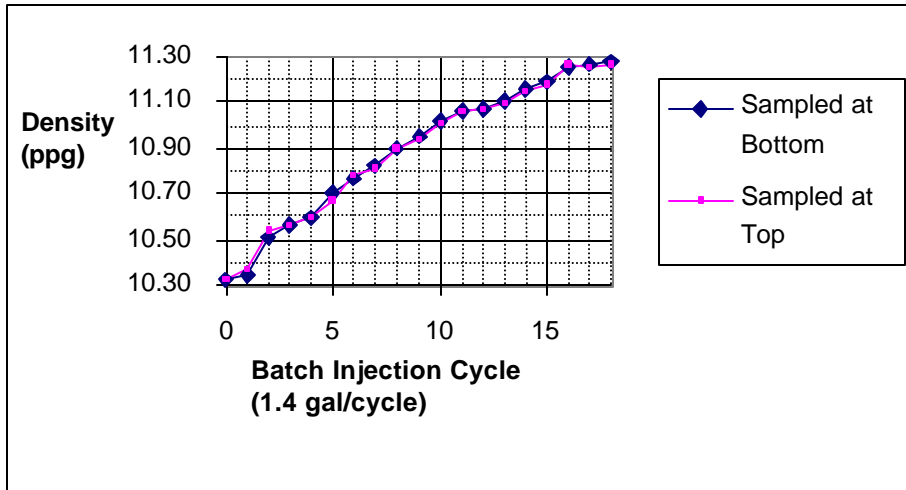
Figure 31.   Annular density change in Experiment 3.
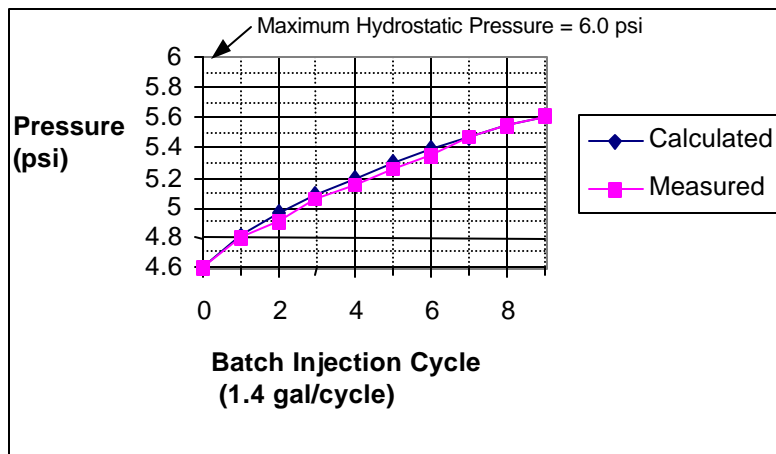
Figure 32. Comparison of Eq. (11) with results of Experiment 2.
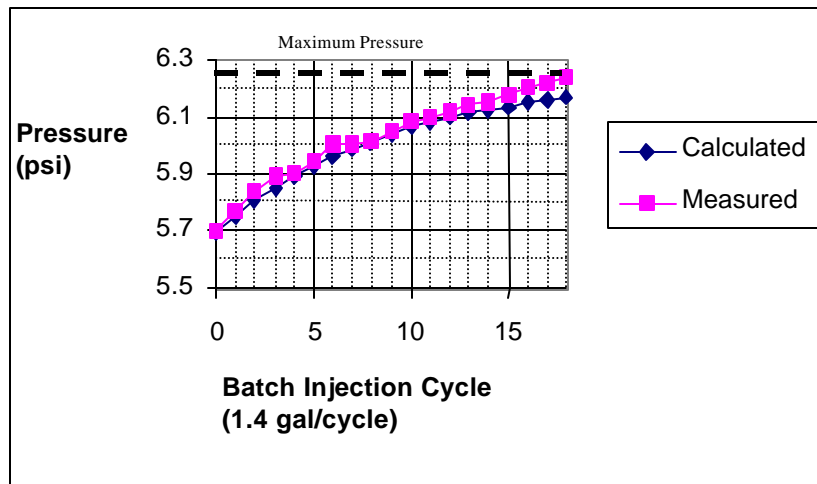
Figure 33. Comparison of Eq. (11) with results of Experiment 3.

Brine (CaCl₂) into Water-base Mud

First, we injected 10.15-ppg brine into the annulus filled with 3-wt% bentonite slurry (Experiment 4). The result was almost the same as that with water. At this concentration of bentonite and calcium chloride, no flocculation was observed as being a problem. However, rheology measurements showed a clear rheology change caused by calcium flocculation, as shown in Table 7.
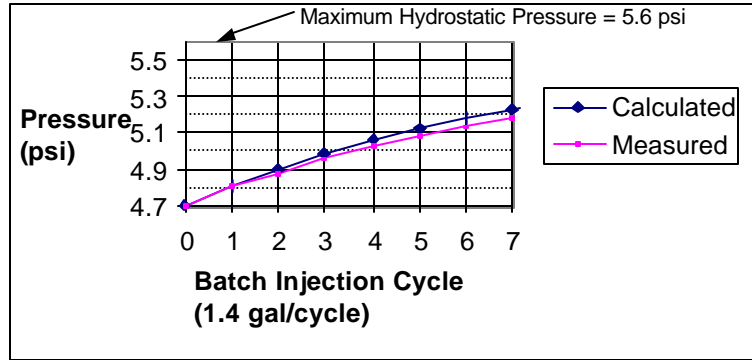
Figure 34. Comparison of Eq. (11) with results of Experiment 4.

Table 7. Rheology of Annular Fluid in Experiment 4

Viscometer Reading	Original Rheology	Final Rheology
600	10	11
300	6	8
200	5	6
100	3	5
6	1	3.5
3	0.9	2

Next, to investigate the effect of the bentonite content, we conducted Experiment 5 using 10.3 brine (CaCl₂) and 6-wt % bentonite slurry. After single-cycle injection, we noticed less fluid returned compared to the volume injected. Since the bentonite slurry was flocculated, its high gel strength prevented annular flow return. In other words, the excess hydrostatic pressure on the inside pipe over the hydrostatic pressure in the annulus was smaller than the friction force between the annular fluid and the pipes. Then, in the first two cycles, a significant increase of the hydrostatic pressure was observed. However, after the fourth cycle, the hydrostatic pressure remained the same (Fig. 35).

We should keep in mind that sodium montmorillonite can be flocculated by contact with calcium ions, even in low concentrations. If sodium montmorillonite is present in high concentrations, brine with calcium ions may cause flocculation and, thus, the high hydrostatic pressure. As shown in Fig. 36, initially the hydrostatic pressure increased higher than that of CPM. However, the hydrostatic pressure dropped below the CPM performance after the eighth cycle.

Table 8 shows the rheology of the returned fluids from the top valve, and Fig. 37 shows data from a viscometer reading at 3 rpm. Evidently this Bingham fluid had been heavily flocculated. However, the returned fluids were becoming Newtonian fluids after the second cycle of injection. Thus, Fig. 38 shows the density of the returned fluids were coming close to the density of the kill liquid. In other words, the kill liquid was not effective for increasing the annular density.

This phenomenon might be explained as follows: First, when we injected the kill liquid (Condition A in Fig. 39), the flocculation must have been present (Condition B in Fig. 39). The flocculation increased the hydrostatic pressure because of an increased gel strength and yield point. Then, a flocculated "plug" was formed, and it stayed as we bled off (Condition C in Fig. 39). Finally, the flocculated "plug" prevented the kill liquid from a downward movement and further mixing (Condition D in Fig. 39), and then it returned to Condition C as we bled off. Consequently, the system repeated Conditions C and D.

This situation would be ineffective in removing SCP. Based on the results for Experiment 5, we believe that the bentonite slurry in the annulus would not work with brines.
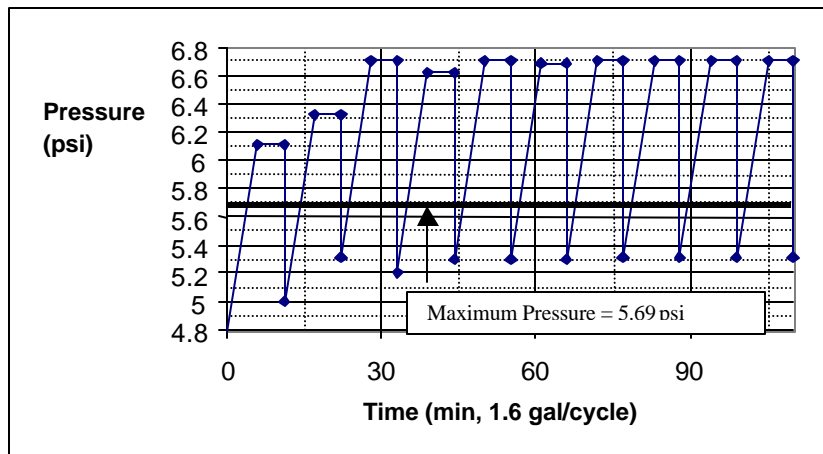
Figure 35. Results of Experiment 5.
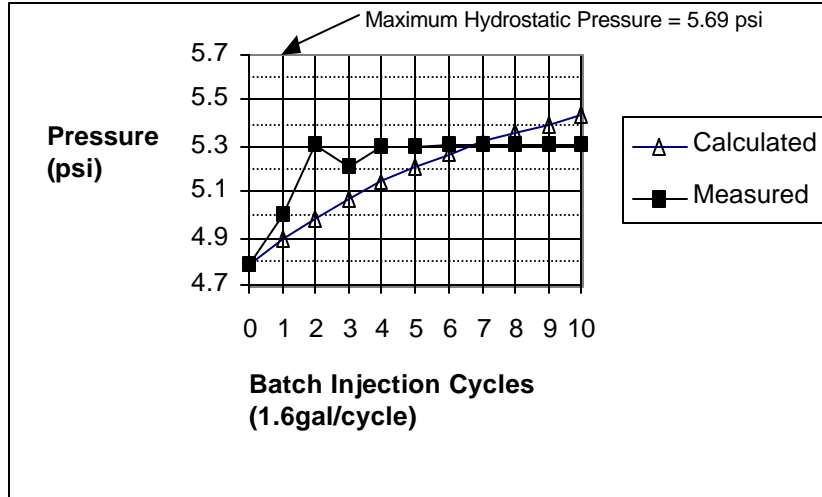
Figure 36. Comparison of Eq. (5.7) with results of Experiment 5.

Table 8. Rheology of Returned Fluid in Experiment 5

Cycle	600 (lb/100 ft^2)	300 (lb/100 ft^2)	200 (lb/100 ft^2)	100 (lb/100 ft^2)	6 (lb/100 ft^2)	3 (lb/100 ft^2)
0	36	22	17	11	5	2
2	38	30	26	22	17	14
4	28	23	20	17	14	11
6	24	18	16	13	10	8
8	21	16	15	12	10	8
10	11	7	6	5	4	3

Table 9. Density of Returned Fluid in Experiment 5

Cycle	Density (ppg)
1	9.12
2	8.89
3	8.70
4	8.80
5	9.21
6	9.19
7	9.20
8	9.40
9	9.45
10	9.60
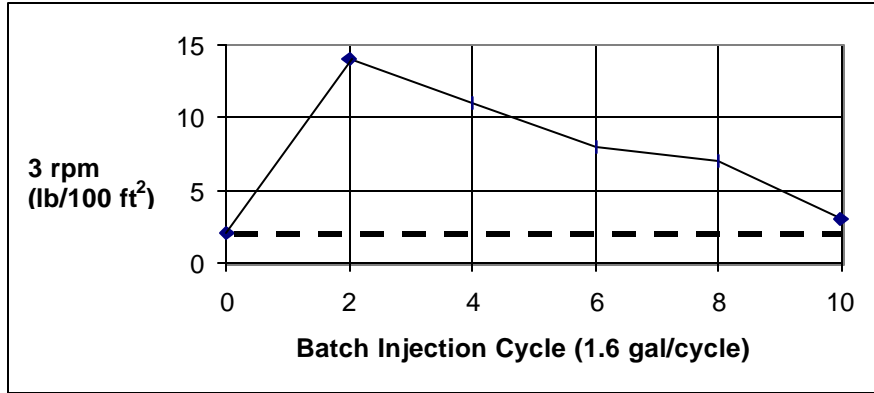
Figure 37. Rheology (3 rpm) of the returned fluid in Experiment 5.
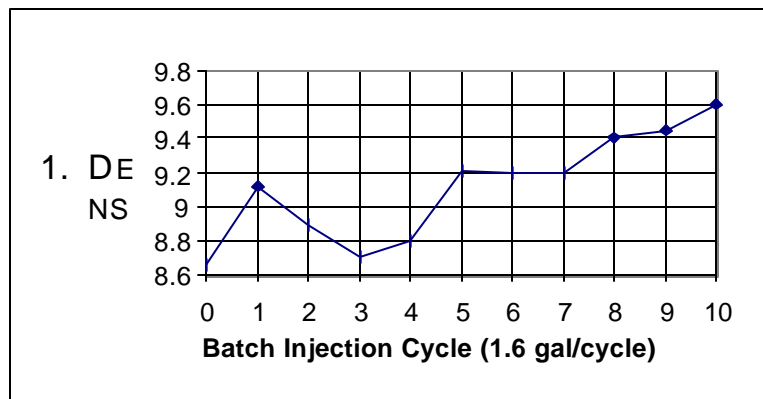
Figure 38. Density of the returned fluid in Experiment 5.

A   B   C   D

Kill Liquid

Flocculated Fluid
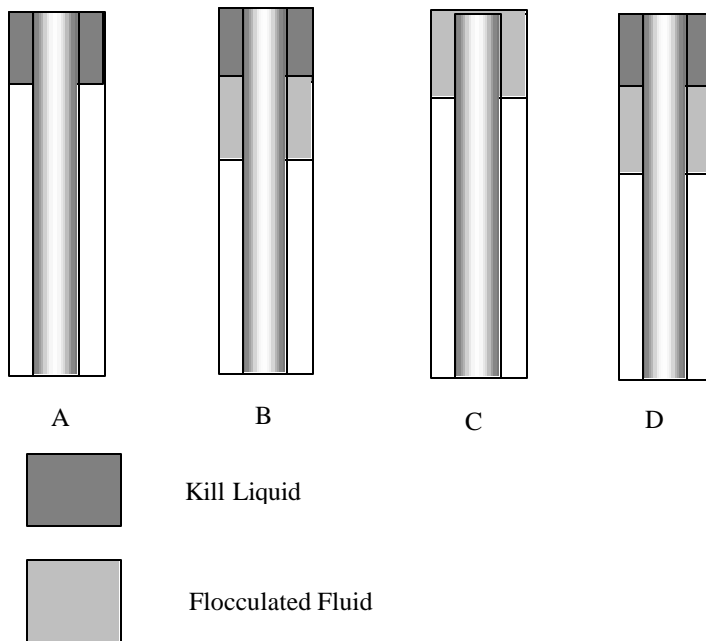
Figure 39. Conceptual model for Experiment 5.

Water-base Mud into Water

Brines are used to increase an annular density because of their high density and lack of solid contents. However, to our knowledge, no investigation has been made to evaluate drilling mud as a kill liquid to be injected into an annulus.

In this section, we conducted experiments to compare bentonite mud and brine ($CaCl_2$). To do this, we performed a 5-cycle injection, pumping until 6 psi of the hydrostatic pressure was achieved for each cycle. Five cycles were the upper limitation for this apparatus to inject the 11.0-ppg-bentonite slurry because barite settling on the bottom was critical to plug the outlet, and only barite was returned when we opened the bottom valve.

The results, shown in Fig. 40, indicated that cyclic injection increased the bottom hole pressure more than that of CPM; this knowledge can be useful in field operations. However, we need further investigation to determine whether this cyclic injection is effective in maintaining hydrostatic pressure in an annulus permanently.
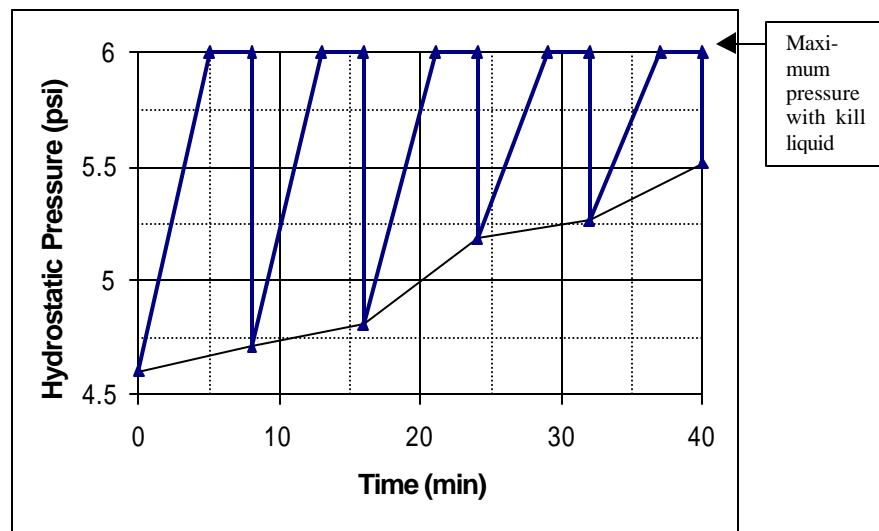
Figure 40. Increase of bottom hole pressure in Experiment 6.

10.2.2 Immiscible Displacement Experiments

Performance of miscible displacement in our experiments was poor. We assumed that a miscible-immiscible combination would be more effective to kill SCP. We conducted two experiments such as brine vs. white oil and bentonite slurry vs. white oil. The results of these experiments showed that both the brine and water-base mud would quickly settle to the bottom and perform as in Case A (Fig. 24).

Brine (CaCl₂) into White Oil

Brine (CaCl$_2$) into White Oil

First, we conducted Experiment 7 to inject brine into white oil (see Fig. 41). The result showed the whole liquid settled to the bottom of the apparatus. The kill liquid parted immediately and dispersed into droplets after entering the white oil from the outlet. Large droplets settled faster than did the small droplets. Stocks Law can explain this phenomenon. The whole volume settled completely to the bottom. The initial hydrostatic pressure by white oil was 3.9 psi. Then after pumping, the brine column was measured 0.8 ft on bottom and the hydrostatic pressure after bleed off was given as 4.04 psi. There was no brine in the returned fluid. In this case, the pumped 11.0-ppg brine provided the maximum hydrostatic pressure. In other words, this combination gave the optimal situation, as shown in Fig. 24, Case A.

Water-base Mud into White Oil

Next, we conducted Experiment 8 using a 11.0-ppg bentonite slurry and white oil. The bentonite slurry behaved differently from brine. The bentonite slurry from the inlet did not part as the brine did and settled onto the bottom, as shown in Fig. 42. The initial hydrostatic pressure in the white oil was 3.9 psi. After pumping, a column of bentonite slurry was measured at 0.95 ft, and the hydrostatic pressure after bleed off was 4.07 psi. There was no slurry in the returned fluid. In this case, the pumped 11.0-ppg slurry provided the maximum hydrostatic pressure. This was also the same result shown in Fig. 24, Case A.
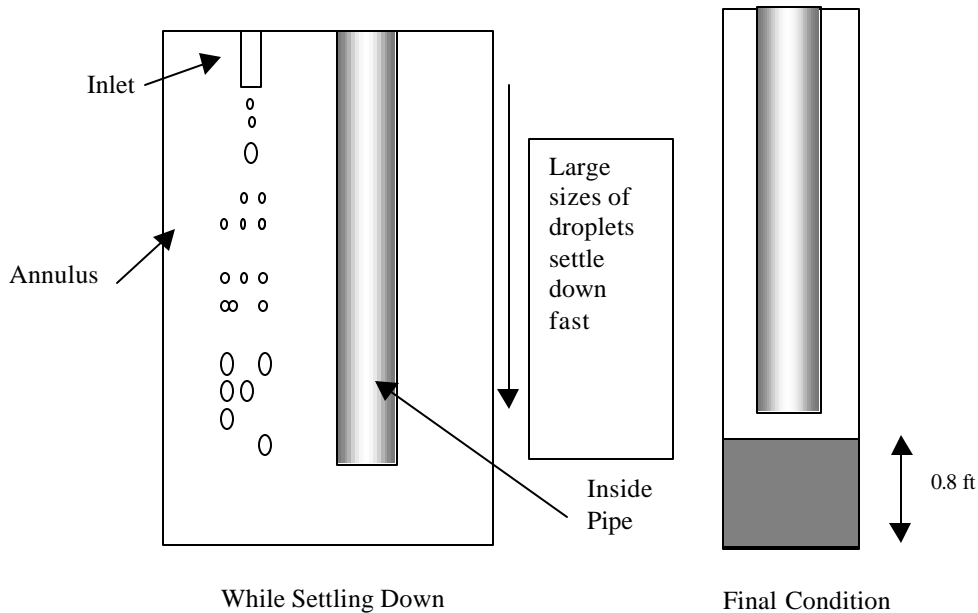
Figure 41. Brine injection into white oil in Experiment 7.
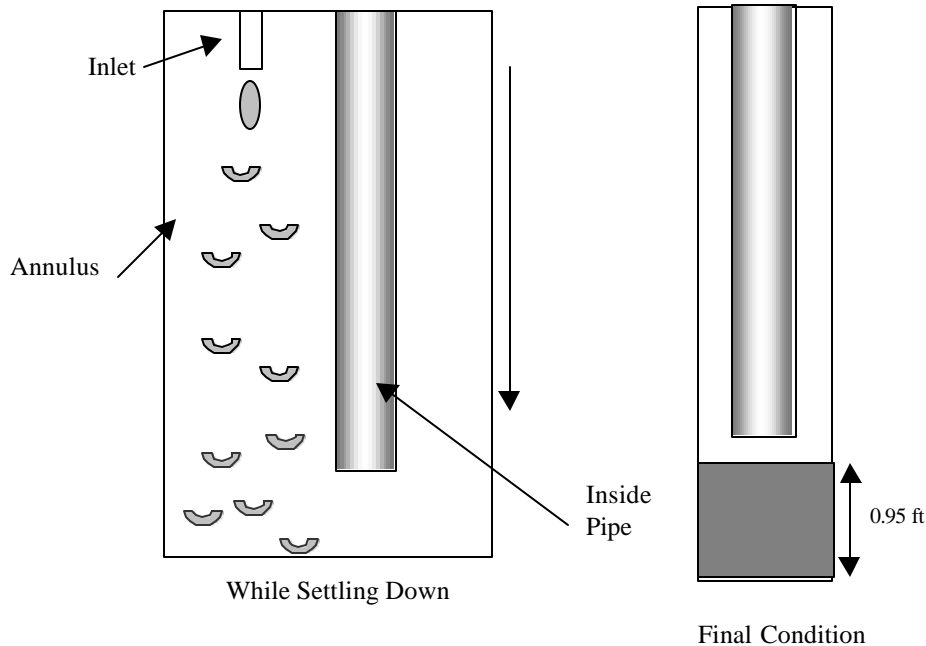
Figure 42. Water-base mud injection into white oil in Experiment 8.

12. SCP REMEDIATION – CONCLUSIONS AND RECOMMENDATIONS

Conclusions:
Results of this study show that a strong relation exists between the performance of cyclic injection and chemical interaction of the brines with fluids (usually drilling muds) already in the annulus. Depending upon fluid compatibility, the performance might range from total elimination of casing pressure to extreme cases of no effect at all. Field observations have confirmed this conclusion.

The following specific conclusions can be drawn from this study:

● The assessment of compatibility is critical for the selection of a kill liquid and an annular fluid. Such an assessment could be done using the methodology and testing equipment developed in this work.

● A brine kill liquid placed in an annulus filled with water gives a desirable hydrostatic pressure. The density increases by perfect mixing, and perfect mixing occurs rapidly in a short annulus. This result shows that removal of SCP might be effective if the fluid in the annulus is Newtonian and miscible. Brine is not a good candidate kill fluid for an annulus filled with water-based drilling fluid. The brine would flocculate the annulus mud and the displacement process would stop.

● An immiscible combination of kill and annulus fluids provides the most desirable performance for cyclic injection. In this case, the injected fluid would displace the annular fluid and kill SCP.

Recommendations:

Based upon results of this work, we recommend follow-up studies to develop and implement a fluid sampling and testing procedure to be used before injecting a kill fluid into the well's annulus. Future work in this area should focus on developing a laboratory or pilot-size method and equipment for sampling and testing the synergy and performance of fluids used to mitigate the SCP problem by annular injection (bleed-and-lube) or circulation (CARS) methods. The testing procedure should be suitable for evaluation and selection of various fluids and compounds to be used in specific wells. The method should ideally also provide experimental verification of the potential of displacing fluids (or compounds) for permanent containment of casing pressure.

- The displacement experiment involving two Newtonian fluids showed that a complete displacement is achievable by large number of injection cycles.
- If the well's annulus is filled up with thin drilling mud, the displacement pattern will full that for Newtonian fluid. More testing is needed, however, to determine maximum clay concentration in the mud.
- A mathematical model using data from a mixing test can predict the required number of cycles for the Newtonian-type displacement.
- The immiscible-displacement experiments involving injection of brine or bentonite slurry into synthetic-oil-filled annulus resulted in complete displacement with a minimum volume of injected fluid and maximum value of the final bottom-hole pressure.
- Bleed-and-Lube method did not worth when brine was lubricated into the annulus filled with a typical bentonite drilling mud. The treatment resulted in a rapid flocculation and formed a plug, which prevented the brine from displacing the annulus.
- Performance of the pressure Bleed-and-Lube method for control of SCP depends entirely upon annular fluid displacement with the injected heavy fluid. In the closed-ended annulus, the displacement is controlled by combination of two phenomena: diffusive mixing and gravity settling.
- The performance can be evaluated and predicted by analyzing rheology of the annular fluid and testing the two annular fluids interaction using a pressurized scaled-down physical analog of the Bleed-and-Lube process – similar to the experimental apparatus used in this research study.
- Three parameters represent Bleed-and-Lube process design; batch volume of a single injection cycle, total required number of cycles, and maximum final pressure increase at the top of cement (TOC) at the end of the treatment.

BIBLIOGRAPHY

Appleby, S., and A. Wilson: "Permeability and Suction in Setting Cement," *Chemical Engineering Science* 51:251-267 (1996).

Bourgoyne, A. T., Jr., S. L. Scott, and W. Manowski: "A Review of Sustained Casing Pressure (SCP) Occurring on the OCS," Final Report submitted to MMS (March 2000).

Hamrick, R., and C. Landry: "$13^3/_8$ Casing Stair Step Casing Pressure Elimination Project," LSU/MMS Well Control Workshop, November 19-20, 1996.

Johnson, A. B., and D. B. White: "Gas-Rise Velocities During Kicks," SPE 20431 (Schlumberger Education Service, 1989), p. 5-1.

Levine, Dennis C., Eugene W. Thomas, H. P. Bezner, and Glen C. Tolle: "Annular Gas Flow After Cementing: A Look at Practical Solutions," SPE Paper 8255, 1979.

Minerals Management Service: "Notice to Lessees and Operators: Sustained Casinghead Pressure" (Draft), US MMS, GOM OCS Region, January, 2000.

Nishikawa, Somei: "Mechanism of Gas Migration after Cement Placement and Control of Sustained Casing Pressure," M. S. Thesis, Louisiana State University, May 1999.

Nishikawa, S., Wojtanowicz, A.K., and Smith, J.R.: "Experimental Assessment of Bleed-and Lube Method for Removal of Sustained Casing Pressure," CIPC Paper 2001-041, Canadian International Petroleum Conference-2001, Calgary, Alberta, Canada, June 12-14, 2001.

Tinsley, John M., Erik C. Miller, Fred L. Sabins, and Dave L. Sutton: "Study of Factors Causing Annular Gas Flow Following Primary Cementing," SPE Paper 8257, 1979.

Xu, R., and Wojtanowicz, A.K.: "Diagnosis of Sustained Casing Pressure from Bleed-off/Buildup Testing Patterns," SPE Paper 67194, 2001.

SCP DATA BANK

MUA1.xls

MUA2.xls

MUA3.xls

MUA4.xls

MUA5.xls

MUA8.xls

MUA9.xls

MUA10.xls

MUA11.xls

MUA12.xls

MUA15.xls

APTA19.xls

APTA30.xls

APTA31.xls

APTL9.xls

BPTB6.xls

PTCA25C.xls

PTCA7D.xls

B7.xls

HIA1.xls

HIA2.xls

HIA3.xls

Table A1 Pressure Record of Well A-1 - Platform MU-A111

Date	Status	Time	Surf Csg	Cond Csg		SITP	FTP
		days	13 3/8"	20"	26"		
1/3/89	Vent Well	0	0	0			
2/5/89	Vent Well	33	0	0			
3/8/89	Vent Well	64	0	0			
4/7/89	Vent Well	94	0	0			
5/3/89	Vent Well	120	0	0			
6/6/89	Vent Well	154	0	0			
7/3/89	Vent Well	181	10	36			
8/2/89	Vent Well	211	17	24	0		
9/1/89	Vent Well	241	20	46	0		
10/1/89	Vent Well	271	23	?	0		
11/1/89	Vent Well	302	25	10	0		
12/1/89	Vent Well	332	28	27	0		
1/2/90	Vent Well	364	38	28	0		
2/9/90	Vent Well	402	46	30	0		
3/14/90	Vent Well	435	55	25	0		
4/1/90	Vent Well	453	54	22			
5/1/90	Vent Well	483	55	26			
6/2/90	Vent Well	515	55	26			
7/1/90	Vent Well*	544	71	5			
8/1/90	Vent Well	575	58	29			
9/1/90	Vent Well	606	59	28			
10/1/90	Vent Well	636	60	25			
11/1/90	Vent Well	667	65	23			
12/1/90	Vent Well	697	61	21			
1/1/91	Vent Well	728	60	22			
2/1/91	Vent Well	759	55	19			
3/1/91	Vent Well	787	60	25			
4/1/91	Vent Well	818	60	25			
5/1/91	Vent Well	848	70	30			
6/3/91	Vent Well	881	67	30			
7/1/91	Vent Well	909	69	28			
8/9/91	Vent Well	948	68	27			
9/1/91	Vent Well	971	70	26			
10/3/91	Vent Well	1003	70	30			
11/5/91	Vent Well	1036	73	25			
12/4/91	Vent Well	1065	75	25			
1/2/92	Vent Well	1094	72	20			
2/2/92	Vent Well	1125	72	20			
3/2/92	Vent Well	1154	25	25			
4/2/92	Vent Well	1185	80	20			
5/1/92	Vent Well	1214	80	25			
6/1/92	Vent Well	1245	80	25			
7/1/92	Vent Well	1275	75	40			
8/3/92	Vent Well	1308	85	35			
9/2/92	Vent Well	1338	80	30			
10/1/92	Vent Well	1367	10	0			
11/2/92	Vent Well	1399	20	21			
12/15/92	Vent Well	1442	25	20			
1/6/93	Vent Well	1464	25	25			
2/1/93	Vent Well	1490	25	20			
3/3/93	Vent Well	1520	25	20			
4/4/93	Vent Well	1552	25	20			
5/1/93	Vent Well	1579	25	20			
6/1/93	Vent Well	1610	25	25			
7/1/93	Vent Well	1640	30	30			
8/1/93	Vent Well	1671	20	20			
9/1/93	Vent Well	1702	20	20			
10/6/93	SI	1737	40	20			
11/4/93	SI	1766	35	30			
12/1/93	SI	1793	35	35			
1/12/94	SI	1835	30	30			
2/1/94	SI	1855	30	15			
3/1/94	SI	1883	35	25			
4/1/94	SI	1914	35	20			
5/1/94	SI	1944	35	30			
6/2/94	SI	1976	35	25			
7/1/94	SI	2005	35	30			
8/2/94	SI	2037	45	30			
9/4/94	SI	2070	40	35			
10/2/94	SI	2098	40	20			

Fig.A-1-1   13 3/8" x 9 5/8" Annulus of Well MUA1 - Platform MU-A111
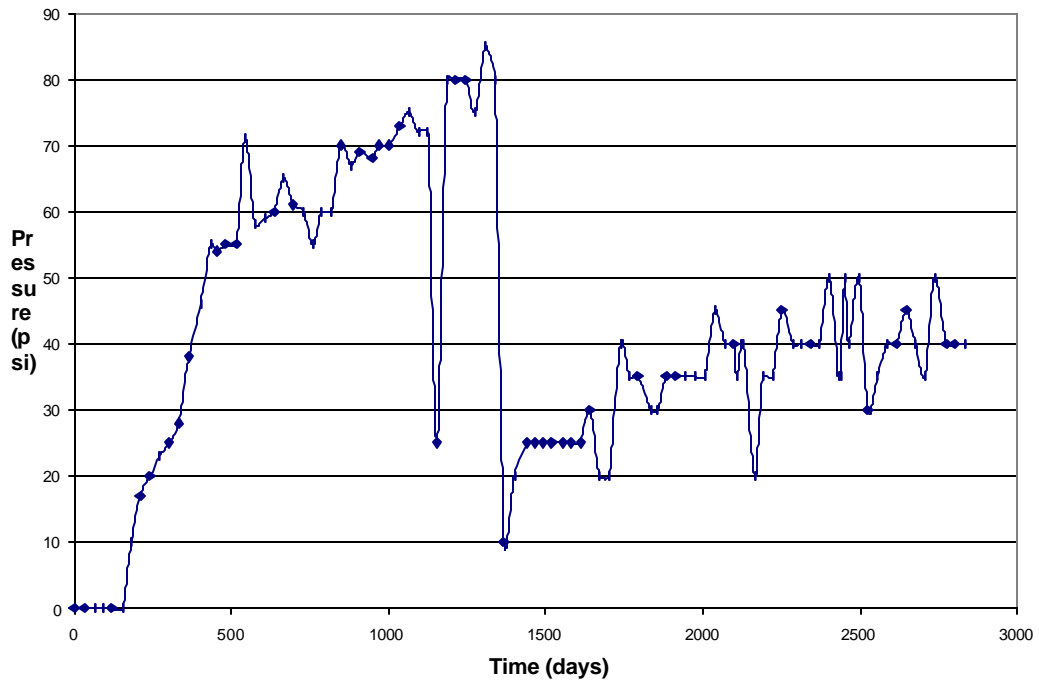
Fig.A-1-2   20" x 13 3/8" Annulus of Well MUA1 - Platform MU-A111
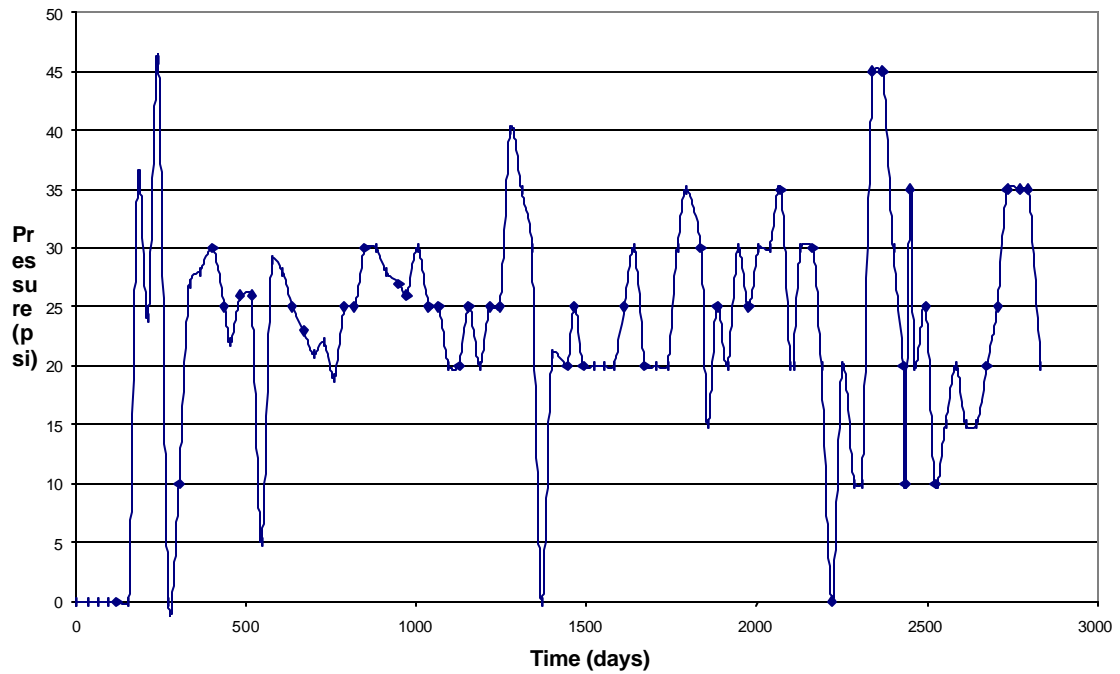
Table A2 Pressure Record of Well A-2 in Platform MU-A111

Date	Status	Time days	Prod Csg 7"	Interm Csg 9 5/8"	Surf Csg 13 3/8"	Cond Csg 20"	SITP	FTP
1/3/89	SI	0	0	0	5	10	3752	
2/5/89	FLOW	33	0	0	0	0	3752	3160
3/8/89	FLOW	64	0	0	0	0	3752	3500
4/7/89	SI	94	5	0	0	5	4950	
5/3/89	SI	120	5	0	0	5	4950	
6/6/89	SI	154	0	0	5	5	4950	
7/3/89	SI	181	0	0	0	0	4950	
8/2/89	SI	211	0	0	0	4	4956	
9/1/89	FLOW	241	0	0	0	0	5092	3942
10/1/89	FLOW	271	7	0	363	10	6012	?
11/1/89	FLOW	302	8	0	402	15	3610	3417
12/1/89	FLOW	332	10	0	357	0	3610	3209
1/2/90	FLOW	364	9	3	80	5	3610	3102
2/9/90	FLOW	402	13	7	329	8	3610	3012
3/14/90	FLOW	435	0	0	275	0	3610	3110
4/1/90	FLOW	453	3	0	228	4	3610	3105
5/1/90	FLOW	483	2	0	173	4	3610	3080
6/2/90	FLOW	515	2	0	332	10	3610	2913
7/1/90	FLOW	544	5	2	311	3	?	?
8/1/90	FLOW	575	5	8	347	17	?	?
9/1/90	FLOW	606	7	4	255	16	3029	2617
10/1/90	FLOW	636	6	3	352	11	3029	?
11/1/90	FLOW	667	9	4	333	13	3029	?
12/1/90	FLOW	697	7	4	155	12	3029	2455
1/1/91	FLOW	728	10	5	385	20	3029	2340
2/1/91	FLOW	759	6	3	285	21	3029	2245
3/1/91	FLOW	787	10	10	280	30	3020	2105
4/1/91	FLOW	818	15	20	60	20	2535	1965
5/1/91	FLOW	848	0	0	390	20		2055
6/3/91	FLOW	881	8	2	185	40		1973
7/1/91	FLOW	909	11	5	415	32		2000
8/9/91	SI;77	948	0	0	20	20		
9/1/91	SI;77	971	2	0	25	42		
10/3/91	SI;77	1003	0	0	30	25		
11/5/91	SI;77	1036	4	0	38	40		
12/4/91	SI;77	1065	5	4	50	45		
1/2/92	SI;77	1094	0	0	48	39		
2/2/92	SI;CODE 43	1125	0	0	59	45		
3/2/92	SI;CODE 43	1154	0	0	60	50		
4/2/92	SI;CODE 43	1185	10	0	70	40		
5/1/92	SI;CODE 43	1214	10	0	70	40		
6/1/92	SI;CODE 43	1245	8	0	70	10		
7/1/92	SI;CODE 43	1275	12	0	70	45		
8/3/92	SI;CODE 43	1308	10	0	65	55		
9/2/92	SI;CODE 43	1338	0	0	60	75		
10/1/92	SI;CODE 43	1367	0	0	0	30		
11/2/92	SI;CODE 43	1399	15	0	21	54		
12/15/92	SI;CODE 43	1442	20	0	30	50		
1/6/93	SI;CODE 43	1464	10	0	40	55		
2/1/93	SI;CODE 43	1490	10	0	40	50		
3/3/93	SI;CODE 43	1520	10	0	40	50		
4/4/93	SI;CODE 43	1552	20	0	20	25		
5/1/93	SI;CODE 43	1579	15	0	25	40		
6/1/93	SI;CODE 43	1610	20	0	30	40		
7/1/93	SI;CODE 43	1640	40	0	40	30		
8/1/93	SI;CODE 43	1671	20	0	30	40		
9/1/93	SI;CODE 43	1702	25	0	30	40		
10/6/93	SI;CODE 43	1737	20	0	30	40		
11/4/93	SI;CODE 43	1766	20	0	40	50		
12/1/93	SI;CODE 43	1793	20	0	50	10		
1/12/94	SI	1835	20	0	50	60		
2/1/94	SI	1855	20	0	45	65		
3/1/94	SI	1883	20	0	50	60		
4/1/94	SI	1914	20	0	50	80		
5/1/94	SI	1944	0	180	420	70		
6/2/94	SI	1976	20	0	60	90		
7/1/94	SI	2005	20	0	55	85		
8/2/94	SI	2037	25	0	55	100		
9/4/94	SI	2070	20	0	50	110		
10/2/94	SI	2098	20	0	50	110		

Fig.A-2-1   7" x 2 7/8" Annulus of Well A-2 - Platform MU-A111
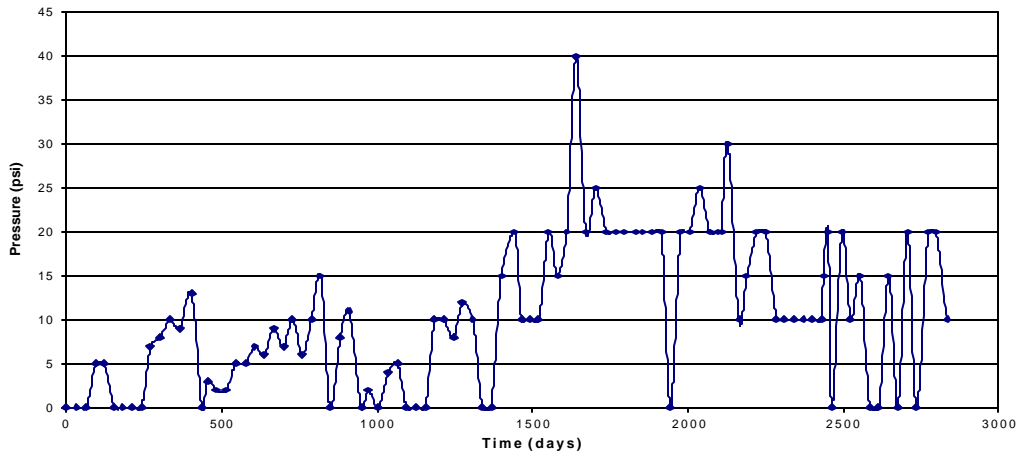
Fig.A-2-2   13 3/8" x 9 5/8" Annulus of Well A-2 - Platform MU-A111

Fig.A-2-3   20" x 13 3/8" Annulus of Well A-2 - Platform MU-A111

51
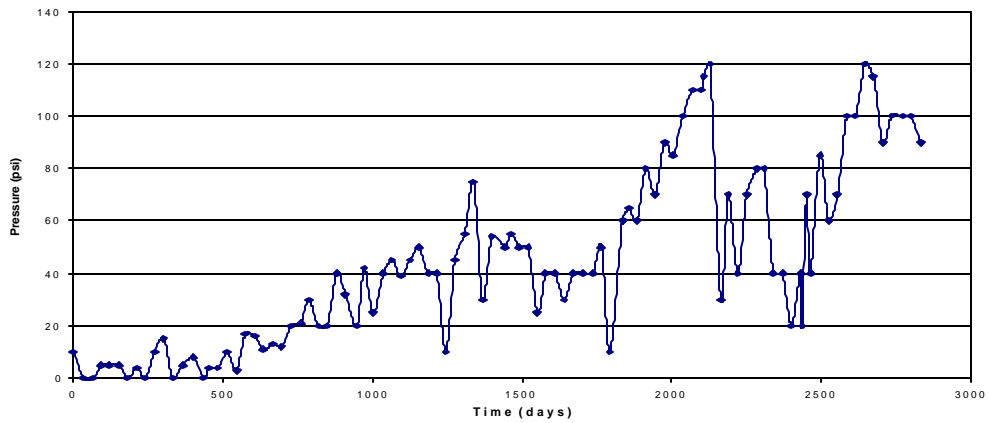
Table A3 Pressure Record of Well A-3 - Platform MU-A111

Date	Status	Time	Prod Csg	Interm Csg	Surf Csg	SITP	FTP
		days	7"	9 5/8"	13 3/8"		
1/3/89	SI	0	0	245	0	2216	
2/5/89	FLOW	33	0	179	0	2219	1557
3/8/89	FLOW	64	0	40	0	2216	2000
4/7/89	FLOW	94	0	45	0	2200	1650
5/3/89	FLOW	120	0	95	0	2200	1650
6/6/89	SI	154	0	120	5	2200	
7/3/89	SI	181	208	156	0	2200	
8/2/89	SI	211	25	90	0	2154	
9/1/89	FLOW	241	354	93	0	2010	1430
10/1/89	FLOW	271	1134	157	0	?	?
11/1/89	FLOW	302	1120	160	0	1907	1330
12/1/89	FLOW	332	1028	145	0	1917	1356
1/2/90	FLOW	364	632	136	0	1917	1246
2/9/90	FLOW	402	397	170	0	1805	1754
3/14/90	FLOW	435	235	65	0	1940	1725
4/1/90	FLOW	453	693	176	0	1940	1455
5/1/90	FLOW	483	725	200	0	1940	1395
6/2/90	SI Rate ADT	515	509	170	0	1940	
7/1/90	FLOW	544	873	206	8	?	?
8/1/90	FLOW	575	638	255	12	?	?
9/1/90	FLOW	606	805	275	7	1728	1366
10/1/90	FLOW	636	667	305	5	?	?
11/1/90	FLOW	667	519	298	5	1728	966
12/1/90	FLOW	697	557	292	5	1728	1100
1/1/91	FLOW	728	680	290	0	1728	1160
2/1/91	FLOW	759	620	282	0	1728	1270
3/1/91	FLOW	787	880	100	0	?	?
4/1/91	FLOW	818	370	320	0	1625	1210
5/1/91	FLOW	848	610	495	0		1135
6/3/91	FLOW	881	619	568	4		1227
7/1/91	FLOW	909	608	648	4		1125
8/9/91	FLOW	948	667	738	10		1180
9/1/91	FLOW	971	636	780	10		1140
10/3/91	FLOW	1003	450	775	10		1175
11/5/91	FLOW	1036	710		0		1135
12/4/91	FLOW	1065	721	1065	15		1180
1/2/92	FLOW	1094	678	1128	8		1100
2/2/92	FLOW	1125	620	1170	10		1080
3/2/92	FLOW	1154	190	1210	10		1040
4/2/92	FLOW	1185	270	1250	0		1050
5/1/92	FLOW	1214	5	120	0		1040
6/1/92	FLOW	1245	62	433	0		1080
7/1/92	FLOW	1275	105	635	0		1050
8/3/92	FLOW	1308	80	590	0		1060
9/2/92	SI;CODE 77	1338	105	310	30		
10/1/92	SI;CODE 77	1367	40	240	0		
11/2/92	FLOW	1399	116	680	6		1150
12/15/92	SI;CODE 77	1442	200	655	0		
1/6/93	FLOW	1464	290	845	0		1260
2/1/93	SI;CODE 43	1490	350	920	0		1260
3/3/93	FLOW	1520	120	1190	10		
4/4/93	SI;CODE 82	1552	110	360	0		
5/1/93	FLOW	1579	270	170	0		1110
6/1/93	SI	1610	280	310	0		
7/1/93	FLOW	1640	400	400	40		1140
8/1/93	FLOW	1671	440	500	40		1100
9/1/93	FLOW	1702	420	700	30		1100
10/6/93	FLOW	1737	48	440	40		1140
11/4/93	FLOW	1766	570	820	30		
12/1/93	FLOW	1793	560	900	30		1100
1/12/94	FLOW	1835	680	10	0		1140
2/1/94	FLOW	1855	760	10	0		
3/1/94	FLOW	1883	720	40	20		1100
4/1/94	SI	1914	620	160	20		
5/1/94	SI	1944	440	240	10		
6/2/94	FLOW	1976	555	220	15		
7/1/94	FLOW	2005	795	320	0		1100
8/2/94	SI	2037	40	25	0		
9/4/94	SI	2070	420	330	0		
10/2/94	SI	2098	660	450	0		

Fig.A-3-1   7" x 2 7/8" Annulus of Well A-3 - Platform MU-A111

Fig.A-3-2   9 5/8" x 7" Annulus of Well A-3 - Platform MU-A111

Fig.A-3-3   13 3/8" x 9 5/8" Annulus of Well A-3 - Platform MU-A111
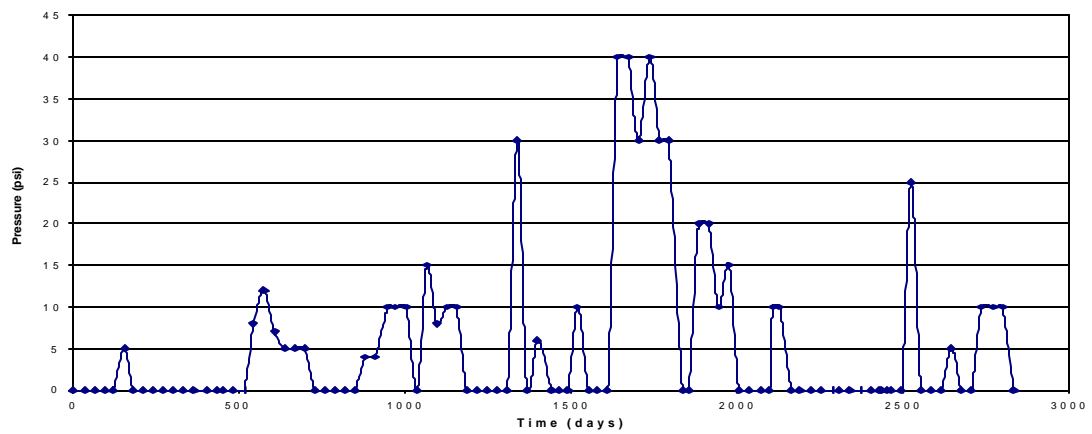
Table A4 Pressure Record of Well A-4 - Platform MU-A111

Date	Status	Time	Prod Csg	Interm Csg	Surf Csg	SITP	FTP
		days	7"	9 5/8"	13 3/8"		
1/3/89	work on rig	0					
2/5/89	FLOW	33	0	0	0	2996	8248
3/8/89	FLOW	64	0	0	0	8858	2690
4/7/89	FLOW	94	20	0	0	2200	1650
5/3/89	FLOW	120	20	0	0	9100	3600
6/6/89	FLOW	154	540	0	0	9100	2400
7/3/89	SI	181	90	610	0	9100	
8/2/89	SI	211	570	550	0	7882	
9/1/89	FLOW	241	1355	921	0	?	?
10/1/89	FLOW	271	1448	1004	0	7637	1464
11/1/89	FLOW	302	1369	548	0	7001	1861
12/1/89	FLOW	332	1391	532	0	7001	1451
1/2/90	FLOW	364	1360	847	0	7001	1391
2/9/90	FLOW	402	758	157	0	7854	1130
3/14/90	Loaded up	435	1110	240	5	6300	
4/1/90	Loaded up	453	1229	195	8	6600	
5/1/90	Loaded up	483	1415	163	8	6660	
6/2/90	Loaded up	515	910	106	7	6640	
7/1/90	Loaded up	544	1214	282	9	6656	
8/1/90	Loaded up	575	1361	187	8	6731	
9/1/90	Loaded up	606	1487	155	6	4660	
10/1/90	Loaded up	636	1558	114	5	4540	
11/1/90	Loaded up	667	1627	74	6	4550	
12/1/90	Loaded up	697	1692	54	4	3280	
1/1/91	Loaded up	728	1700	38	0	3280	
2/1/91	Loaded up	759	1725	15	0	3780	
3/1/91	Loaded up	787	1740	25	0	3780	
4/1/91	Loaded up	818	1770	25	0	3780	
5/1/91	41-SI	848	1785	0	0		
6/3/91	41-SI	881	1800	10	0		
7/1/91	41-SI	909	1776	26	2		
8/9/91	41-SI	948	1719	60	30		
9/1/91	41-SI	971	1720	45	20		
10/3/91	41-SI	1003	1745	55	20		
11/5/91	41-SI	1036	1710	30	14		
12/4/91	41-SI	1065	1745	35	10		
1/2/92	41-SI	1094	1710	10	8		
2/2/92	41-SI	1125	1730	0	0		
3/2/92	41-SI	1154	1735	25	0		
4/2/92	41-SI	1185	1740	230	0		
5/1/92	41-SI	1214	1740	310	15		
6/1/92	41-SI	1245	1715	280	10		
7/1/92	41-SI	1275	1775	115	40		
8/3/92	41-SI	1308	1800	370	50		
9/2/92	41-SI	1338	860	320	80		
10/1/92	41-SI	1367	200	30	0		
11/2/92	41-SI	1399	720	92	0		
12/15/92	41-SI	1442	470	120	15		
1/6/93	41-SI	1464	780	170	0		
2/1/93	41-SI	1490	1000	200	10		
3/3/93	41-SI	1520	390	70	20		
4/4/93	41-SI	1552	870	110	20		
5/1/93	41-SI	1579	1110	210	20		
6/1/93	41-SI	1610	1260	230	20		
7/1/93	43-SI	1640	1130	40	20		
8/1/93	43-SI	1671	590	40	26		
9/1/93	SI	1702	700	220	40		
10/6/93	SI	1737	220	240	30		
11/4/93	SI	1766	760	280	0		
12/1/93	SI	1793	890	320	30		
1/12/94	SI	1835	1050	310	20		
2/1/94	FLOW	1855	0	30	0		
3/1/94	FLOW	1883	730	320	20		
4/1/94	SI	1914	1010	390	25		
5/1/94	SI	1944	430	320	20		
6/2/94	FLOW	1976	865	310	30		
7/1/94	FLOW	2005	990	150	20		
8/2/94	SI	2037	1000	280	25		
9/4/94	SI	2070	830	140	0		
10/2/94	SI	2098	1180	280	0		

Fig.A-4-1   7" x 2 7/8" Annulus of Well A-4 - Platform MU-A111

Fig.A-4-2   7" x 2 7/8" Annulus of Well A-4 - Platform MU-A111

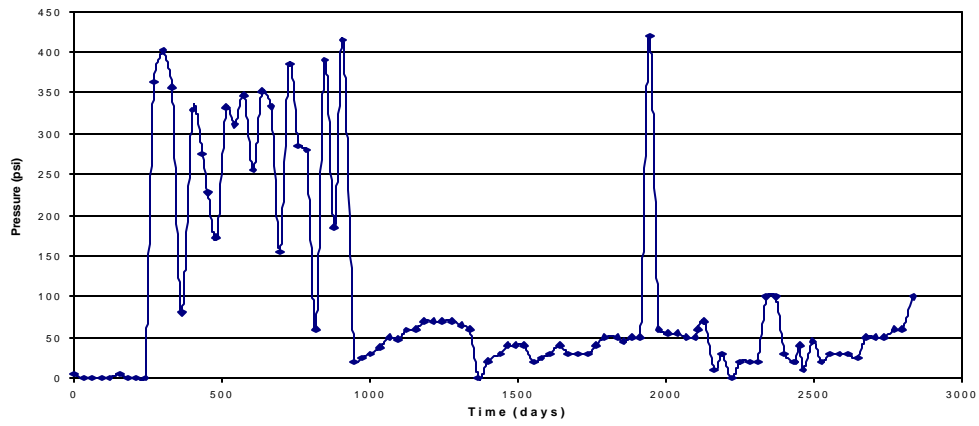**Fig.A-4-3   13 3/8" x 9 5/8" Annulus of Well A-4 - Platform MU-A111**

55
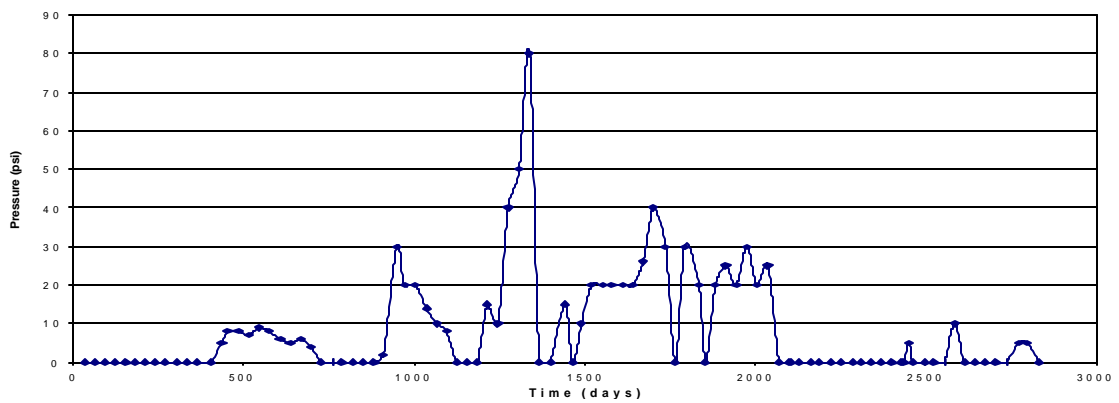
Table A5 Pressure Record of Well A-5 - Platform MU-A111

Date	Status	Time	Prod Csg	Interm Csg	Surf Csg	SITP	FTP
		days	7"	9 5/8"	13 3/8"		
1/3/89	SI	0	0	0	0	5152	
2/5/89	FLOW	33	0	0	0	4772	5152
3/8/89	FLOW	64	0	0	0	4370	5152
4/7/89	FLOW	94		0	0	6200	4190
5/3/89	FLOW	120		0	0	6200	4000
6/6/89	SI	154	0	0	0	6200	
7/3/89	SI	181	0	0	0	6200	
8/2/89	SI	211	0	0	0	6200	
9/1/89	FLOW	241	0	0	0	6202	4755
10/1/89	FLOW	271	100	0	0	6202	4729
11/1/89	FLOW	302	0	15	0	4895	4389
12/1/89	FLOW	332	15	29	0	4985	4431
1/2/90	FLOW	364	0	26	0	4985	4371
2/9/90	FLOW	402	15	27	0	4665	4198
3/14/90	FLOW	435	0	30	0	4665	4360
4/1/90	FLOW	453	5	41	3	4665	4345
5/1/90	FLOW	483	4	46	4	4760	4250
6/2/90	FLOW	515	VAC	44	0	4760	4222
7/1/90	FLOW	544	VAC	46	0	?	?
8/1/90	FLOW	575	35	55	2	4913	4142
9/1/90	FLOW	606	10	58	0	4583	4065
10/1/90	FLOW	636	VAC	56	0	4583	4115
11/1/90	FLOW	667	VAC	62	1		
12/1/90	FLOW	697	VAC	63	VAC	4583	4060
1/1/91	FLOW	728	VAC	62	VAC	4510	4060
2/1/91	FLOW	759	0	65	0	4510	4025
3/1/91	FLOW	787	10	80	0		
4/1/91	FLOW	818	0	75	0	4460	3330
5/1/91	FLOW	848	5	70	0		4000
6/3/91	FLOW	881	19	66	0		3980
7/1/91	FLOW	909	8	74	7		3940
8/9/91	FLOW	948	8	78	0		3947
9/1/91	FLOW	971	2	78	0		3920
10/3/91	FLOW	1003	0	75	VAC		3850
11/5/91	FLOW	1036	4	85	VAC		3560
12/4/91	FLOW	1065	0	85	0		3390
1/2/92	FLOW	1094	19	89	0		3125
2/2/92	FLOW	1125	20	99	0		2845
3/2/92	FLOW	1154	0	90	0		2700
4/2/92	FLOW	1185	0	100	0		2340
5/1/92	FLOW	1214	0	100	5		1940
6/1/92	FLOW	1245	5	110	10		1920
7/1/92	FLOW	1275	12	105	0		1820
8/3/92	FLOW	1308	570	115	20		1820
9/2/92	FLOW	1338	0	70	0		1540
10/1/92	FLOW	1367	240	100	10		1420
11/2/92	FLOW	1399	20	78	0		1300
12/15/92	43-SI	1442	0	60	0		
1/6/93	43-SI	1464	0	60	0		
2/1/93	43-SI	1490	VAC	65	0		
3/3/93	43-SI	1520	0	65	0		
4/4/93	43-SI	1552	0	70	0		
5/1/93	80-SI	1579	0	0	0		
6/1/93	80-SI	1610	180	60	0		
7/1/93	80-SI	1640	180	80	30		
8/1/93	80-SI	1671	100	80	0		
9/1/93	80-SI	1702	80	50	0		
10/6/93	43-SI	1737	0	70	0		
11/4/93	SI	1766	0	60	0		
12/1/93	SI	1793	0	60	0		
1/12/94	SI	1835	0	60	0		
2/1/94	SI	1855	0	55	0		
3/1/94	SI	1883	0	65	0		
4/1/94	SI	1914	15	65	0		
5/1/94	SI	1944	30	60	0		
6/2/94	SI	1976	325	15	0		
7/1/94	FLOW	2005	185	40	0		4240
8/2/94	FLOW	2037	0	40	0		
9/4/94	SI	2070	50	40	0		
10/2/94	SI	2098	0	30	0		

Fig.A-5-1   7" x 2 7/8" Annulus of Well A-5 - Platform MU-A111
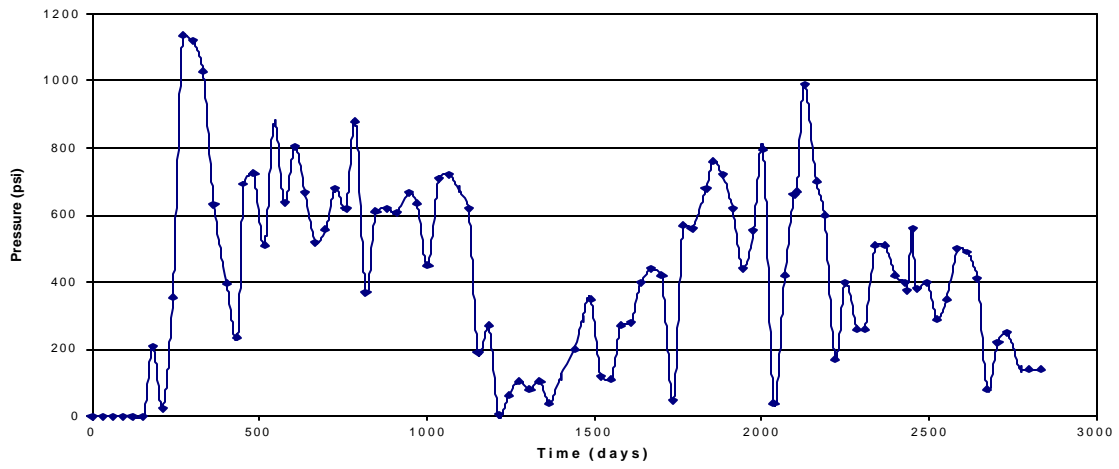

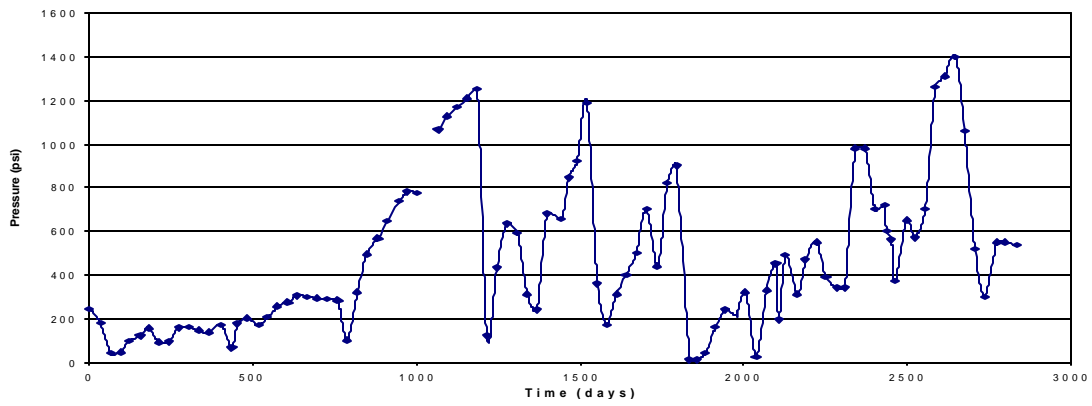**Fig.A-5-2   9 5/8" x 7" Annulus of Well A-5 - Platform MU-A111**

**Fig.A-5-3   13 3/8" x 9 5/8" Annulus of Well A-5 - Platform MU-A111**
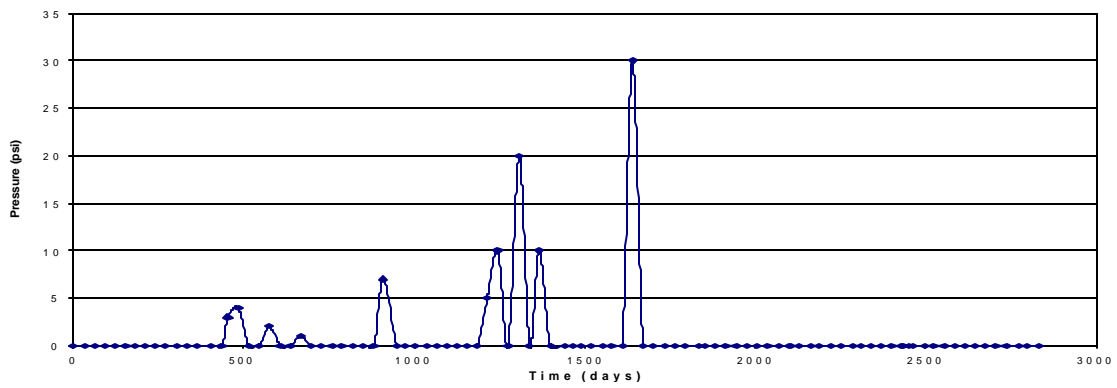
Table A6 Pressure Record of Well A-8 - Platform MU-A111

Date	Status	Time	Prod Csg	Interm Csg	Surf Csg	SITP	FTP
		days	7"	9 5/8"	13 3/8"		
1/3/89	SI	0	510	345	0	2355	1713
2/5/89	FLOW	33	570	45	0	2355	1493
3/8/89	FLOW	64	630	225	0	2174	1440
4/7/89	FLOW	94	525	155	0	2100	1700
5/3/89	FLOW	120	520	155	0	2100	1700
6/6/89	FLOW	154	205	270	0	2100	1520
7/3/89	FLOW	181	265	243	0	2100	1703
8/2/89	SI	211	45	180	VAC	2102	
9/1/89	FLOW	241	147	268	0	2119	1739
10/1/89	FLOW	271	191	251	0	2119	1731
11/1/89	SI; SAND	302	245	95	0	2119	
12/1/89	SI; SAND	332	430	97	0	2119	
1/2/90	SI; SAND	364	362	118	2	2119	
2/9/90	SI; SAND	402	295	115	5	2119	
3/14/90	SI; SAND	435	495	140	0	2119	
4/1/90	SI; SAND	453	538	139	2	2119	
5/1/90	SI; SAND	483	608	152	0	2119	
6/2/90	SI; SAND	515	669	171	0	2119	
7/1/90	SI; SAND	544	713	190	3	2119	
8/1/90	SI; SAND	575	744	248	2	2078	
9/1/90	SI; SAND	606	791	231	3	2116	
10/1/90	SI; SAND	636	811	245	0	2116	
11/1/90	SI; SAND	667	840	240	11	2090	
12/1/90	SI; SAND	697	849	283	0	2024	
1/1/91	SI; SAND	728	230	280	0	2024	
2/1/91	SI; SAND	759		293	0	2024	
3/1/91	SI; SAND	787	158	304	0	2021	
4/1/91	SI; SAND	818	575	320	10	2024	
5/1/91	SI; SAND	848	650	325	0		
6/3/91	41-SI	881	728	350	5		
7/1/91	41-SI	909	780	358	6		
8/9/91	41-SI	948	810	369	65		
9/1/91	41-SI	971	845	387	63		
10/3/91	41-SI	1003	880	380	57		
11/5/91	41-SI	1036	925	340	50		
12/4/91	41-SI	1065	985	360	52		
1/2/92	41-SI	1094	1024	375	55		
2/2/92	41-SI	1125	1062	440	55		
3/2/92	41-SI	1154	1080	350	75		
4/2/92	41-SI	1185	1100	395	80		
5/1/92	41-SI	1214	960	355	10		
6/1/92	41-SI	1245	1005	390	15		
7/1/92	41-SI	1275	1075	440	20		
8/3/92	41-SI	1308	1110	450	20		
9/2/92	41-SI	1338	410	390	20		
10/1/92	41-SI	1367	120	170	0		
11/2/92	41-SI	1399	440	232	0		
12/15/92	41-SI	1442	230	260	0		
1/6/93	41-SI	1464	500	300	0		
2/1/93	41-SI	1490	645	340	0		
3/3/93	41-SI	1520	400	250	0		
4/4/93	41-SI	1552	320	275	20		
5/1/93	41-SI	1579	570	290	10		
6/1/93	41-SI	1610	750	340	10		
7/1/93	41-SI	1640	900	410	20		
8/1/93	41-SI	1671	710	310	30		
9/1/93	41-SI	1702	950	450	60		
10/6/93	41-SI	1737	500	280	30		
11/4/93	SI	1766	680	530	30		
12/1/93	SI	1793	760	440	40		
1/12/94	SI	1835	870	430	30		
2/1/94	SI	1855	530	450	35		
3/1/94	SI	1883	740	520	40		
4/1/94	SI	1914	880	530	30		
5/1/94	SI	1944	750	380	20		
6/2/94	SI	1976	910	450	40		
7/1/94	SI	2005	900	470	40		
8/2/94	SI	2037	255	315	40		
9/4/94	SI	2070	670	420	40		
10/2/94	SI	2098	20	450	40		

Fig.A-6-1   7" x 2 7/8" Annulus of Well A-8 - Platform MU-A111
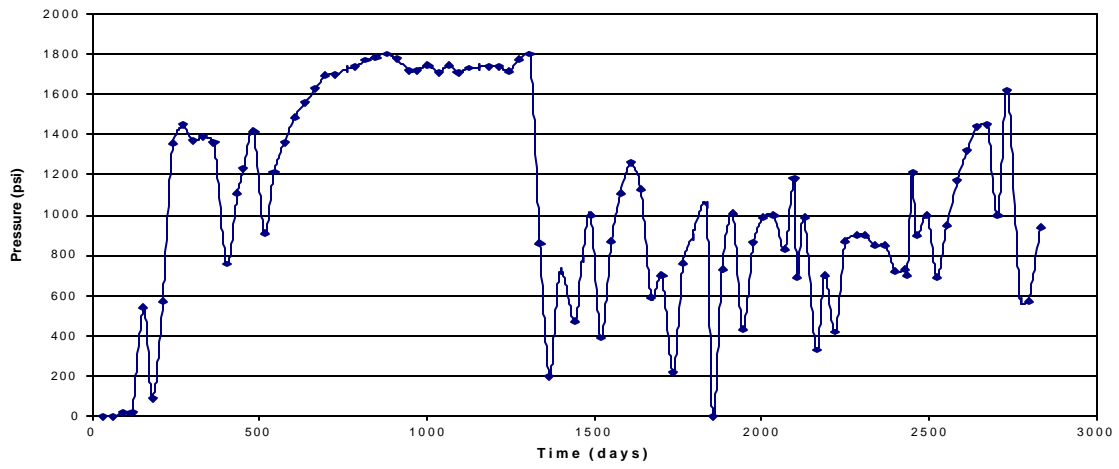

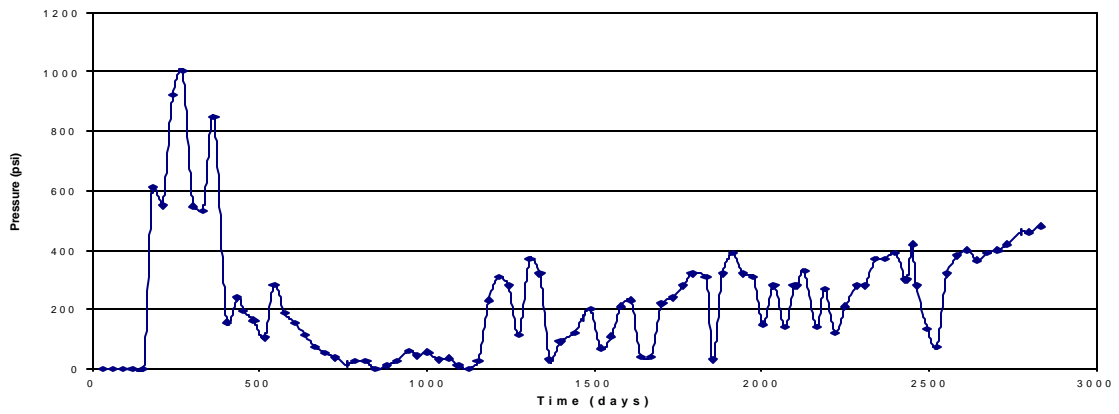**Fig.A-6-2   9 5/8" x 7" Annulus of Well A-8 - Platform MU-A111**

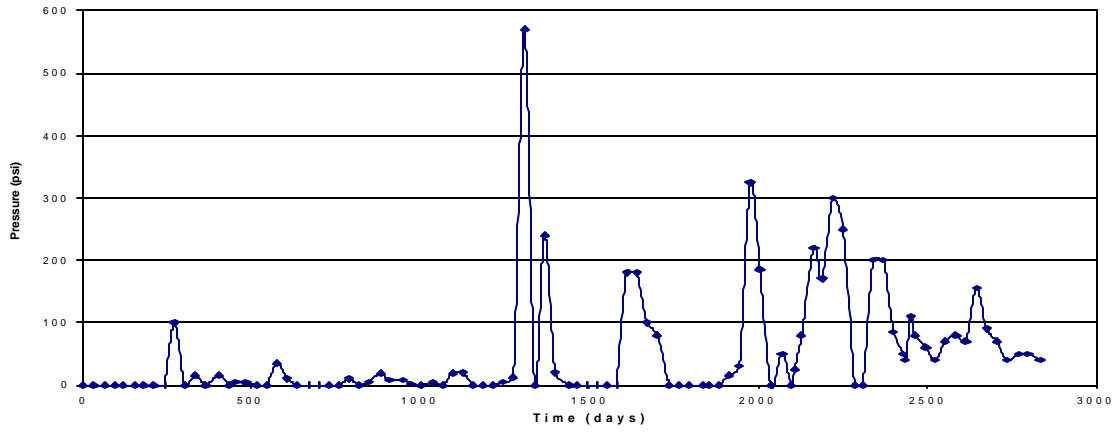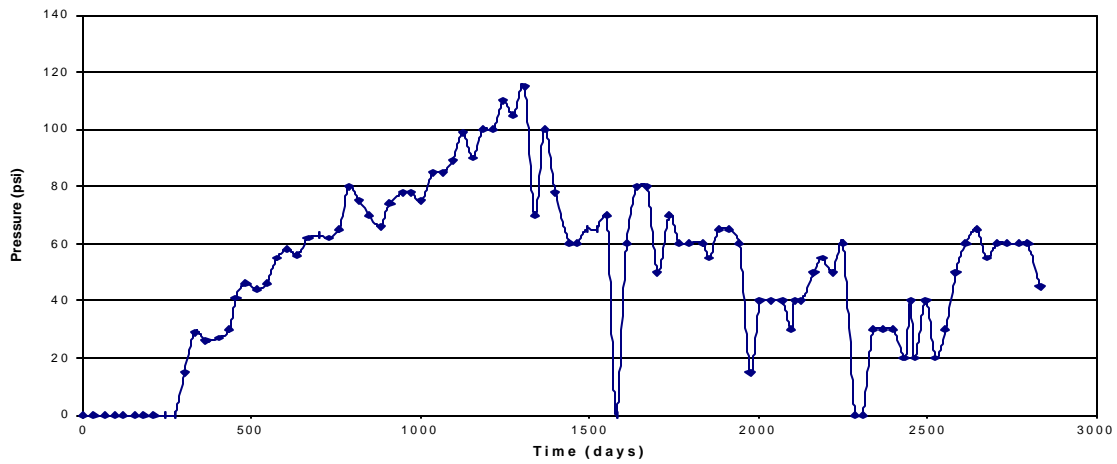**Fig.A-6-3   13 3/8" x 9 5/8" Annulus of Well A-8 - Platform MU-A111**

59
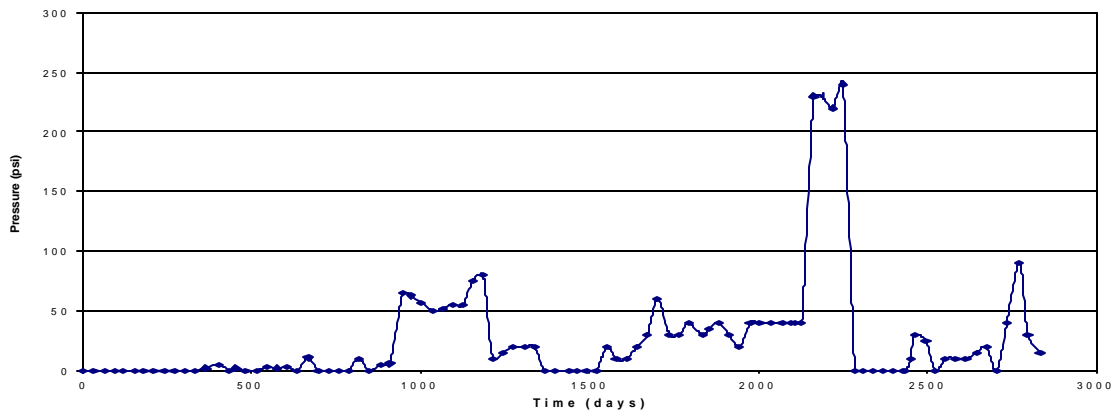
Table A7 Pressure Record of Well A-9 - Platform MU-A111

Date	Status	Time	Prod Csg	Interm Csg	Surf Csg	Cond Csg	SITP	FTP
		days	7"	9 5/8"	13 3/8"	20"		
1/3/89	SI	0	20	0	0	0	4856	4377
2/5/89	FLOW	33	0	0	0	0	4856	4197
3/8/89	FLOW	64	580	0	0	0	4749	4100
4/7/89	FLOW	94	0	0	0	0	4700	4350
5/3/89	FLOW	120	0	0	0	0	4700	4350
6/6/89	FLOW	154	0	0	0	80	4700	4420
7/3/89	FLOW	181	575	0	0	136	4700	4501
8/2/89	SI	211	15	0	VAC	75	4702	
9/1/89	FLOW	241	1518	0	5	163	4688	4106
10/1/89	FLOW	271	1743	25	45	161	4688	2974
11/1/89	FLOW	302	1542	17	22	160	4456	3721
12/1/89	FLOW	332	1591	25	38	162	4456	3750
1/2/90	FLOW	364	1887	38	46	165	4456	3109
2/9/90	FLOW	402	9	10	0	58	4345	4412
3/14/90	FLOW	435	VAC	0	0	200	4560	4330
4/1/90	SI; Low Rate	453	VAC	2	VAC	211	4560	
5/1/90	SI; Low Rate	483	VAC	3	VAC	220	4460	
6/2/90	SI; Low Rate	515	VAC	8	2	245	4480	
7/1/90	SI	544	1220	13	6	261	4376	?
8/1/90	SI	575	VAC	14	VAC	222	4376	
9/1/90	FLOW	606	1862	14	37	261	4407	3721
10/1/90	FLOW	636	1866	20	39	259	4407	3617
11/1/90	FLOW	667	1832	20	51	261	4407	?
12/1/90	FLOW	697	1745	13	47	4	4407	3430
1/1/91	FLOW	728	932	18	10	190	4330	3850
2/1/91	FLOW	759	1710	20	25	200	4330	3330
3/1/91	FLOW	787	646	5	0	200	4198	
4/1/91	FLOW	818	580	10	20	250	4100	3400
5/1/91	FLOW	848	1760	10	0	240		3290
6/3/91	FLOW	881	863	20	20	220		3276
7/1/91	FLOW	909	344	25	40	234		3820
8/9/91	FLOW	948	1580	200	90	265		3300
9/1/91	FLOW	971	1555	18	55	265		3250
10/3/91	FLOW	1003	1390	0	70	265		3060
11/5/91	FLOW	1036	1550	2	70	240		2920
12/4/91	FLOW	1065	1410	20	79	250		3280
1/2/92	FLOW	1094	1440	21	80	255		2860
2/2/92	FLOW	1125	1355	16	65	248		2695
3/2/92	FLOW	1154	1115	25	80	245		2540
4/2/92	FLOW	1185	790	30	75	240		2985
5/1/92	FLOW	1214	760	45	75	50		2480
6/1/92	FLOW	1245	167	32	59	95		3010
7/1/92	FLOW	1275	525	60	75	115		2200
8/3/92	FLOW	1308	470	50	85	110		2120
9/2/92	FLOW	1338	190	310	30	40		2360
10/1/92	FLOW	1367	0	10	0	0		1865
11/2/92	FLOW	1399	80	15	10	4		1710
12/15/92	FLOW	1442	180	40	10	40		
1/6/93	FLOW	1464	145	40	15	35		1600
2/1/93	FLOW	1490	140	25	15	50		1550
3/3/93	FLOW	1520	10	20	10	90		
4/4/93	82-SI	1552	0	10	0	190		
5/1/93	FLOW	1579	240	50	20	250		1520
6/1/93	SI	1610	0	20	10	50		
7/1/93	FLOW	1640	60	30	30	150		1560
8/1/93	FLOW	1671	90	20	0	70		1520
9/1/93	FLOW	1702	250	40	30	100		1500
10/6/93	FLOW	1737	140	40	20	120		1500
11/4/93	FLOW	1766	VAC	10	20	120		
12/1/93	FLOW	1793	200	40	30	180		1850
1/12/94	FLOW	1835	160	60	25	190		1750
2/1/94	FLOW	1855	420	30	0	200		
3/1/94	FLOW	1883	265	60	15	255		1600
4/1/94	SI	1914	0	25	15	270		
5/1/94	FLOW	1944	50	60	280	275		1500
6/2/94	FLOW	1976	50	50	40	325		
7/1/94	FLOW	2005	170	50	45	300		1910
8/2/94	FLOW	2037	290	40	70	330		
9/4/94	SI	2070	0	40	65	340		
10/2/94	FLOW	2098	0	40	100	350		1920

Fig.A-7-1   7" x 2 7/8" Annulus of Well A-9 - Platform MU-A111

Fig.A-7-2   9 5/8" x 7" Annulus of Well A-9- Platform MU-A111

**Fig.A-7-3   13 3/8" x 9 5/8" Annulus of Well A-9- Platform MU-A111**

Fig.A-7-4   20" x 13 3/8" Annulus of Well A-9 - Platform MU-A111

Table A8 Pressure Record of Well A-10 - Platform MU-A111

Date	Status	Time	Prod Csg	Interm Csg	Surf Csg	SITP	FTP
		days	7"	9 5/8"	13 3/8"		
1/3/89	SI	0	3484	3990	145	755	
2/5/89	FLOW	33	500	3590	261	2374	2167
3/8/89	FLOW	64	1800	2800	75	2374	2000
4/7/89	FLOW	94	2450	3125	38	2250	2090
5/3/89	FLOW	120	2450	3175	88	2250	2090
6/6/89	FLOW	154	2600	3300	105	2750	1730
7/3/89	FLOW	181	1460	3390	156	2750	2110
8/2/89	SI	211	650	3170	110	2299	
9/1/89	FLOW	241	870	2511	210	2171	1706
10/1/89	FLOW	271	1810	3020	317	2278	1846
11/1/89	FLOW	302	125	2865	316	2143	1786
12/1/89	FLOW	332	330	3422	362	2143	1653
1/2/90	FLOW	364	800	2366	332	2143	1338
2/9/90	SI	402	1411	2384	174	2108	
3/14/90	FLOW	435	1550	3505	145	1980	1550
4/1/90	SI; Low Rate	453	1500	3565	150	1980	
5/1/90	FLOW	483	2360	4060	303	1935	1700
6/2/90	SI; Low Rate	515	1670	3560	170	1935	
7/1/90	SI	544	1657	3740	166	1935	
8/1/90	SI	575	1525	3720	179	1943	
9/1/90	SI	606	6	28	174	1913	
10/1/90	SI	636	5	5	177	1913	
11/1/90	SI	667	0	16	191	1913	
12/1/90	FLOW	697	39	21	270	1859	1340
1/1/91	FLOW	728	28	23	190	1780	1340
2/1/91	FLOW	759	25	20	285	1780	1325
3/1/91	FLOW	787	15	18	262	1780	1735
4/1/91	FLOW	818	108	6	205	1680	1325
5/1/91	FLOW	848	32	125	0		1280
6/3/91	Flow/Vent in 9 5/8"	881	147	2.5	411		1245
7/1/91	77/43-SI	909	610	771	140		
8/9/91	77-SI	948	633	830	169		
9/1/91	FLOW	971	1110	700	395		1150
10/3/91	FLOW	1003	995	630	275		1240
11/5/91	FLOW	1036	1120	520	360		1130
12/4/91	FLOW	1065	1040	1000	370		1182
1/2/92	FLOW	1094	320	881	335		1135
2/2/92	FLOW	1125	655	1255	355		1120
3/2/92	77-SI	1154	700	1050	205		
4/2/92	77-SI	1185	770	945	190		
5/1/92	77-SI	1214	175	675	190		
6/1/92	77-SI	1245	640	1270	196		
7/1/92	77-SI	1275	820	1145	200		
8/3/92	77-SI	1308	670	800	390		
9/2/92	FLOW	1338	780	780	480		1300
10/1/92	FLOW	1367	370	520	80		1300
11/2/92	77-SI	1399	828	125	90		
12/15/92	FLOW	1442	560	320	150		
1/6/93	FLOW	1464	450	1000	180		1230
2/1/93	FLOW	1490	430	1000	250		1150
3/3/93	FLOW	1520	110	1000	220		
4/4/93	82-SI	1552	395	1000	65		
5/1/93	43-SI	1579	790	1000	100		
6/1/93	43-SI	1610	30	1020	20		
7/1/93	43-SI	1640	0	120	60		
8/1/93	43-SI	1671	100	1000	50		
9/1/93	43-SI	1702	170	970	90		
10/6/93	43-SI	1737	440	200	100		
11/4/93	SI	1766	0	0	120		
12/1/93	SI	1793	130	70	70		
1/12/94	SI	1835	60	50	190		
2/1/94	SI	1855	45	200	45		
3/1/94	SI	1883	285	10	90		
4/1/94	SI	1914	710	200	110		
5/1/94	SI	1944	200	200	60		
6/2/94	SI	1976	680	390	90		
7/1/94	SI	2005	810	1000	100		
8/2/94	SI	2037	50	1700	20		
9/4/94	SI	2070	660	990	100		
10/2/94	SI	2098	0	1000	100		

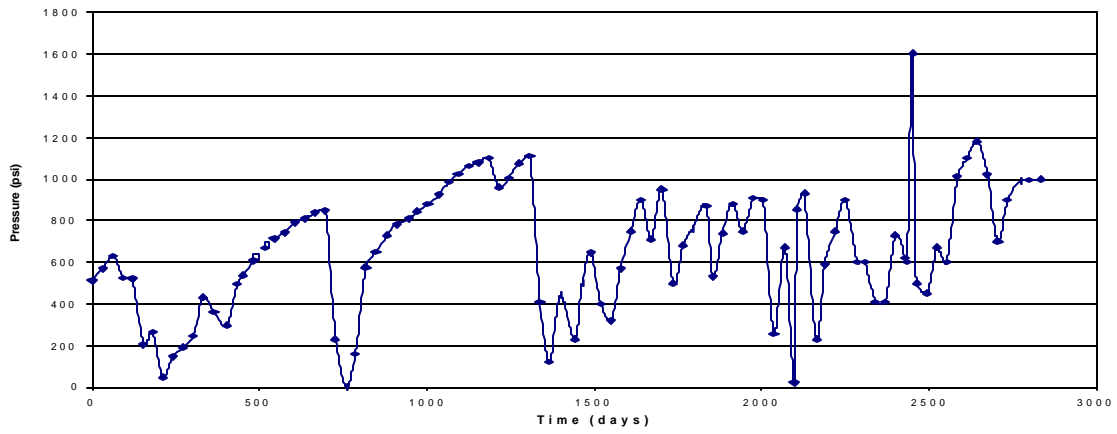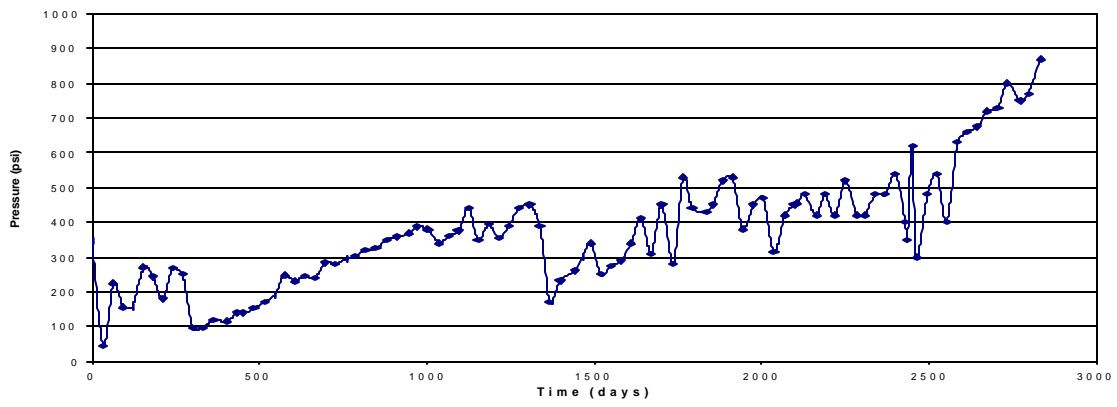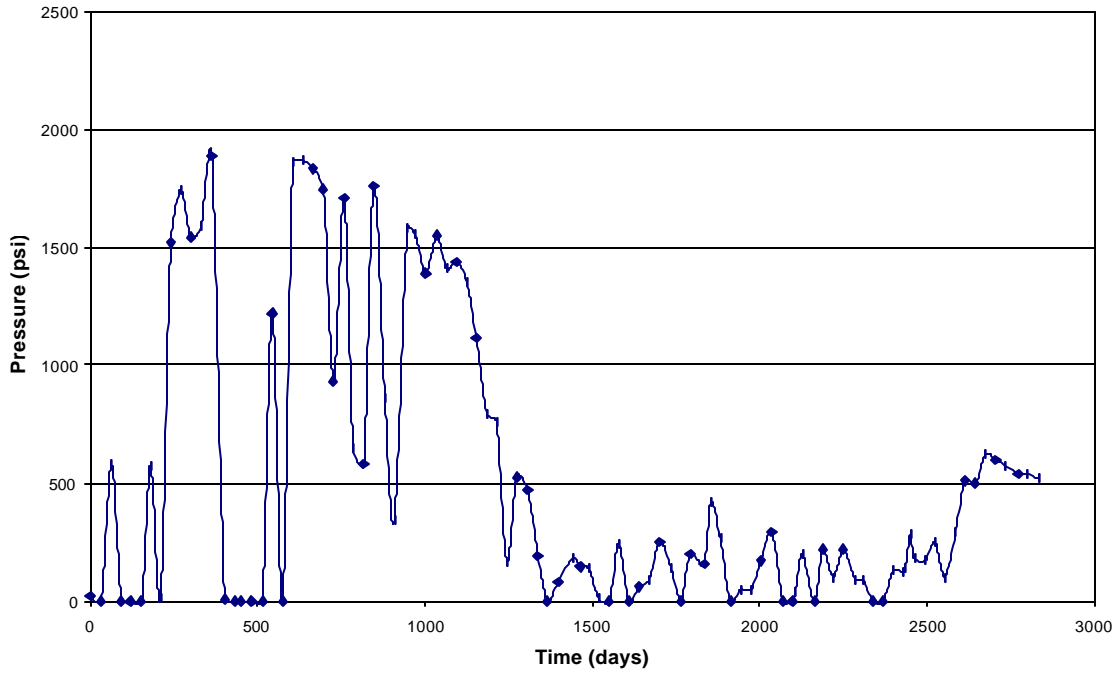Fig.A-8-1   7" x 2 7/8" Annulus of Well A-10 - Platform MU-A111

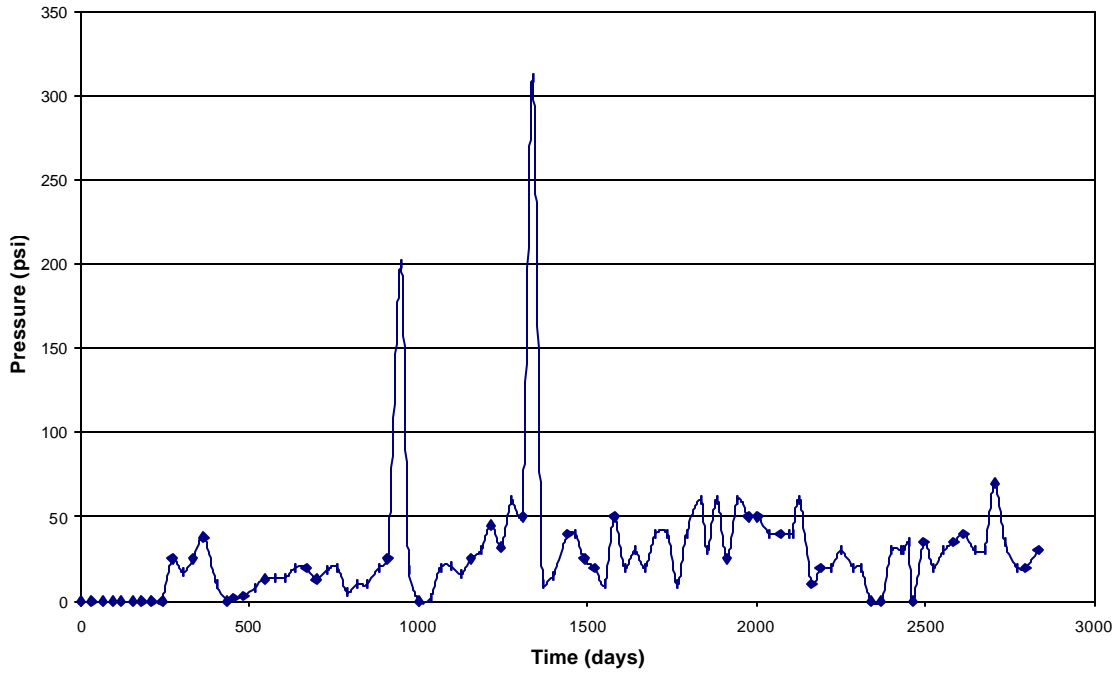Fig.A-8-2   9 5/8" x 7" Annulus of Well A-10- Platform MU-A111

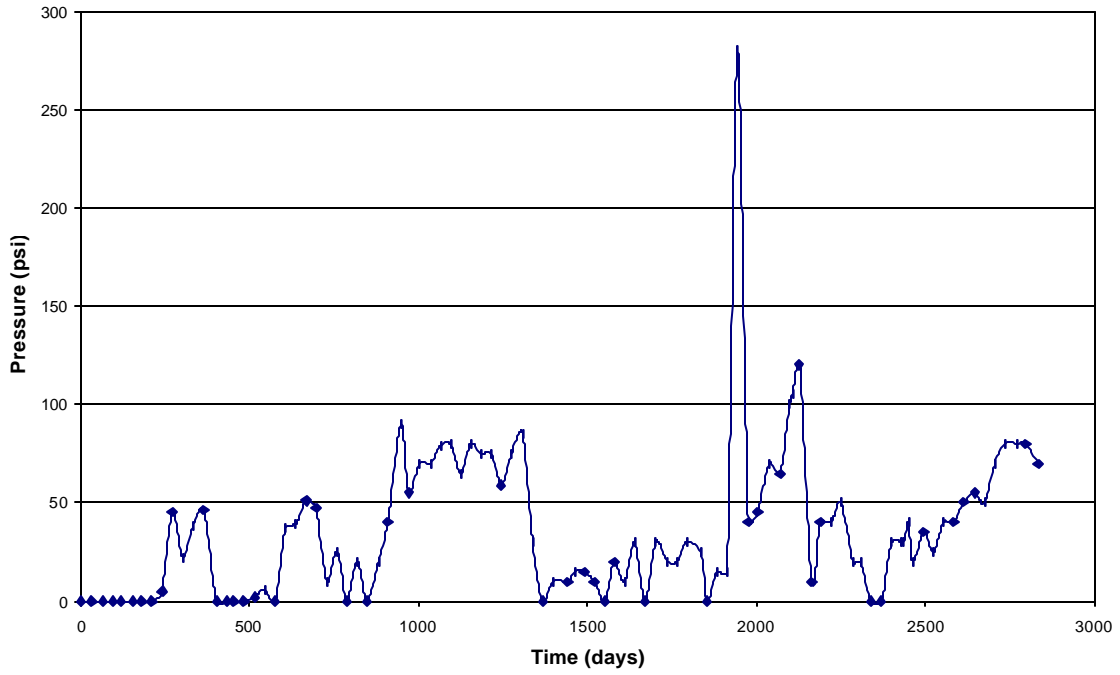Fig.A-8-3   13 3/8" x 9 5/8" Annulus of Well A-10- Platform MU-A111
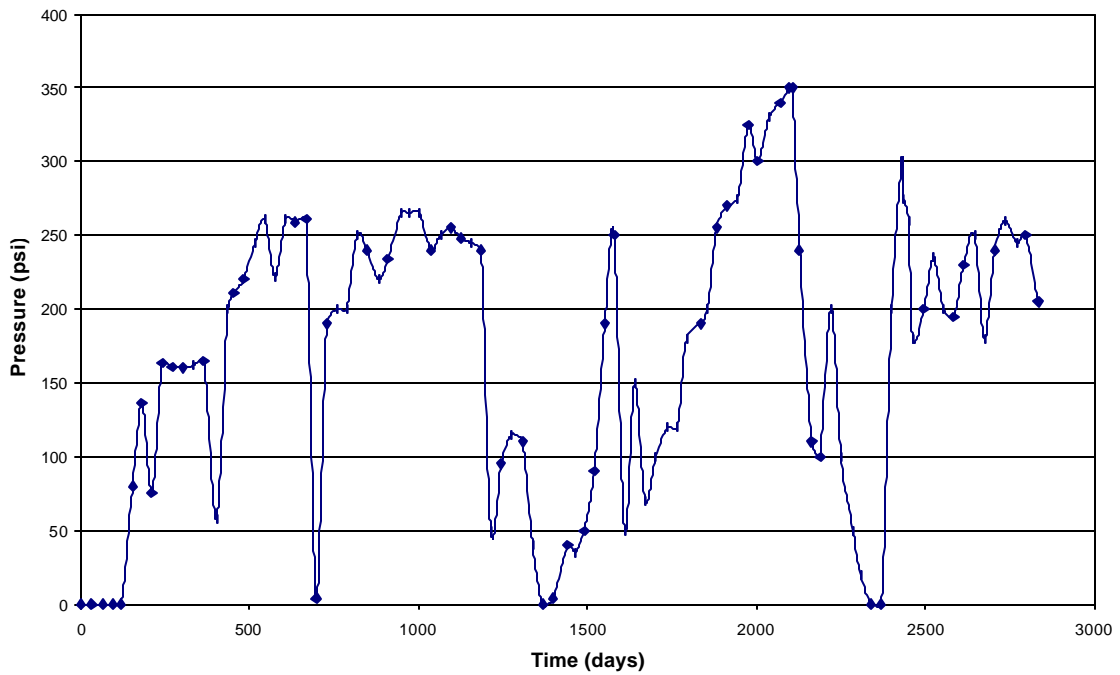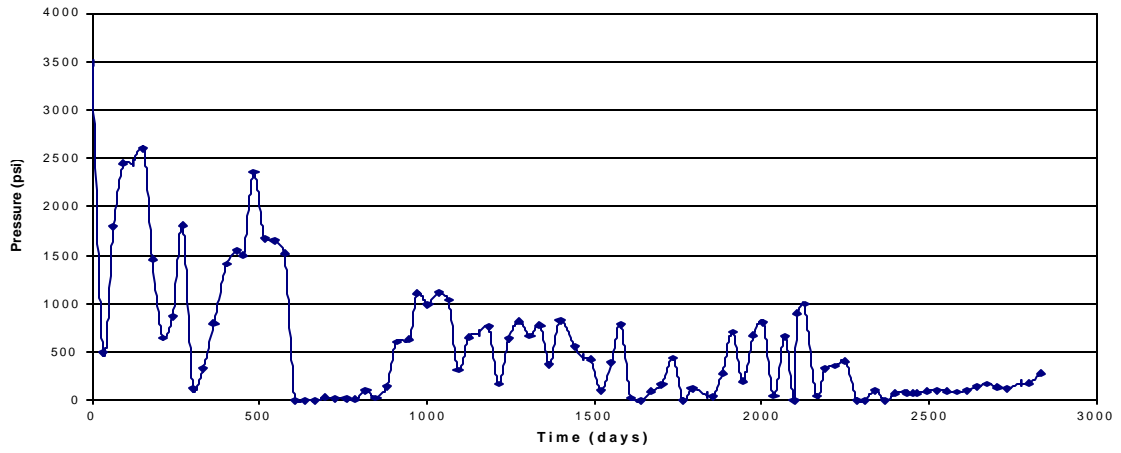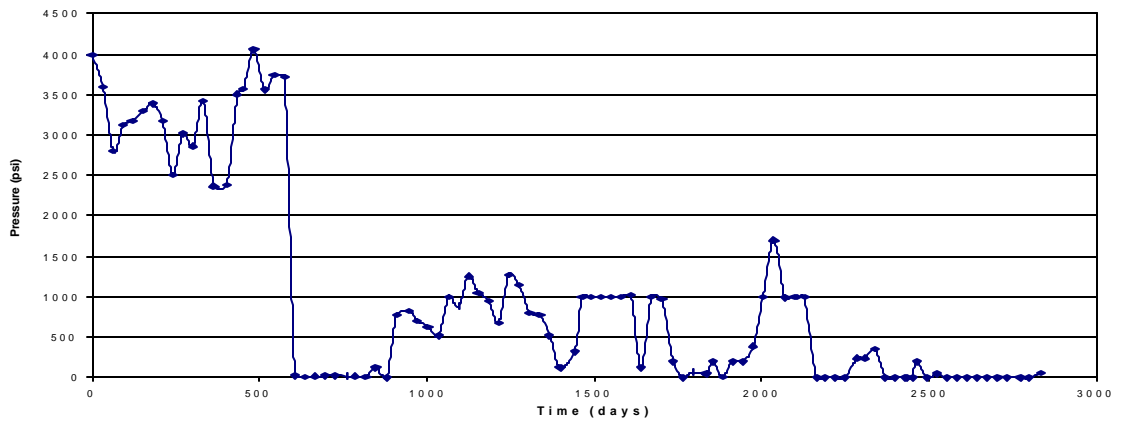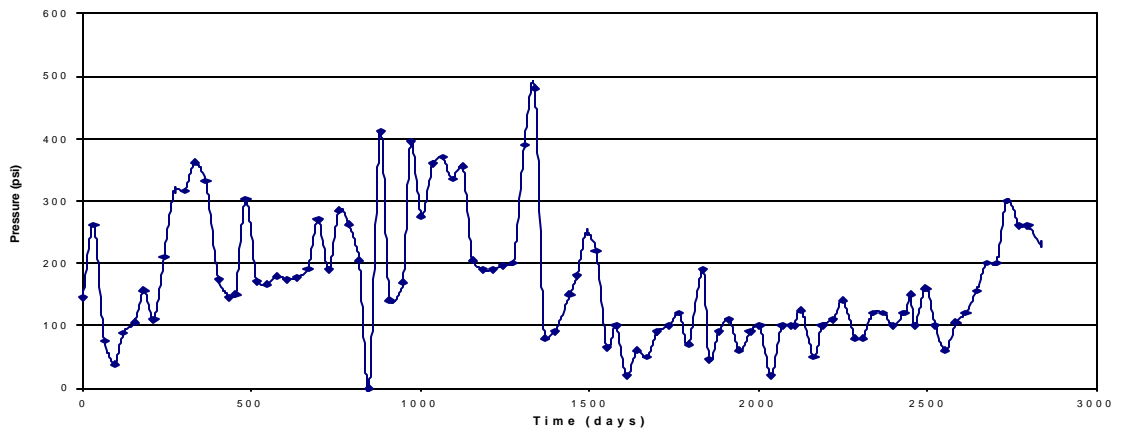
Table A9 Pressure Record of Well A -11 - Platform MU-A111

Date	Status	Time	Prod Csg	Interm Csg	Surf Csg	Cond Csg	SITP	FTP
		days	6 5/8"	8 5/8"	11 3/4"	16"		
1/3/89	SI	0	10	0	160	0	1906	
2/5/89	SI	33	12	0	148	0	1906	
3/8/89	SI	64	20	0	100	0		
4/7/89	SI	94	5	0	120	10	4150	
5/3/89	SI	120	5	0	120	5	4150	
6/6/89	SI; Depleted	154	10	0	125	0	4300	
7/3/89	SI; Depleted	181	12	0	146	30	4300	
8/2/89	SI; Depleted	211	10	0	90	20	4300	
9/1/89	SI; Depleted	241	4	0	114	24	4165	
10/1/89	SI; Depleted	271	0	0	144	30	4393	
11/1/89	SI; Depleted	302	0	0	147	25	4693	
12/1/89	SI; Depleted	332	0	15	162	23	4493	
1/2/90	SI; Depleted	364	2	2	189	24	4693	
2/9/90	SI; Depleted	402	5	2	187	28	4693	
3/14/90	SI; Depleted	435	0	0	0	165	4693	
4/1/90	SI; Depleted	453	4	2	3	170	4693	
5/1/90	SI; Depleted	483	3	2	4	160	4693	
6/2/90	SI; Depleted	515	0	0	0	180	4693	
7/1/90	SI; Depleted	544	4	6	5	166	4376	
8/1/90	SI; Depleted	575	1	2	1	178	5274	
9/1/90	SI; Depleted	606	2	1	1	174	5274	
10/1/90	SI; Depleted	636	2	1	1	180	5274	
11/1/90	SI; Depleted	667	5	1	1		5361	
12/1/90	SI; Depleted	697	1	2	3	6	5364	
1/1/91	SI; Depleted	728	2	0	0	145	5364	
2/1/91	SI; Depleted	759	0	0	0	140	5364	
3/1/91	SI; Depleted	787	0	0	0	150	5364	
4/1/91	SI; Depleted	818	0	0	0	165	5364	
5/1/91	31-SI	848	0	0	0	160		
6/3/91	31-SI	881	2	0	0	160		
7/1/91	31-SI	909	8	27	53	35		
8/9/91	31-SI	948	0	0	150	35		
9/1/91	31-SI	971	5	0	0	252		
10/3/91	31-SI	1003	0	0	0	160		
11/5/91	FLOW	1036	8	0	0	120		2320
12/4/91	36-SI	1065	6	2	0	137		
1/2/92	36-SI	1094	4	0	131	38		
2/2/92	36-SI	1125	5	0	141	39		
3/2/92	36-SI	1154	0	0	130	30		
4/2/92	36-SI	1185	0	0	130	30		
5/1/92	36-SI	1214	10	10	140	40		
6/1/92	36-SI	1245	0	0	150	40		
7/1/92	77-SI	1275	0	0	160	0		
8/3/92	77-SI	1308	0	0	140	40		
9/2/92	77-SI	1338	0	0	150	30		
10/1/92	77-SI	1367	0	0	110	30		
11/2/92	77-SI	1399	0	0	139	38		
12/15/92	77-SI	1442	0	0	135	35		
1/6/93	77-SI	1464	0	0	135	35		
2/1/93	77-SI	1490	0	0	130	30		
3/3/93	77-SI	1520	0	0	140	30		
4/4/93	82-SI	1552	0	0	150	30		
5/1/93	77-SI	1579	0	0	145	30		
6/1/93	77-SI	1610	0	0	110	30		
7/1/93	77-SI	1640	0	30	170	20		
8/1/93	77-SI	1671	10	5	130	40		
9/1/93	77-SI	1702	0	0		40		
10/6/93	77-SI	1737	0	0	260	0		
11/4/93	77-SI	1766	0	0	150	150		
12/1/93	SI	1793	0	0	0	150		
1/12/94	SI	1835	0	0	0	160		
2/1/94	SI	1855	0	0	0	0		
3/1/94	SI	1883	0	0	0	150		
4/1/94	SI	1914	0	0	0	15		
5/1/94	SI	1944	0	0	0	15		
6/2/94	SI	1976	10	0	150	20		
7/1/94	SI	2005	10	0	0	140		
8/2/94	SI	2037	0	0	0	150		
9/4/94	SI	2070	0	0	0	0		
10/2/94	SI	2098	0	0	0	20		

Fig.A-9-1   6 5/8" x 2 7/8" Annulus of Well A-11 - Platform MU-A111

Fig.A-9-2   8 5/8" x 6 5/8" Annulus of Well A-11 - Platform MU-A111

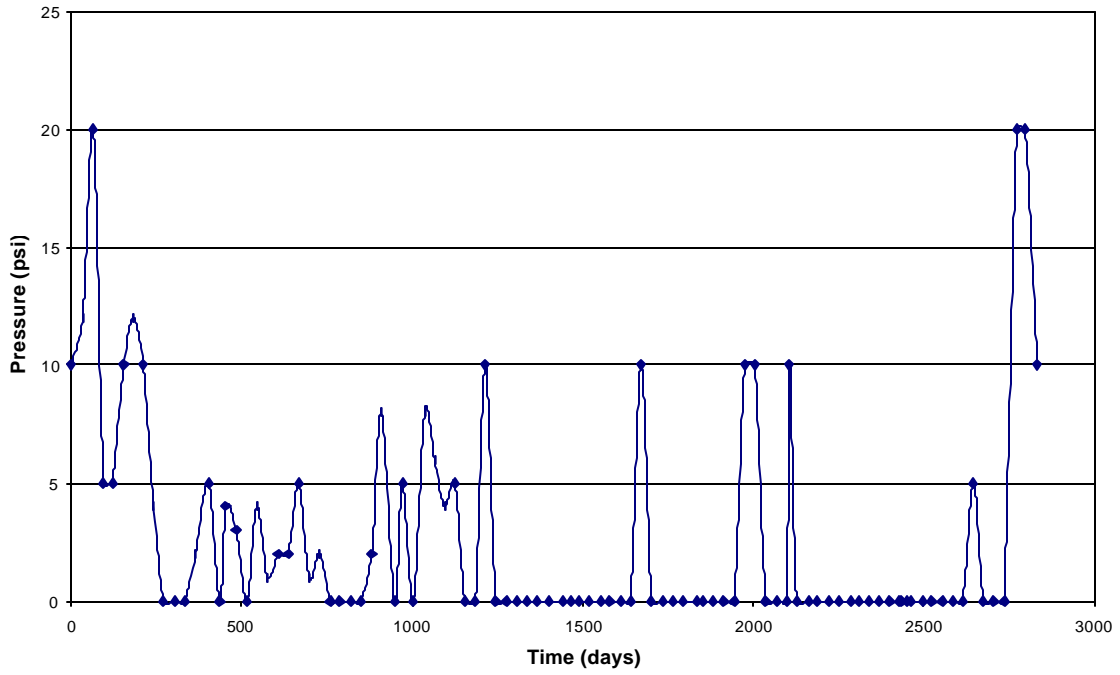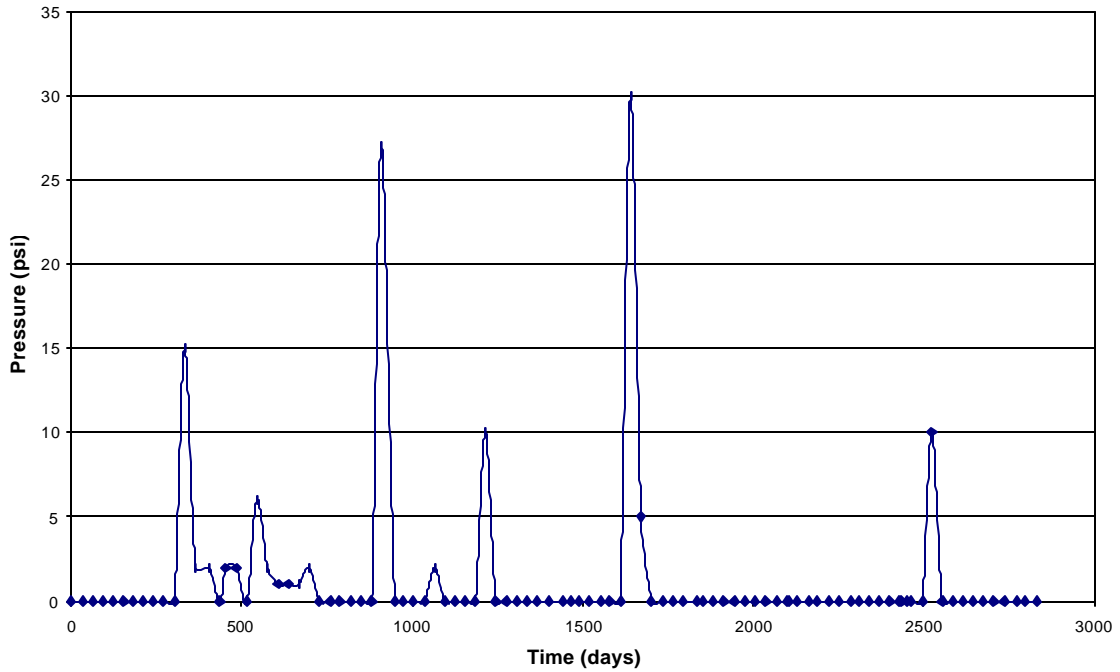**Fig.A-9-3   11 3/4" x 8 5/8" Annulus of Well A-11 - Platform MU-A111**
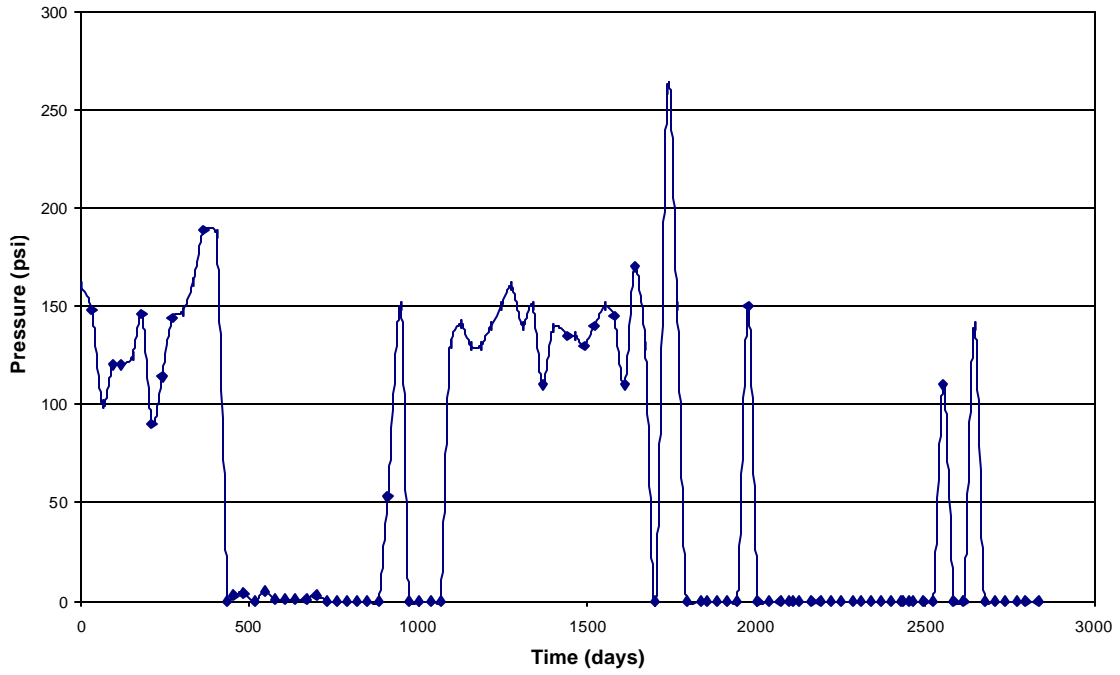

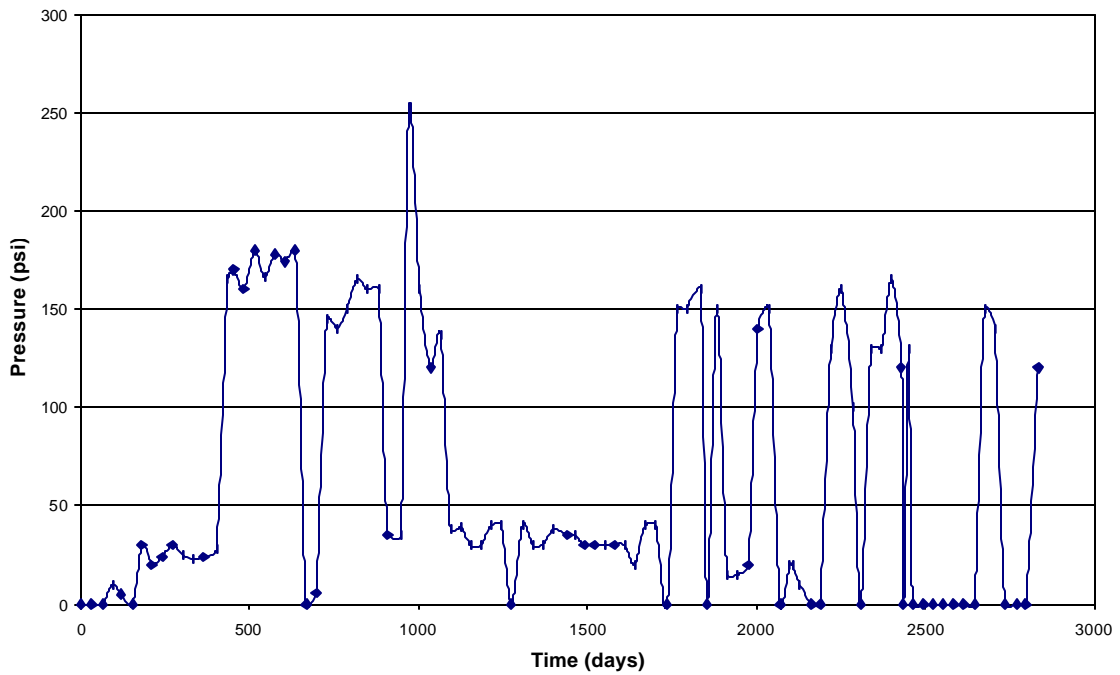**Fig.A-9-4   16" x 11 3/4" Annulus of Well A-11 - Platform MU-A111**

Table A10 Pressure Record of Well A -12 - Platform MU-A111

Date	Status	Time	Prod Csg	Interm Csg	Surf Csg	SITP	FTP
		days	7"	9 5/8"	13 3/8"		
1/3/89	FLOW	0	30	175	0	2443	1892
2/5/89	FLOW	33	218	167	0	2443	1901
3/8/89	FLOW	64	375	155	0	2443	1840
4/7/89	FLOW	94	570	200	0	2443	1800
5/3/89	FLOW	120	570	200	0	2443	1800
6/6/89	Loaded up	154	120	345	0	2300	
7/3/89	Loaded up	181	242	430	0	2300	
8/2/89	Loaded up	211	30	485	0	2300	
9/1/89	Loaded up	241	121	498	0	2255	
10/1/89	Loaded up	271	240	465	10	2255	
11/1/89	Loaded up	302	327	454	21	2255	
12/1/89	Loaded up	332	408	473	30	2255	
1/2/90	Loaded up	364	493	489	45	2255	
2/9/90	Loaded up	402	35	410	41	2255	
3/14/90	Loaded up	435	125	465	65	2255	
4/1/90	SI; Sand	453	171	479	69	2255	
5/1/90	SI; Sand	483	245	500	85	2255	
6/2/90	SI; Sand	515	323	509	26	2255	
7/1/90	SI; Sand	544	385	245	69	2255	
8/1/90	SI; Sand	575	446	639	82	1906	
9/1/90	SI; Sand	606	512	736	111	1910	
10/1/90	SI; Sand	636	559	739	139	1910	
11/1/90	Sand up	667	609	922	169	1872	
12/1/90	Sand up	697	654	839	189	1872	
1/1/91	Sand up	728	330	280	210	1872	
3/1/91	Sand up	787	418	370	215	1872	
4/1/91	Sand up	818	475	867	300	1872	
5/1/91	41-SI; Sand up	848	510	920	305		
6/3/91	41-SI; Sand up	881	568	980	308		
7/1/91	41-SI; Sand up	909	604	1075	329		
8/9/91	41-SI; Sand up	948	660	1110	395		
9/1/91	41-SI; Sand up	971	680	1030	420		
10/3/91	41-SI; Sand up	1003	650	970	560		
11/5/91	41-SI	1036	660	910	450		
12/4/91	41-SI	1065	692	920	480		
1/2/92	41-SI	1094	720	905	593		
2/2/92	41-SI	1125	760	901	511		
3/2/92	41-SI	1154	780	900	510		
4/2/92	41-SI	1185	815	900	500		
5/1/92	41-SI	1214	770	920	155		
6/1/92	41-SI	1245	775	960	215		
7/1/92	41-SI	1275	830	1050	255		
8/3/92	41-SI	1308	870	1060	345		
9/2/92	41-SI	1338	310	1070	135		
10/1/92	41-SI	1367	10	340	20		
11/2/92	41-SI	1399	42	572	12		
12/15/92	41-SI	1442	0	720	10		
1/6/93	41-SI	1464	40	800	50		
2/1/93	41-SI	1490	85	860	90		`
3/3/93	41-SI	1520	40	530	25		
4/4/93	41-SI	1552	25	630	40		
5/1/93	41-SI	1579	70	660	70		
6/1/93	41-SI	1610	0	720	110		
7/1/93	36-SI	1640	0	790	140		
8/1/93	36-SI	1671	0	520	125		
9/1/93	36-SI	1702	0	570	160		
10/6/93	36-SI	1737	0	860	260		
11/4/93	36-SI	1766	0	0	50		
12/1/93	36-SI	1793	0	0	0		
1/12/94	SI	1835	0	850	250		
2/1/94	SI	1855	0	775	245		
3/1/94	SI	1883	0	800	300		
4/1/94	SI	1914	0	800	320		
5/1/94	SI	1944	0	650	180		
6/2/94	SI	1976	0	760	220		
7/1/94	SI	2005	0	800	230		
8/2/94	SI	2037	0	460	275		
9/4/94	SI	2070	0	650	270		
10/2/94	SI	2098	750	280	30		
10/11/94	SI	2107	0	780	290		

Fig.A-10-1   7" x 2 7/8" Annulus of Well A-12 - Platform MU-A111
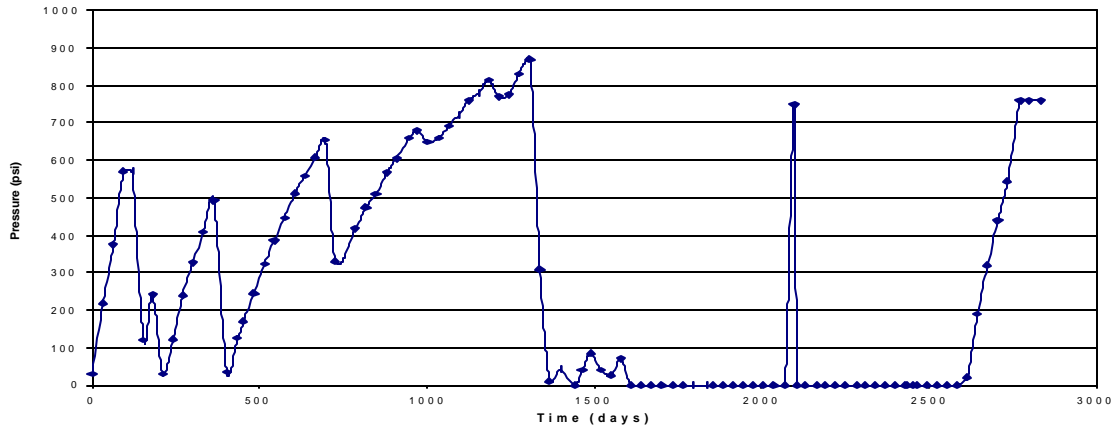
Fig.A-10-2   9 5/8" x 7" Annulus of Well A-12- Platform MU-A111

Fig.A-10-3   13 3/8" x 9 5/8" Annulus of Well A-12- Platform MU-A111
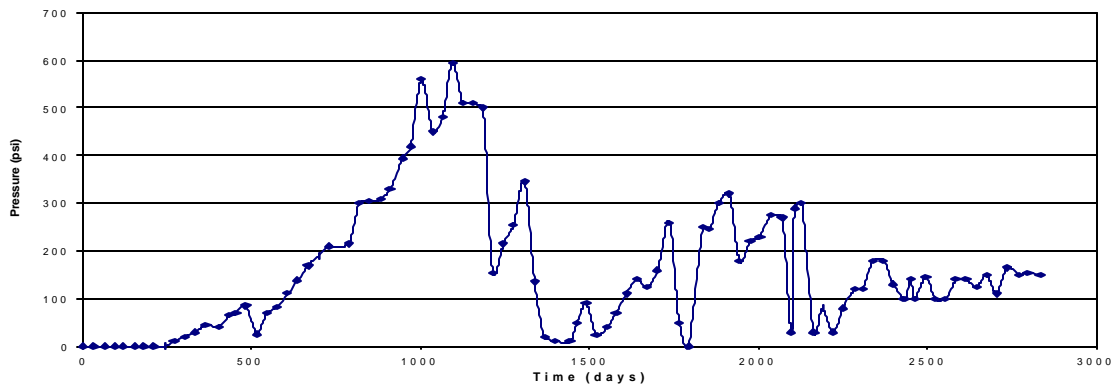
Table A11 Pressure Record of Well A -15 - Platform MU-A111

Date	Status	Time	Prod Csg	Interm Csg	Surf Csg	SITP	FTP
		days	7"	9 5/8"	13 3/8"		
11/4/93	SI	0	400	0	0		
12/1/93	FLOW	27	510	0	0		1140
1/12/94	SI	69	0	0	0		
2/1/94	SI	89	0	0	0		
3/1/94	SI	117	0	0	0		
4/1/94	SI	148	0	0	0		
5/1/94	SI	178	20	0	20		
6/2/94	SI	210	0	0	0		
7/1/94	SI	239	0	95	0		
8/2/94	SI	271	20	115	0		
9/4/94	SI	304	20	180	20		
10/2/94	SI	332	40	220	20		
10/11/94	SI	341	0	210	0		
11/1/94	SI	362	60	0	0		
12/7/94	SI	398	0	130	0		
1/1/95	SI	423	0	120	0		
2/2/95	SI	455	0	20	0		
3/4/95	SI	485	0	0	0		
4/8/95	SI	520	0	20	0		
5/1/95	SI	543	0	20	0		
6/1/95	SI	574	0	0	0		
7/1/95	SI	604	0	0	0		
8/1/95	SI	635	0	70	0		
8/30/95	SI	664	5	130	20		
9/5/95	SI	670	0	100	0		
9/20/95	SI	685	0	120	0		
10/2/95	SI	697	0	0	0		
11/4/95	SI	730	0	175	0		
12/2/95	SI	758	0	175	0		
1/1/96	SI	788	0	190	0		
2/1/96	SI	819	0	350	0		
3/1/96	SI	848	0	350	0		
4/2/96	SI	880	0	450	0		
5/1/96	SI	909	0	560	0		
6/1/96	SI	940	0	600	0		
7/1/96	SI	970	0	30	0		
8/7/96	SI	1007	0	760	0		
9/1/96	SI	1032	0	760	0		
10/7/96	SI	1068	0	795	0		

Fig.A-11-1　7" x 2 7/8" Annulus of Well A-15 - Platform MU-A111

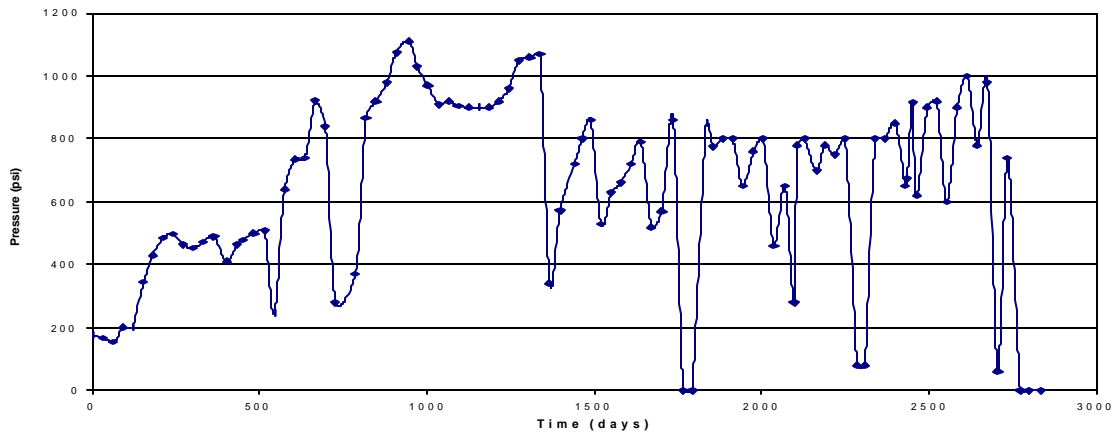**Fig.A-11-2　9 5/8" x 7" Annulus of Well A-15 - Platform MU-A111**

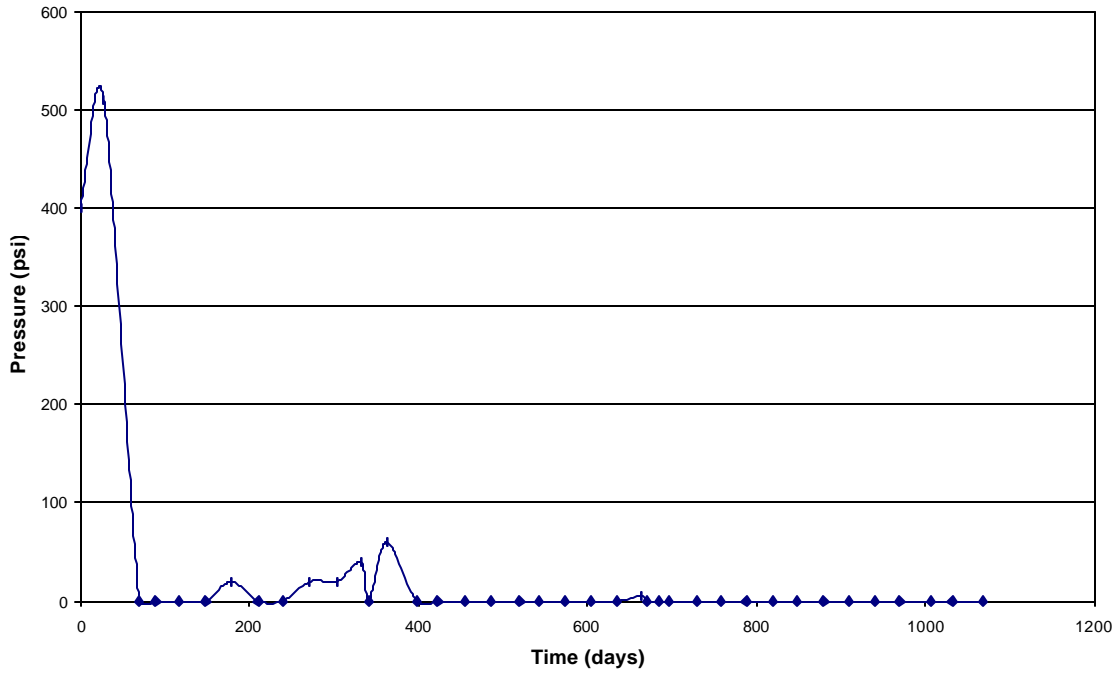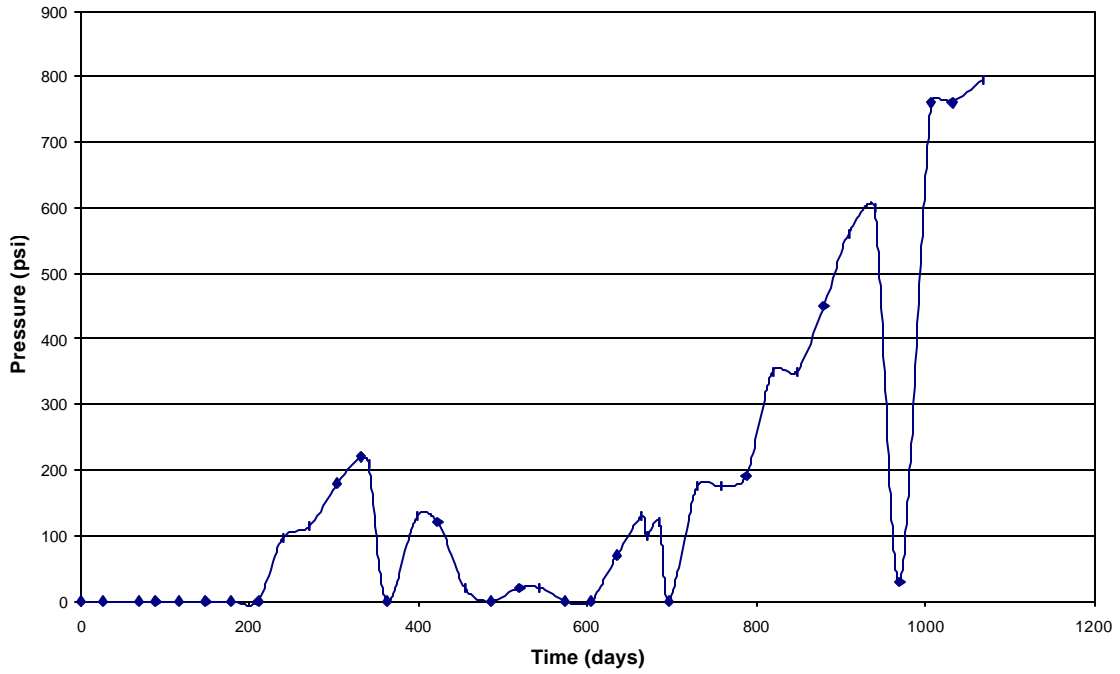**Table A12 10 3/4" Casing Pressure of Well APTA19 - South Timbalier-300A**

Time		Pressure	Time		Pressure
Recorded	Hours	10 3/4"	Recorded	Hours	10 3/4"
7/13/97 8:30	0.0	1177.5	7/15/97 17:30	0.0	1178.2
7/13/97 9:00	0.5	1177.5	7/15/97 18:00	0.5	1178.2
7/13/97 9:30	1.0	1176.7	7/15/97 18:30	1.0	761.2
7/13/97 10:00	1.5	1176.7	7/15/97 19:00	1.5	881.2
7/13/97 10:30	2.0	1176.7	7/15/97 19:30	2.0	901.5
7/13/97 11:00	2.5	1175.2	7/15/97 20:00	2.5	911.2
7/13/97 11:30	3.0	1175.2	7/15/97 20:30	3.0	919.5
7/13/97 12:00	3.5	1175.2	7/15/97 21:00	3.5	925.5
7/13/97 12:30	4.0	1175.2	7/15/97 21:30	4.0	930.8
7/13/97 13:00	4.5	1174.5	7/15/97 22:00	4.5	936
7/13/97 13:30	5.0	1174.5	7/15/97 22:30	5.0	940.5
7/13/97 14:00	5.5	1175.2	7/15/97 23:00	5.5	945
7/13/97 14:30	6.0	1174.5	7/15/97 23:30	6.0	948
7/13/97 15:00	6.5	1175.2	7/16/97 0:00	6.5	952.5
7/13/97 15:30	7.0	1173.7	7/16/97 0:30	7.0	954
7/13/97 16:00	7.5	1173.7	7/16/97 1:00	7.5	957
7/13/97 16:30	8.0	1174.5	7/16/97 1:30	8.0	959.3
7/13/97 17:00	8.5	1174.5	7/16/97 2:00	8.5	963
7/13/97 17:30	9.0	1173.7	7/16/97 2:30	9.0	964.5
7/13/97 18:00	9.5	1173.7	7/16/97 3:00	9.5	967.5
7/13/97 18:30	10.0	1173.7	7/16/97 3:30	10.0	970.5
7/13/97 19:00	10.5	1173.7	7/16/97 4:00	10.5	974.2
7/13/97 19:30	11.0	1173.7	7/16/97 4:30	11.0	975
7/13/97 20:00	11.5	1173.7	7/16/97 5:00	11.5	978
7/13/97 20:30	12.0	1173.7	7/16/97 5:30	12.0	979.5
7/13/97 21:00	12.5	1173.7	7/16/97 6:00	12.5	980.2
7/13/97 21:30	13.0	1173.7	7/16/97 6:30	13.0	982.5
7/13/97 22:00	13.5	1173.7	7/16/97 7:00	13.5	983.2
7/13/97 22:30	14.0	1173.7	7/16/97 7:30	14.0	984.7
7/13/97 23:00	14.5	1174.5	7/16/97 8:00	14.5	985.5
7/13/97 23:30	15.0	1173.7	7/16/97 8:30	15.0	986.3
7/14/97 0:00	15.5	1173.7	7/16/97 9:00	15.5	988.5
7/14/97 0:30	16.0	1173	7/16/97 9:30	16.0	990
7/14/97 1:00	16.5	1172.2	7/16/97 10:00	16.5	990
7/14/97 1:30	17.0	1173	7/16/97 10:30	17.0	990.7
7/14/97 2:00	17.5	1173	7/16/97 11:00	17.5	991.5
7/14/97 2:30	18.0	1173	7/16/97 11:30	18.0	992.2
7/14/97 3:00	18.5	1173	7/16/97 12:00	18.5	993
7/14/97 3:30	19.0	1172.2	7/16/97 12:30	19.0	993
7/14/97 4:00	19.5	1173	7/16/97 13:00	19.5	993.8
7/14/97 4:30	20.0	1176	7/16/97 13:30	20.0	993.8
7/14/97 5:00	20.5	1176	7/16/97 14:00	20.5	994.5
7/14/97 5:30	21.0	1175.2	7/16/97 14:30	21.0	994.5
7/14/97 6:00	21.5	1175.2	7/16/97 15:00	21.5	995.2
7/14/97 6:30	22.0	1175.2	7/16/97 15:30	22.0	994.5
7/14/97 7:00	22.5	1175.2	7/16/97 16:00	22.5	996
7/14/97 7:30	23.0	1174.5	7/16/97 16:30	23.0	996
7/14/97 8:00	23.5	1174.5	7/16/97 17:00	23.5	996.7
7/14/97 8:30	24.0	1174.5	7/16/97 17:30	24.0	997.5
7/14/97 9:00	24.5	1173	7/16/97 18:00	24.5	999.7
7/14/97 9:30	25.0	1173	7/16/97 18:30	25.0	577.5
7/14/97 10:00	25.5	1172.2	7/16/97 19:00	25.5	1000.5
7/14/97 10:30	26.0	1173	7/16/97 19:30	26.0	1002
7/14/97 11:00	26.5	1172.2			
7/14/97 11:30	27.0	1172.2			
7/14/97 12:00	27.5	1172.2			
7/14/97 12:30	28.0	1172.2			
7/14/97 13:00	28.5	1170			
7/14/97 13:30	29.0	1174.5			
7/14/97 14:00	29.5	1179.7			
7/14/97 14:30	30.0	1177.5			
7/14/97 15:00	30.5	1176			
7/14/97 15:30	31.0	1173.7			
7/14/97 16:00	31.5	1173			
7/14/97 16:30	32.0	1172.2			

Fig.A-12-1   10 3/4" Casing Pressure of Well APTA 19 - South Timbalier-300A
(July 13 to 14)

Fig.A-12-2   10 3/4" Casing Pressure of Well APTA 19 - South Timbalier-300A
(July 15 to 16)

73
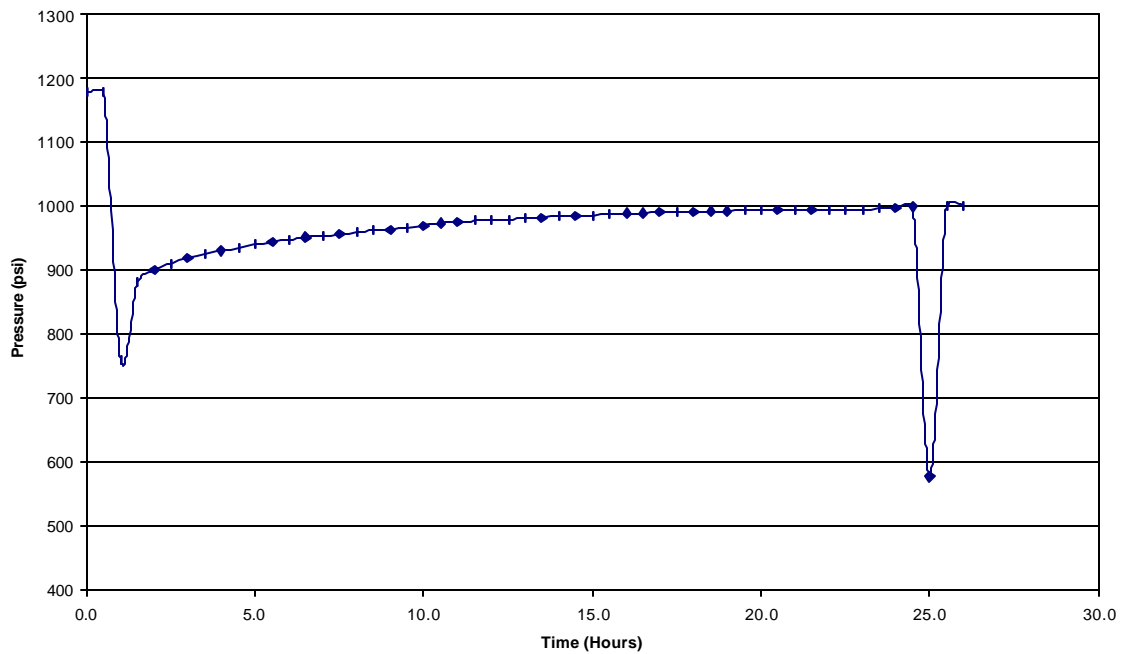
Table A13 16" Casing Pressure for Well APTA30 - South Timbalier-300A

Time		Pressure
Recorded	Hours	16"
7/15/97 17:30	0.0	221.2
7/15/97 18:00	0.5	220.5
7/15/97 18:30	1.0	180.8
7/15/97 19:00	1.5	130.5
7/15/97 19:30	2.0	144
7/15/97 20:00	2.5	148.5
7/15/97 20:30	3.0	150.8
7/15/97 21:00	3.5	153
7/15/97 21:30	4.0	154.5
7/15/97 22:00	4.5	157.5
7/15/97 22:30	5.0	157.5
7/15/97 23:00	5.5	159
7/15/97 23:30	6.0	160.5
7/16/97 0:00	6.5	161.3
7/16/97 0:30	7.0	162
7/16/97 1:00	7.5	161.3
7/16/97 1:30	8.0	163.5
7/16/97 2:00	8.5	163.5
7/16/97 2:30	9.0	164.3
7/16/97 3:00	9.5	165
7/16/97 3:30	10.0	165
7/16/97 4:00	10.5	166.5
7/16/97 4:30	11.0	165.8
7/16/97 5:00	11.5	165.8
7/16/97 5:30	12.0	166.5
7/16/97 6:00	12.5	167.3
7/16/97 6:30	13.0	167.3
7/16/97 7:00	13.5	168.8
7/16/97 7:30	14.0	167.3
7/16/97 8:00	14.5	168.8
7/16/97 8:30	15.0	169.5
7/16/97 9:00	15.5	170.3
7/16/97 9:30	16.0	170.3
7/16/97 10:00	16.5	170.3
7/16/97 10:30	17.0	170.3
7/16/97 11:00	17.5	169.5
7/16/97 11:30	18.0	169.5
7/16/97 12:00	18.5	170.3
7/16/97 12:30	19.0	170.3
7/16/97 13:00	19.5	170.3
7/16/97 13:30	20.0	170.3
7/16/97 14:00	20.5	170.3
7/16/97 14:30	21.0	170.3
7/16/97 15:00	21.5	170.3
7/16/97 15:30	22.0	170.3
7/16/97 16:00	22.5	170.3
7/16/97 16:30	23.0	170.3
7/16/97 17:00	23.5	170.3
7/16/97 17:30	24.0	170.3
7/16/97 18:00	24.5	170.3
7/16/97 18:30	25.0	171
7/16/97 19:00	25.5	170.3

Fig.A-13-1   16" Casing Pressure of Well APTA 30 - South Timbalier-300A

74

Table A14 10 3/4" Casing Pressure of Well APTA31 - South Timbalier-300A

Time		Pressure	Time		Pressure
Recorded	Hours	10 3/4"	Recorded	Hours	10 3/4"
7/13/97 8:30	0.0	1406.2	7/15/97 17:30	0.0	1377.7
7/13/97 9:00	0.5	1404.7	7/15/97 18:00	0.5	1377.7
7/13/97 9:30	1.0	1404	7/15/97 18:30	1.0	1378.5
7/13/97 10:00	1.5	1406.2	7/15/97 19:00	1.5	1378.5
7/13/97 10:30	2.0	1407	7/15/97 19:30	2.0	1377.7
7/13/97 11:00	2.5	1407.7	7/15/97 20:00	2.5	1379.2
7/13/97 11:30	3.0	1409.2	7/15/97 20:30	3.0	1017.7
7/13/97 12:00	3.5	1410.7	7/15/97 21:00	3.5	1182
7/13/97 12:30	4.0	1414.5	7/15/97 21:30	4.0	1223.2
7/13/97 13:00	4.5	1414.5	7/15/97 22:00	4.5	1249.5
7/13/97 13:30	5.0	1416	7/15/97 22:30	5.0	1272
7/13/97 14:00	5.5	1418.2	7/15/97 23:00	5.5	1291.5
7/13/97 14:30	6.0	1419.7	7/15/97 23:30	6.0	1306.5
7/13/97 15:00	6.5	1419	7/16/97 0:00	6.5	1319.2
7/13/97 15:30	7.0	1073.2	7/16/97 0:30	7.0	1327.5
7/13/97 16:00	7.5	1200.7	7/16/97 1:00	7.5	1334.2
7/13/97 16:30	8.0	1249.5	7/16/97 1:30	8.0	1339.5
7/13/97 17:00	8.5	1278	7/16/97 2:00	8.5	1344.7
7/13/97 17:30	9.0	1301.2	7/16/97 2:30	9.0	1350.7
7/13/97 18:00	9.5	1320.7	7/16/97 3:00	9.5	1354.5
7/13/97 18:30	10.0	1337.2	7/16/97 3:30	10.0	1357.5
7/13/97 19:00	10.5	1351.5	7/16/97 4:00	10.5	1360.5
7/13/97 19:30	11.0	1361.2	7/16/97 4:30	11.0	1361.2
7/13/97 20:00	11.5	1370.2	7/16/97 5:00	11.5	1361.2
7/13/97 20:30	12.0	1375.5	7/16/97 5:30	12.0	1361.2
7/13/97 21:00	12.5	1380.7	7/16/97 6:00	12.5	1362
7/13/97 21:30	13.0	1384.5	7/16/97 6:30	13.0	1361.2
7/13/97 22:00	13.5	1386.7	7/16/97 7:00	13.5	1361.2
7/13/97 22:30	14.0	1389	7/16/97 7:30	14.0	1361.2
7/13/97 23:00	14.5	1389.7	7/16/97 8:00	14.5	1361.2
7/13/97 23:30	15.0	1391.2	7/16/97 8:30	15.0	1360.5
7/14/97 0:00	15.5	1392	7/16/97 9:00	15.5	1361.2
7/14/97 0:30	16.0	1393.5	7/16/97 9:30	16.0	1360.5
7/14/97 1:00	16.5	1394.2	7/16/97 10:00	16.5	1361.2
7/14/97 1:30	17.0	1395	7/16/97 10:30	17.0	1362.7
7/14/97 2:00	17.5	1396.5	7/16/97 11:00	17.5	1362
7/14/97 2:30	18.0	1398.7	7/16/97 11:30	18.0	1363.5
7/14/97 3:00	18.5	1400.2	7/16/97 12:00	18.5	1365
7/14/97 3:30	19.0	1401	7/16/97 12:30	19.0	1364.2
7/14/97 4:00	19.5	1404	7/16/97 13:00	19.5	1365.7
7/14/97 4:30	20.0	1404	7/16/97 13:30	20.0	1368
7/14/97 5:00	20.5	1405.2	7/16/97 14:00	20.5	1368
7/14/97 5:30	21.0	1407.7	7/16/97 14:30	21.0	1369.5
7/14/97 6:00	21.5	1410.7	7/16/97 15:00	21.5	1371
7/14/97 6:30	22.0	1414.5	7/16/97 15:30	22.0	1371.7
7/14/97 7:00	22.5	1416	7/16/97 16:00	22.5	1373.2
7/14/97 7:30	23.0	1417.5	7/16/97 16:30	23.0	1372.5
7/14/97 8:00	23.5	1417.5	7/16/97 17:00	23.5	1374.7
7/14/97 8:30	24.0	1417.5	7/16/97 17:30	24.0	1374.7
7/14/97 9:00	24.5	1419	7/16/97 18:00	24.5	1373.2
7/14/97 9:30	25.0	1421.2	7/16/97 18:30	25.0	1374.7
7/14/97 10:00	25.5	1422.7	7/16/97 19:00	25.5	1375.5
7/14/97 10:30	26.0	1422.7	7/16/97 19:30	26.0	1374.7
7/14/97 11:00	26.5	1425			
7/14/97 11:30	27.0	1425.7			
7/14/97 12:00	27.5	1427.2			
7/14/97 12:30	28.0	1427.2			
7/14/97 13:00	28.5	1425.7			
7/14/97 13:30	29.0	1072.5			
7/14/97 14:00	29.5	1115.2			
7/14/97 14:30	30.0	1206			
7/14/97 15:00	30.5	1238.2			
7/14/97 15:30	31.0	1265.2			
7/14/97 16:00	31.5	1284.7			
7/14/97 16:30	32.0	1302.7			

Fig.A-14-1   10 3/4" Casing Pressure of Well APTA 31- South Timbalier-300A
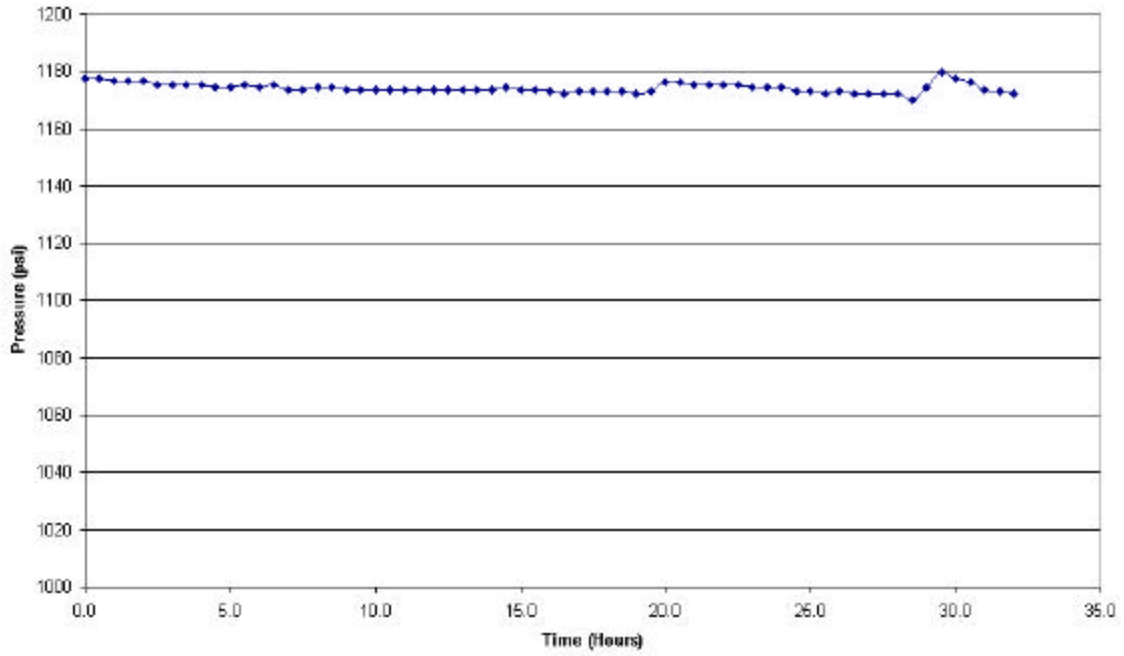**(July 13 to 14)**

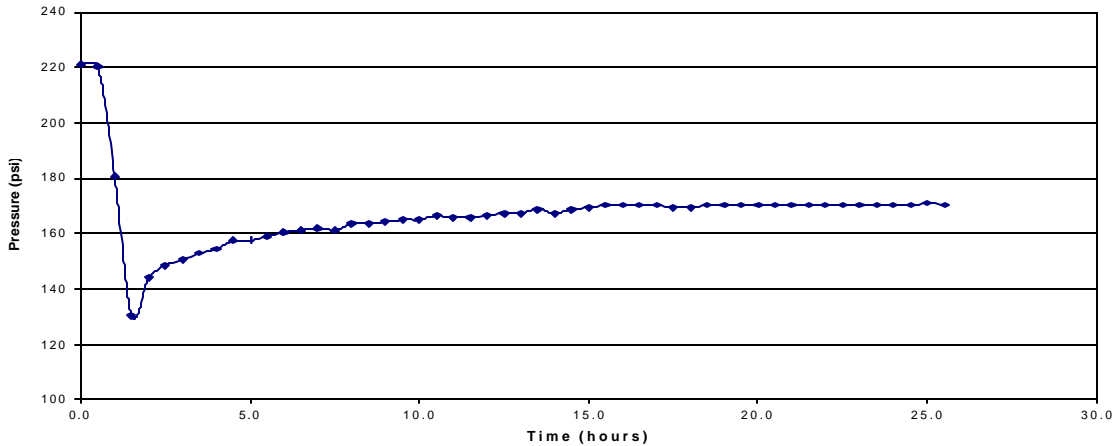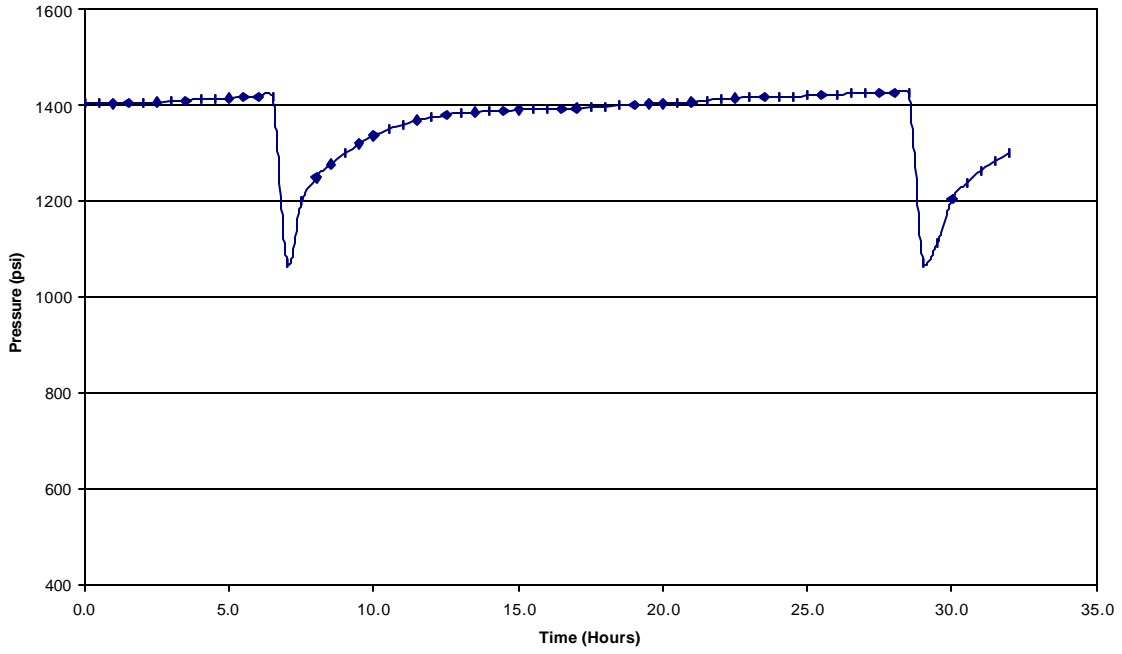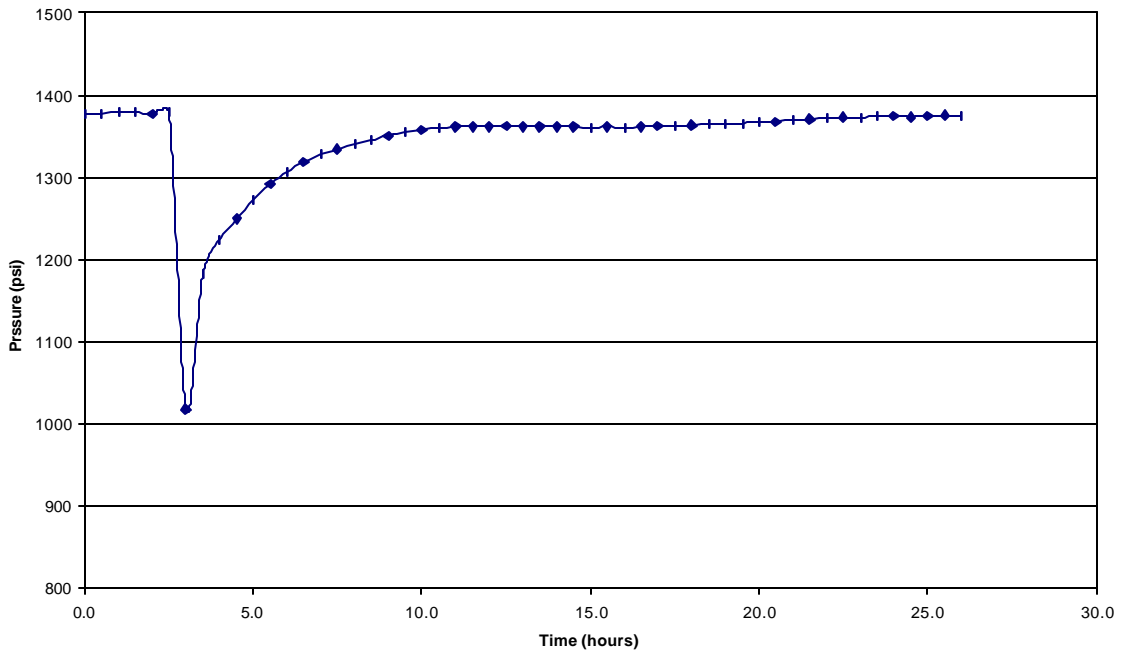**Fig.A-14-2   10 3/4" Casing Pressure of Well APTA 31- South Timbalier-300A**
(July 15 to 16)

Table A15 10 3/4" Casing Pressure of Well APTL9 - South Timbalier-300A

Time Recorded	Hours	Pressure 10 3/4"	Time Recorded	Hours	Pressure 10 3/4"
7/13/97 8:30	0.0	1257.7	7/15/97 17:30	0.0	1236.7
7/13/97 9:00	0.5	1263	7/15/97 18:00	0.5	1239
7/13/97 9:30	1.0	1269	7/15/97 18:30	1.0	1239.7
7/13/97 10:00	1.5	1273.5	7/15/97 19:00	1.5	189.8
7/13/97 10:30	2.0	1278	7/15/97 19:30	2.0	365.5
7/13/97 11:00	2.5	1284	7/15/97 20:00	2.5	337.5
7/13/97 11:30	3.0	1290	7/15/97 20:30	3.0	393
7/13/97 12:00	3.5	1295.2	7/15/97 21:00	3.5	435
7/13/97 12:30	4.0	1300.5	7/15/97 21:30	4.0	469.5
7/13/97 13:00	4.5	1307.2	7/15/97 22:00	4.5	501.8
7/13/97 13:30	5.0	1313.2	7/15/97 22:30	5.0	528.7
7/13/97 14:00	5.5	1320.7	7/15/97 23:00	5.5	552.7
7/13/97 14:30	6.0	1325.2	7/15/97 23:30	6.0	575.2
7/13/97 15:00	6.5	1329.7	7/16/97 0:00	6.5	595.5
7/13/97 15:30	7.0	1335.7	7/16/97 0:30	7.0	612.7
7/13/97 16:00	7.5	1089	7/16/97 1:00	7.5	627.7
7/13/97 16:30	8.0	822.7	7/16/97 1:30	8.0	640.2
7/13/97 17:00	8.5	867	7/16/97 2:00	8.5	654
7/13/97 17:30	9.0	899.2	7/16/97 2:30	9.0	666
7/13/97 18:00	9.5	926.2	7/16/97 3:00	9.5	678.7
7/13/97 18:30	10.0	945	7/16/97 3:30	10.0	689.2
7/13/97 19:00	10.5	962.2	7/16/97 4:00	10.5	698.2
7/13/97 19:30	11.0	971.2	7/16/97 4:30	11.0	707.2
7/13/97 20:00	11.5	982.5	7/16/97 5:00	11.5	716.2
7/13/97 20:30	12.0	987.7	7/16/97 5:30	12.0	724.5
7/13/97 21:00	12.5	992.2	7/16/97 6:00	12.5	732
7/13/97 21:30	13.0	996	7/16/97 6:30	13.0	737.2
7/13/97 22:00	13.5	1000.5	7/16/97 7:00	13.5	744.7
7/13/97 22:30	14.0	1005	7/16/97 7:30	14.0	750
7/13/97 23:00	14.5	1008.7	7/16/97 8:00	14.5	755.2
7/13/97 23:30	15.0	1011	7/16/97 8:30	15.0	760.5
7/14/97 0:00	15.5	1015.5	7/16/97 9:00	15.5	764.3
7/14/97 0:30	16.0	1019.2	7/16/97 9:30	16.0	769.5
7/14/97 1:00	16.5	1023.7	7/16/97 10:00	16.5	772.5
7/14/97 1:30	17.0	1028	7/16/97 10:30	17.0	775.5
7/14/97 2:00	17.5	1032	7/16/97 11:00	17.5	779.2
7/14/97 2:30	18.0	1036.5	7/16/97 11:30	18.0	781.5
7/14/97 3:00	18.5	1040.2	7/16/97 12:00	18.5	784.5
7/14/97 3:30	19.0	1040	7/16/97 12:30	19.0	786.7
7/14/97 4:00	19.5	1039.5	7/16/97 13:00	19.5	789.7
7/14/97 4:30	20.0	1043	7/16/97 13:30	20.0	792
7/14/97 5:00	20.5	1045.2	7/16/97 14:00	20.5	793.5
7/14/97 5:30	21.0	1048.5	7/16/97 14:30	21.0	796.5
7/14/97 6:00	21.5	1050.7	7/16/97 15:00	21.5	798.8
7/14/97 6:30	22.0	1053	7/16/97 15:30	22.0	800.2
7/14/97 7:00	22.5	1056	7/16/97 16:00	22.5	801.7
7/14/97 7:30	23.0	1058.2	7/16/97 16:30	23.0	803.2
7/14/97 8:00	23.5	1060.5	7/16/97 17:00	23.5	804.7
7/14/97 8:30	24.0	1062.7	7/16/97 17:30	24.0	807
7/14/97 9:00	24.5	1065	7/16/97 18:00	24.5	807.7
7/14/97 9:30	25.0	1065.7	7/16/97 18:30	25.0	809.2
7/14/97 10:00	25.5	1068	7/16/97 19:00	25.5	810
7/14/97 10:30	26.0	1070.2			
7/14/97 11:00	26.5	1073.2			
7/14/97 11:30	27.0	1075.5			
7/14/97 12:00	27.5	1078.5			
7/14/97 12:30	28.0	1080			
7/14/97 13:00	28.5	1082.2			
7/14/97 13:30	29.0	1085.2			
7/14/97 14:00	29.5	1088.2			
7/14/97 14:30	30.0	1089.7			
7/14/97 15:00	30.5	1092.7			
7/14/97 15:30	31.0	1095.7			
7/14/97 16:00	31.5	1098.7			
7/14/97 16:30	32.0	1101.7			

Fig.A-15-1   10 3/4" Casing Pressure of Well APTL 9 - South Timbalier-300A
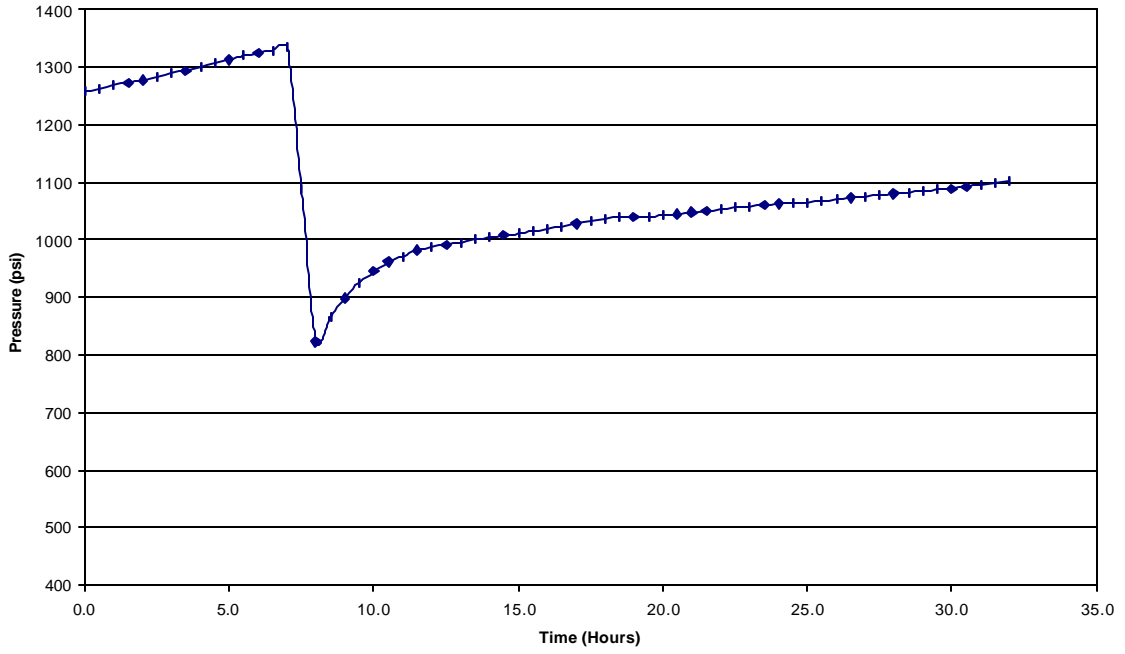**(July 13 to 14)**

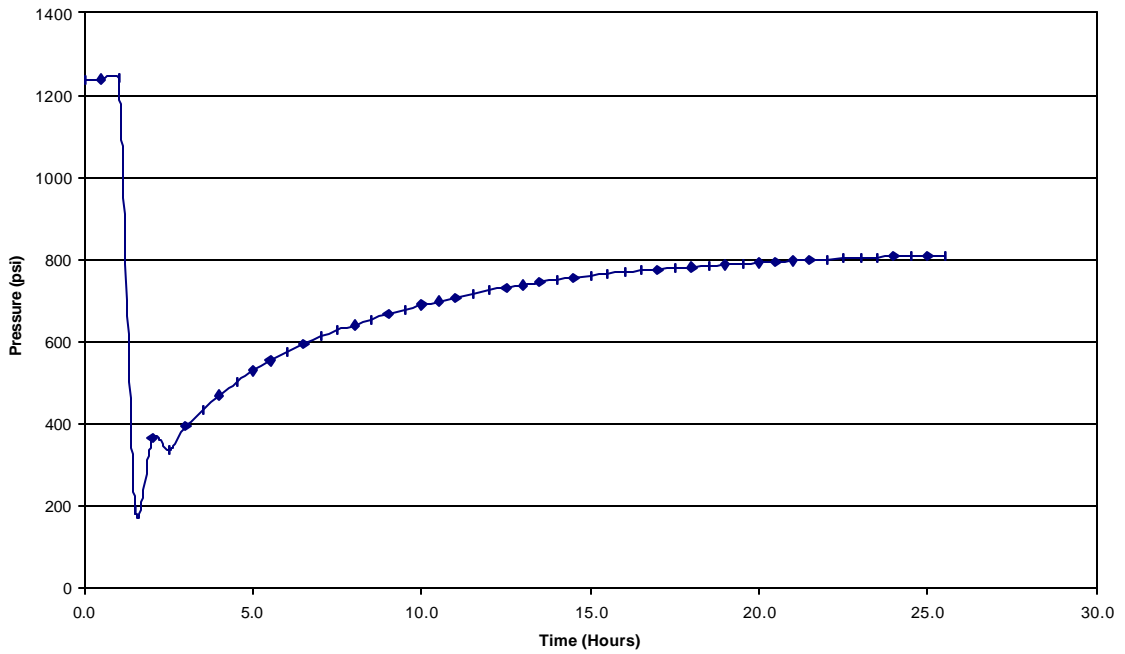**Fig.A-15-2   10 3/4" Casing Pressure of Well APTL 9 - South Timbalier-300A**
(July 15 to 16)

Table A16 10 3/4" Casing Pressure of Well BPTB6 - South Timbalier-300A

Time		Pressure
Recorded	Hours	10 3/4"
7/15/97 17:30	0.0	3
7/15/97 18:00	0.5	3
7/15/97 18:30	1.0	3
7/15/97 19:00	1.5	122.2
7/15/97 19:30	2.0	242.2
7/15/97 20:00	2.5	253.5
7/15/97 20:30	3.0	258.5
7/15/97 21:00	3.5	264
7/15/97 21:30	4.0	265.5
7/15/97 22:00	4.5	267
7/15/97 22:30	5.0	268.5
7/15/97 23:00	5.5	271.5
7/15/97 23:30	6.0	273
7/16/97 0:00	6.5	274.5
7/16/97 0:30	7.0	275.3
7/16/97 1:00	7.5	276.8
7/16/97 1:30	8.0	277.5
7/16/97 2:00	8.5	277.5
7/16/97 2:30	9.0	278.3
7/16/97 3:00	9.5	279.8
7/16/97 3:30	10.0	279
7/16/97 4:00	10.5	280.5
7/16/97 4:30	11.0	281.3
7/16/97 5:00	11.5	282
7/16/97 5:30	12.0	285
7/16/97 6:00	12.5	285
7/16/97 6:30	13.0	286.5
7/16/97 7:00	13.5	286.5
7/16/97 7:30	14.0	287.3
7/16/97 8:00	14.5	288
7/16/97 8:30	15.0	289.5
7/16/97 9:00	15.5	290.3
7/16/97 9:30	16.0	289.5
7/16/97 10:00	16.5	290.3
7/16/97 10:30	17.0	291.8
7/16/97 11:00	17.5	291
7/16/97 11:30	18.0	291
7/16/97 12:00	18.5	291
7/16/97 12:30	19.0	291.8
7/16/97 13:00	19.5	291.8
7/16/97 13:30	20.0	291.8
7/16/97 14:00	20.5	293.2
7/16/97 14:30	21.0	293.2
7/16/97 15:00	21.5	294
7/16/97 15:30	22.0	294.7
7/16/97 16:00	22.5	294.7
7/16/97 16:30	23.0	295.5
7/16/97 17:00	23.5	296.3
7/16/97 17:30	24.0	298.5
7/16/97 18:00	24.5	298.5
7/16/97 18:30	25.0	298.5
7/16/97 19:00	25.5	300.8

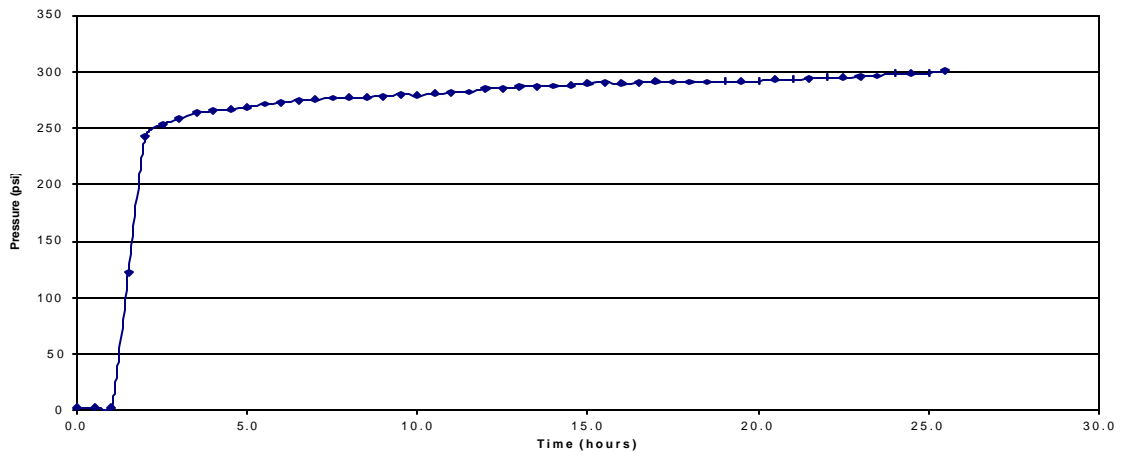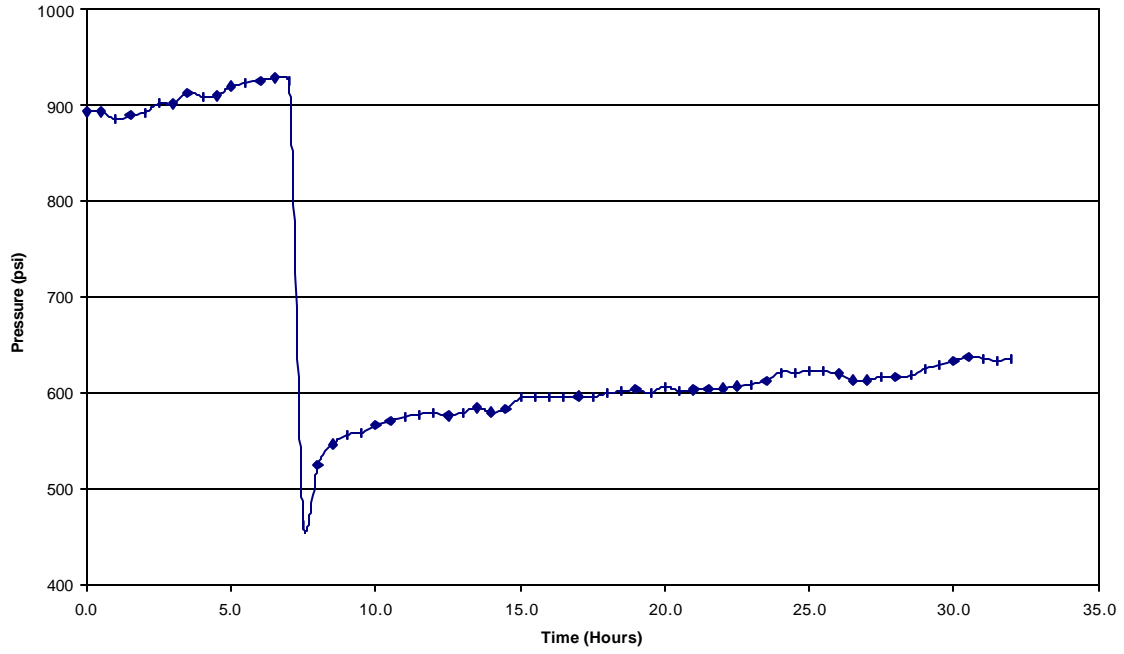**Fig.A-16-1   10 3/4" Casing Pressure of Well BPTB 6 - South Timbalier-300A**

Table A17 10 3/4" Casing Pressure of Well PTCA25C - South Timbalier-300A

Time Recorded	Hours	Pressure 10 3/4"	Time Recorded	Hours	Pressure 10 3/4"
7/13/97 8:30	0.0	893.5	7/15/97 17:30	0.0	703
7/13/97 9:00	0.5	893.5	7/15/97 18:00	0.5	700.5
7/13/97 9:30	1.0	885.5	7/15/97 18:30	1.0	700.5
7/13/97 10:00	1.5	890	7/15/97 19:00	1.5	529
7/13/97 10:30	2.0	893	7/15/97 19:30	2.0	545.5
7/13/97 11:00	2.5	902.5	7/15/97 20:00	2.5	550.5
7/13/97 11:30	3.0	902	7/15/97 20:30	3.0	558
7/13/97 12:00	3.5	914	7/15/97 21:00	3.5	562.5
7/13/97 12:30	4.0	909.5	7/15/97 21:30	4.0	560.5
7/13/97 13:00	4.5	910.5	7/15/97 22:00	4.5	562
7/13/97 13:30	5.0	920.5	7/15/97 22:30	5.0	570
7/13/97 14:00	5.5	923.5	7/15/97 23:00	5.5	573
7/13/97 14:30	6.0	926.5	7/15/97 23:30	6.0	566
7/13/97 15:00	6.5	929	7/16/97 0:00	6.5	566.5
7/13/97 15:30	7.0	925.5	7/16/97 0:30	7.0	570.5
7/13/97 16:00	7.5	462	7/16/97 1:00	7.5	574
7/13/97 16:30	8.0	525.5	7/16/97 1:30	8.0	571
7/13/97 17:00	8.5	547	7/16/97 2:00	8.5	570
7/13/97 17:30	9.0	557	7/16/97 2:30	9.0	571
7/13/97 18:00	9.5	559	7/16/97 3:00	9.5	568.5
7/13/97 18:30	10.0	566.5	7/16/97 3:30	10.0	571.5
7/13/97 19:00	10.5	572	7/16/97 4:00	10.5	577
7/13/97 19:30	11.0	575.5	7/16/97 4:30	11.0	572
7/13/97 20:00	11.5	578	7/16/97 5:00	11.5	575
7/13/97 20:30	12.0	580	7/16/97 5:30	12.0	572
7/13/97 21:00	12.5	576.5	7/16/97 6:00	12.5	567
7/13/97 21:30	13.0	580	7/16/97 6:30	13.0	572
7/13/97 22:00	13.5	585	7/16/97 7:00	13.5	572.5
7/13/97 22:30	14.0	580.5	7/16/97 7:30	14.0	568.5
7/13/97 23:00	14.5	583	7/16/97 8:00	14.5	568
7/13/97 23:30	15.0	595.5	7/16/97 8:30	15.0	568.5
7/14/97 0:00	15.5	595.5	7/16/97 9:00	15.5	568
7/14/97 0:30	16.0	595.5	7/16/97 9:30	16.0	575
7/14/97 1:00	16.5	595.5	7/16/97 10:00	16.5	576.5
7/14/97 1:30	17.0	597	7/16/97 10:30	17.0	579.5
7/14/97 2:00	17.5	596	7/16/97 11:00	17.5	579
7/14/97 2:30	18.0	600.5	7/16/97 11:30	18.0	571.5
7/14/97 3:00	18.5	602	7/16/97 12:00	18.5	574.5
7/14/97 3:30	19.0	604	7/16/97 12:30	19.0	575.5
7/14/97 4:00	19.5	600.5	7/16/97 13:00	19.5	578
7/14/97 4:30	20.0	607	7/16/97 13:30	20.0	578.5
7/14/97 5:00	20.5	602.5	7/16/97 14:00	20.5	572
7/14/97 5:30	21.0	603.5	7/16/97 14:30	21.0	571.5
7/14/97 6:00	21.5	604	7/16/97 15:00	21.5	571
7/14/97 6:30	22.0	605.5	7/16/97 15:30	22.0	573
7/14/97 7:00	22.5	607.5	7/16/97 16:00	22.5	575.5
7/14/97 7:30	23.0	609.5	7/16/97 16:30	23.0	574
7/14/97 8:00	23.5	613.5	7/16/97 17:00	23.5	573
7/14/97 8:30	24.0	622	7/16/97 17:30	24.0	574
7/14/97 9:00	24.5	622	7/16/97 18:00	24.5	580
7/14/97 9:30	25.0	623	7/16/97 18:30	25.0	580
7/14/97 10:00	25.5	622.5	7/16/97 19:00	25.5	577.5
7/14/97 10:30	26.0	620.5	7/16/97 19:30	26.0	578
7/14/97 11:00	26.5	614			
7/14/97 11:30	27.0	614			
7/14/97 12:00	27.5	617			
7/14/97 12:30	28.0	617			
7/14/97 13:00	28.5	618.5			
7/14/97 13:30	29.0	625.5			
7/14/97 14:00	29.5	630			
7/14/97 14:30	30.0	634.5			
7/14/97 15:00	30.5	638			
7/14/97 15:30	31.0	636.5			
7/14/97 16:00	31.5	634			
7/14/97 16:30	32.0	636.5			

Fig.A-17-1   10 3/4" Casing Pressure of Well PTCA 25C - South Timbalier-300A
(July 13 to 14)

Fig.A-17-2   10 3/4" Casing Pressure of Well PTCA 25C - South Timbalier-300A
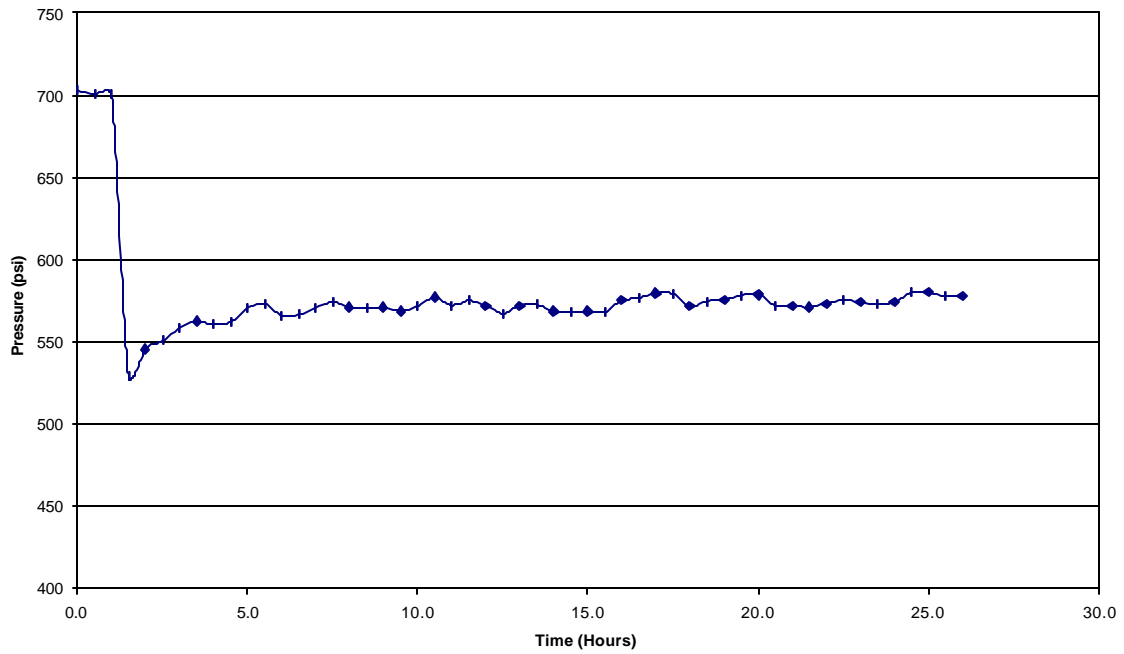**(July 15 to 16)**

Table A18 13 3/8" Casing Pressure of Well PTCA7D - South Timbalier-300A

Time		Pressure
Recorded	Hours	13 3/8"
7/15/97 18:00	0.0	967
7/15/97 18:30	0.5	965.5
7/15/97 19:00	1.0	967
7/15/97 19:30	1.5	128.5
7/15/97 20:00	2.0	88.5
7/15/97 20:30	2.5	34.5
7/15/97 21:00	3.0	34
7/15/97 21:30	3.5	35
7/15/97 22:00	4.0	64
7/15/97 22:30	4.5	78
7/15/97 23:00	5.0	84.5
7/15/97 23:30	5.5	90
7/16/97 0:00	6.0	93.5
7/16/97 0:30	6.5	97.5
7/16/97 1:00	7.0	101.5
7/16/97 1:30	7.5	104.5
7/16/97 2:00	8.0	108
7/16/97 2:30	8.5	110
7/16/97 3:00	9.0	112
7/16/97 3:30	9.5	114.5
7/16/97 4:00	10.0	116
7/16/97 4:30	10.5	117.5
7/16/97 5:00	11.0	119
7/16/97 5:30	11.5	120.5
7/16/97 6:00	12.0	121.5
7/16/97 6:30	12.5	122
7/16/97 7:00	13.0	123.5
7/16/97 7:30	13.5	124.5
7/16/97 8:00	14.0	125.5
7/16/97 8:30	14.5	126
7/16/97 9:00	15.0	126.5
7/16/97 9:30	15.5	127.5
7/16/97 10:00	16.0	128
7/16/97 10:30	16.5	129
7/16/97 11:00	17.0	129
7/16/97 11:30	17.5	129.5
7/16/97 12:00	18.0	129.5
7/16/97 12:30	18.5	129.5
7/16/97 13:00	19.0	130
7/16/97 13:30	19.5	131
7/16/97 14:00	20.0	131
7/16/97 14:30	20.5	131
7/16/97 15:00	21.0	131
7/16/97 15:30	21.5	131
7/16/97 16:00	22.0	131
7/16/97 16:30	22.5	131
7/16/97 17:00	23.0	131
7/16/97 17:30	23.5	131
7/16/97 18:00	24.0	131.5
7/16/97 18:30	24.5	131.5
7/16/97 19:00	25.0	132
7/16/97 19:30	25.5	132.5

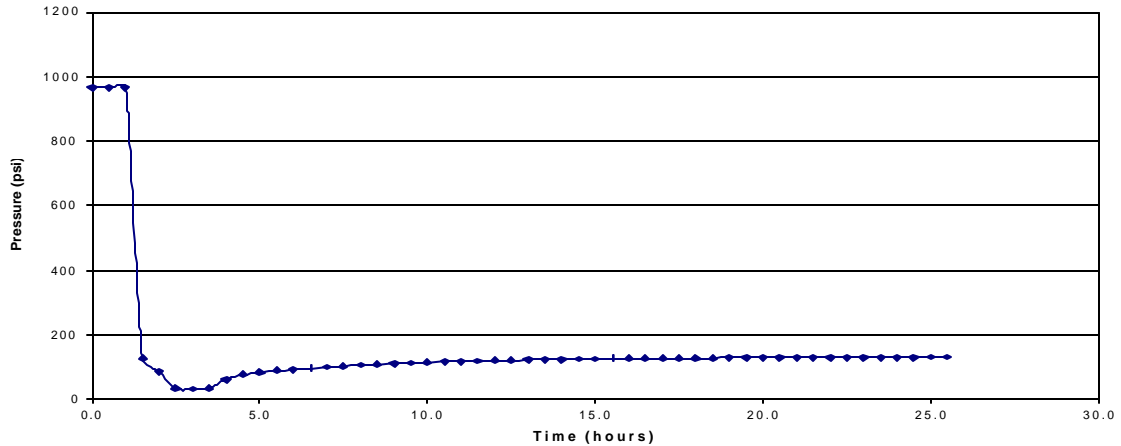**Fig.A-18-1   10 3/4" Casing Pressure of Well PTCA 7D - South Timbalier-300A**

82

Table A19 10 3/4" ´ 7" Annulus Pressure of Well B-7 - South Timbalier-301

time	Pressure
months	10 3/4"
0	200
1	300
2	600
3	830
4	1100
5	1200
6	1320
7	1450
8	1580
9	1600

Fig.A-19-1   10 3/4" x 7" Annulus of Well B-7 - South Timbalier-300A
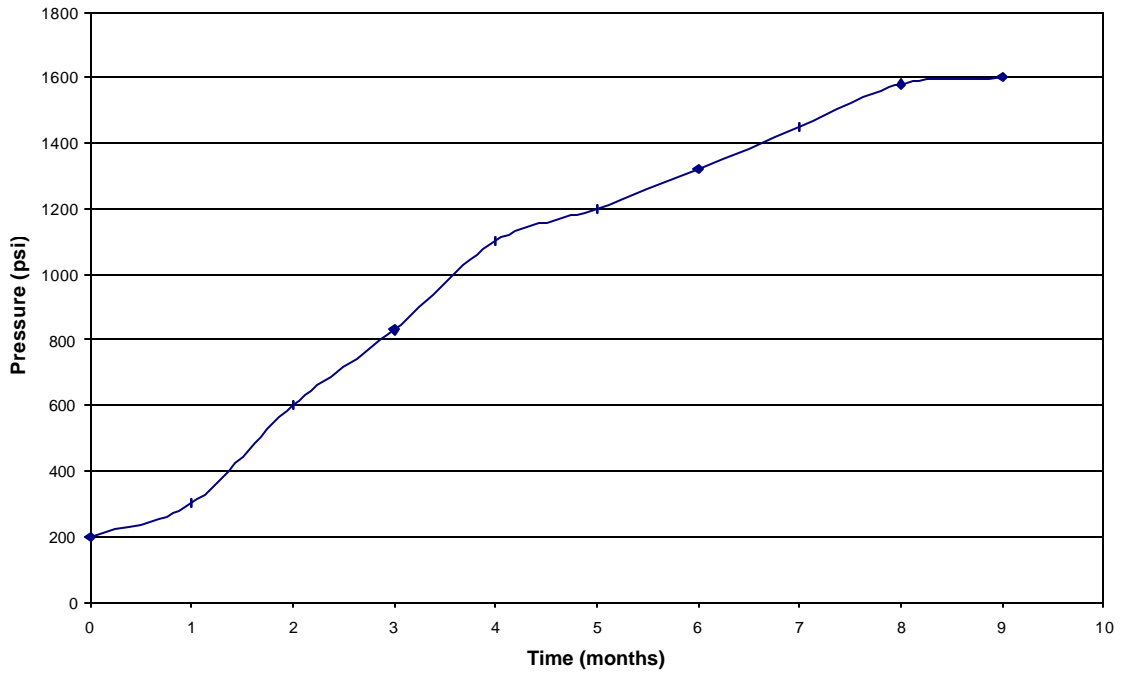
Table A20 10 3/4" ´ 7 5/8" Annulus Pressure of Well A-1 - HIGH ISLAND A-557

Time		Pressure	Time		Pressure
Date	days	10 3/4"	Date	days	10 3/4"
7/10/96	0	420	9/18/96	0	680
7/11/96	1	460	9/19/96	1	700
7/12/96	2	515	9/20/96	2	820
7/13/96	3	560	9/21/96	3	880
7/14/96	4	610	9/22/96	4	960
7/15/96	5	650	9/23/96	5	1000
7/16/96	6	690	9/24/96	6	1020
7/17/96	7	720	9/25/96	7	1040
7/18/96	8	745	9/26/96	8	1050
7/19/96	9	770	9/27/96	9	1070
7/20/96	10	785	9/28/96	10	1060
7/21/96	11	810	9/29/96	11	1080
7/22/96	12	825	9/30/96	12	1080
7/23/96	13	845	10/1/96	13	1085
7/24/96	14	860	10/2/96	14	1090
7/25/96	15	865	10/3/96	15	1100
7/26/96	16	880	10/4/96	16	1090
7/27/96	17	890	10/5/96	17	1080
7/28/96	18	900	10/6/96	18	1080
7/29/96	19	910	10/7/96	19	1070
7/30/96	20	920	10/8/96	20	1080
7/31/96	21	930	10/9/96	21	1100
8/1/96	22	930	10/10/96	22	1120
8/2/96	23	935	10/11/96	23	1120
8/3/96	24	940	10/12/96	24	1125
8/4/96	25	945	10/13/96	25	1125
8/5/96	26	945			
8/6/96	27	945			
8/7/96	28	950			
8/8/96	29	950			
8/9/96	30	950			
8/10/96	31	950			
8/11/96	32	950			
8/12/96	33	950			
9/18/96	70	680			
9/19/96	71	700			
9/20/96	72	820			
9/21/96	73	880			
9/22/96	74	960			
9/23/96	75	1000			
9/24/96	76	1020			
9/25/96	77	1040			
9/26/96	78	1050			
9/27/96	79	1070			
9/28/96	80	1060			
9/29/96	81	1080			
9/30/96	82	1080			
10/1/96	83	1085			
10/2/96	84	1090			
10/3/96	85	1100			
10/4/96	86	1090			
10/5/96	87	1080			
10/6/96	88	1080			
10/7/96	89	1070			
10/8/96	90	1080			
10/9/96	91	1100			
10/10/96	92	1120			
10/11/96	93	1120			
10/12/96	94	1125			
10/13/96	95	1125			

Fig.A-20-1   10 3/4" x 7 5/8" Annulus of Well A-1 - High Island A-557 in July
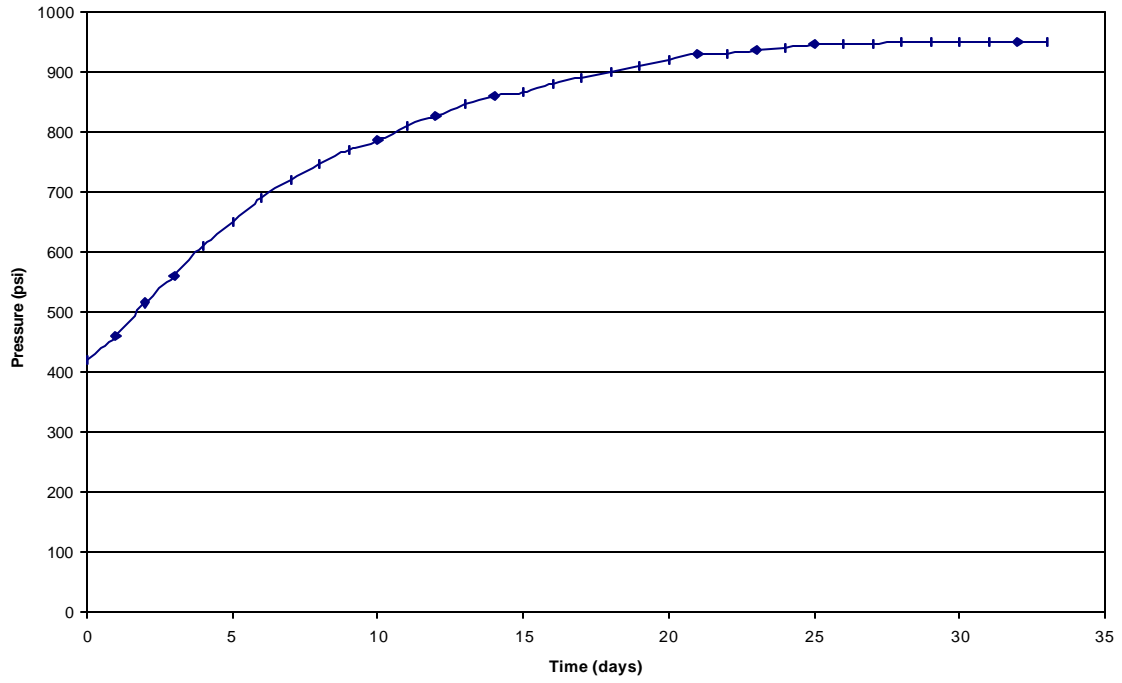

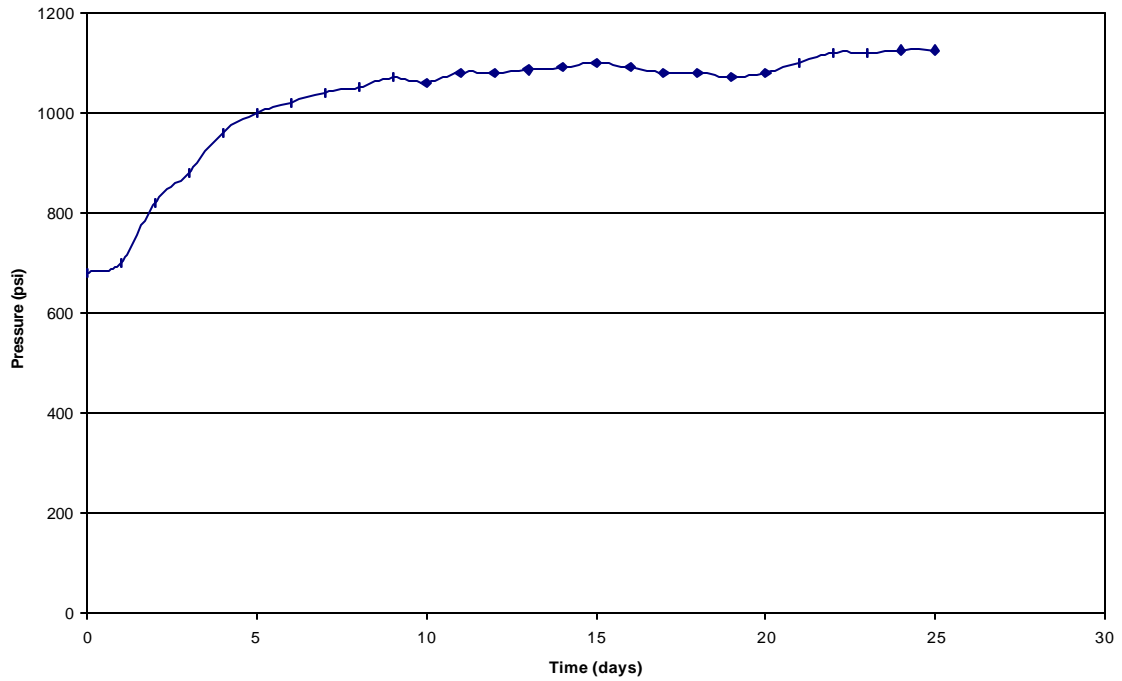**Fig.A-20-2   10 3/4" x 7 5/8" Annulus of Well A-1 - High Island A-557 in September**

Table A21 10 3/4" ´ 7 5/8" Annulus Pressure of Well A-2 - HIGH ISLAND A-557

Time		Pressure	Time		Pressure
Date	days	10 3/4"	Date	days	
7/10/96	0	480	9/19/96	0	680
7/11/96	1	480	9/20/96	1	720
7/12/96	2	520	9/21/96	2	720
7/13/96	3	520	9/22/96	3	740
7/14/96	4	525	9/23/96	4	770
7/15/96	5	530	9/24/96	5	785
7/16/96	6	550	9/25/96	6	800
7/17/96	7	560	9/26/96	7	820
7/18/96	8	560	9/27/96	8	840
7/19/96	9	580	9/28/96	9	850
7/20/96	10	580	9/29/96	10	860
7/21/96	11	590	9/30/96	11	880
7/22/96	12	590	10/1/96	12	900
7/23/96	13	595	10/2/96	13	910
7/24/96	14	600	10/3/96	14	910
7/25/96	15	620	10/4/96	15	900
7/26/96	16	620	10/5/96	16	920
7/27/96	17	625	10/6/96	17	920
7/28/96	18	640	10/7/96	18	940
7/29/96	19	650	10/8/96	19	970
7/30/96	20	660	10/9/96	20	980
7/31/96	21	670	10/10/96	21	1000
8/1/96	22	680	10/11/96	22	1010
8/2/96	23	680	10/12/96	23	1040
8/3/96	24	690			
8/4/96	25	700			
8/5/96	26	700			
8/6/96	27	700			
8/7/96	28	710			
8/8/96	29	720			
8/9/96	30	720			
8/10/96	31	730			
9/19/96	71	680			
9/20/96	72	720			
9/21/96	73	720			
9/22/96	74	740			
9/23/96	75	770			
9/24/96	76	785			
9/25/96	77	800			
9/26/96	78	820			
9/27/96	79	840			
9/28/96	80	850			
9/29/96	81	860			
9/30/96	82	880			
10/1/96	83	900			
10/2/96	84	910			
10/3/96	85	910			
10/4/96	86	900			
10/5/96	87	920			
10/6/96	88	920			
10/7/96	89	940			
10/8/96	90	970			
10/9/96	91	980			
10/10/96	92	1000			
10/11/96	93	1010			
10/12/96	94	1040			

Fig.A-21-1   10 3/4" x 7 5/8" Annulus of Well A-2 - High Island A-557 in July
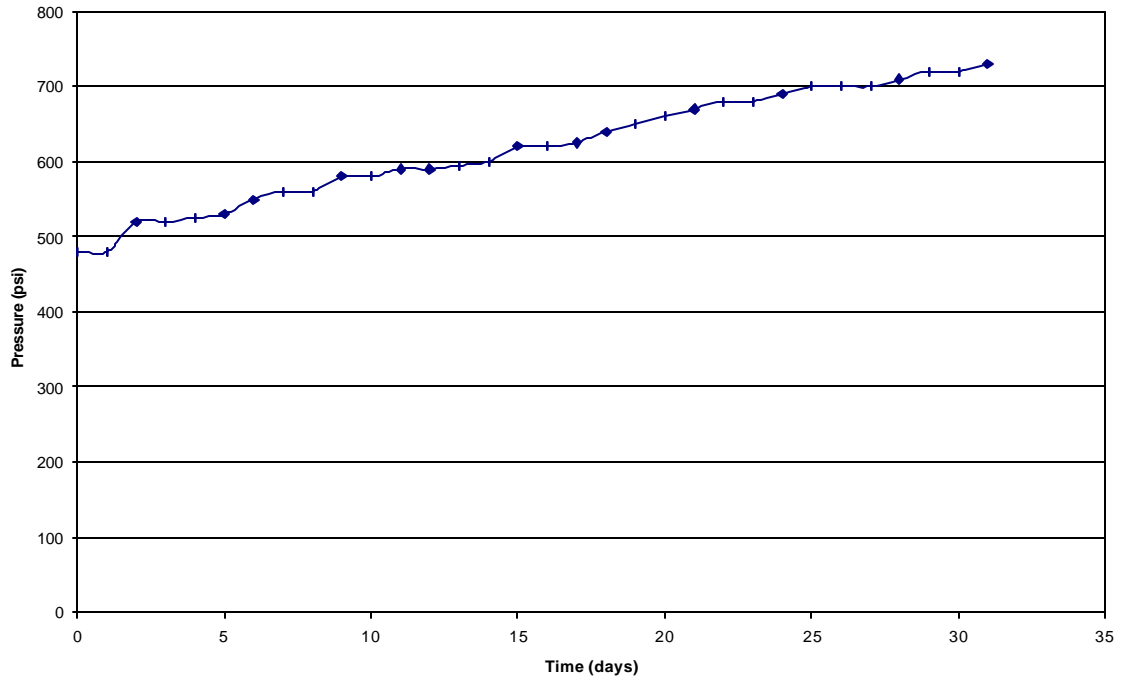

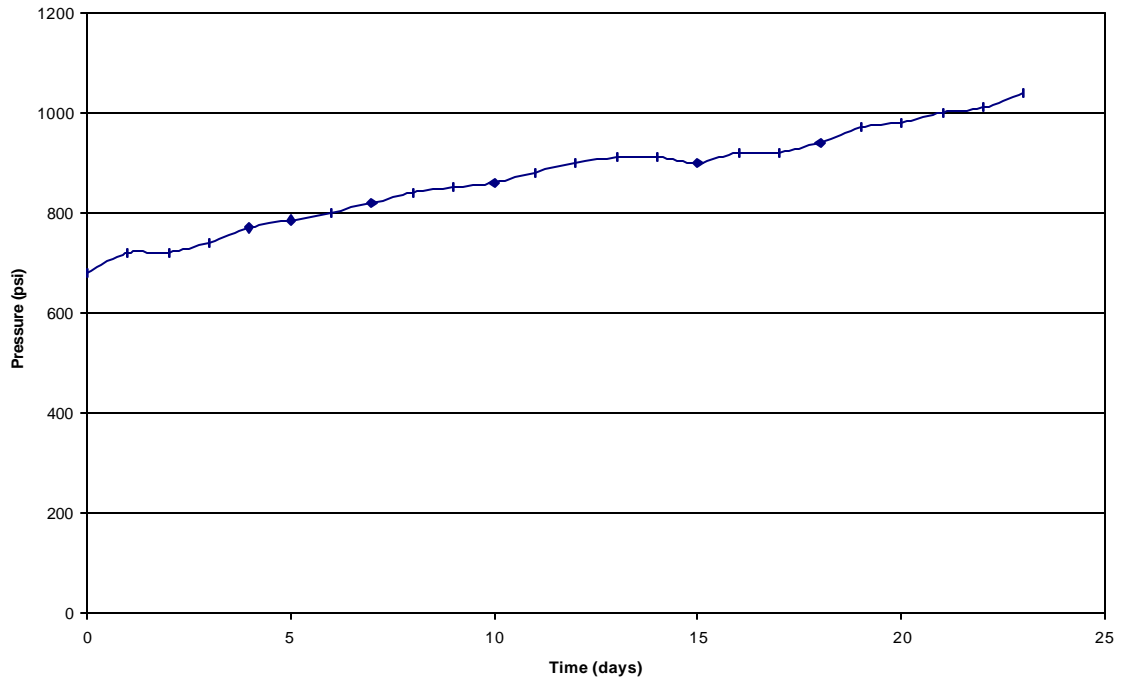**Fig.A-21-2   10 3/4" x 7 5/8" Annulus of Well A-2 - High Island A-557 in September**

Table A22 10 3/4" ´ 7 5/8" Annulus Pressure of Well A-3 - HIGH ISLAND A-557

Time		Pressure	Time		Pressure
Date	days	10 3/4"	Date	days	10 3/4"
7/10/96	0	560	9/19/96	0	635
7/11/96	1	620	9/20/96	1	730
7/12/96	2	745	9/21/96	2	690
7/13/96	3	825	9/22/96	3	655
7/14/96	4	890	9/23/96	4	670
7/15/96	5	940	9/24/96	5	685
7/16/96	6	970	9/25/96	6	695
7/17/96	7	995	9/26/96	7	700
7/18/96	8	1010	9/27/96	8	710
7/19/96	9	1015	9/28/96	9	710
7/20/96	10	1018	9/29/96	10	710
7/21/96	11	1020	9/30/96	11	715
7/22/96	12	1020	10/1/96	12	730
7/23/96	13	1020	10/2/96	13	735
7/24/96	14	1020	10/3/96	14	730
7/25/96	15	1020	10/4/96	15	730
7/26/96	16	1020	10/5/96	16	730
7/27/96	17	1025	10/6/96	17	740
7/28/96	18	1025	10/7/96	18	760
7/29/96	19	1025	10/8/96	19	760
7/30/96	20	1030	10/9/96	20	770
7/31/96	21	1030	10/10/96	21	760
8/1/96	22	1030	10/11/96	22	770
8/2/96	23	1030	10/12/96	23	780
8/3/96	24	1030			
8/4/96	25	1035			
8/5/96	26	1035			
8/6/96	27	1035			
8/7/96	28	1035			
8/8/96	29	1035			
8/9/96	30	1035			
8/10/96	31	1035			
8/11/96	32	1035			
9/19/96	71	635			
9/20/96	72	730			
9/21/96	73	690			
9/22/96	74	655			
9/23/96	75	670			
9/24/96	76	685			
9/25/96	77	695			
9/26/96	78	700			
9/27/96	79	710			
9/28/96	80	710			
9/29/96	81	710			
9/30/96	82	715			
10/1/96	83	730			
10/2/96	84	735			
10/3/96	85	730			
10/4/96	86	730			
10/5/96	87	730			
10/6/96	88	740			
10/7/96	89	760			
10/8/96	90	760			
10/9/96	91	770			
10/10/96	92	760			
10/11/96	93	770			
10/12/96	94	780			

Fig.A-22-1   10 3/4" x 7 5/8" Annulus of Well A-3 - High Island A-557 in July

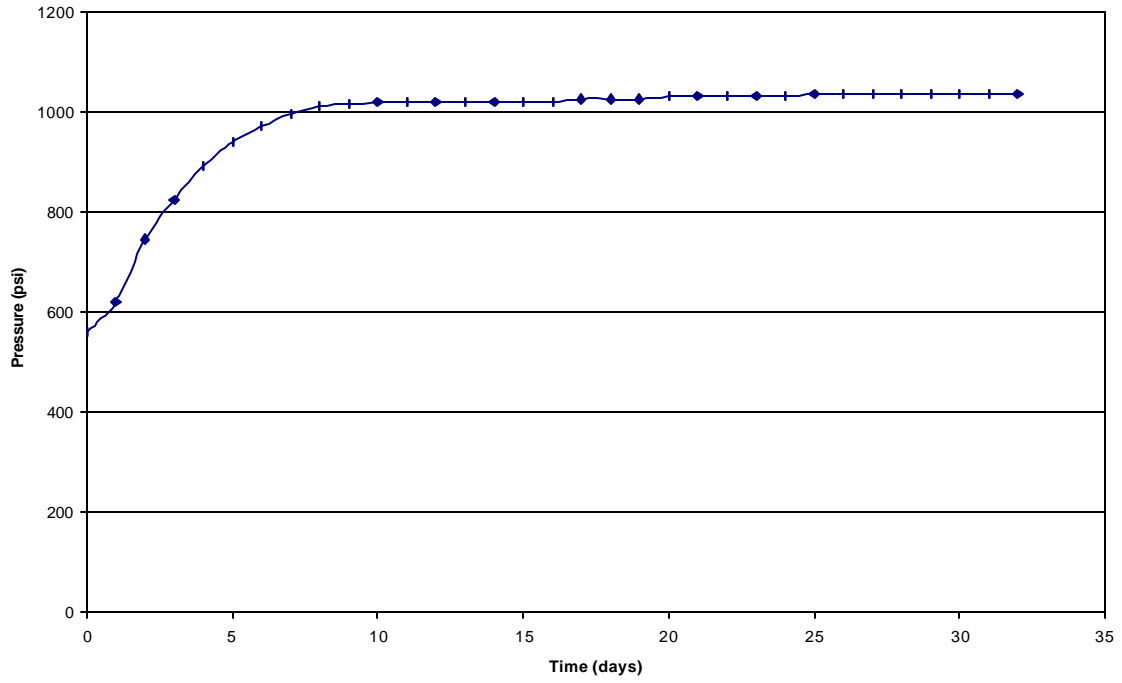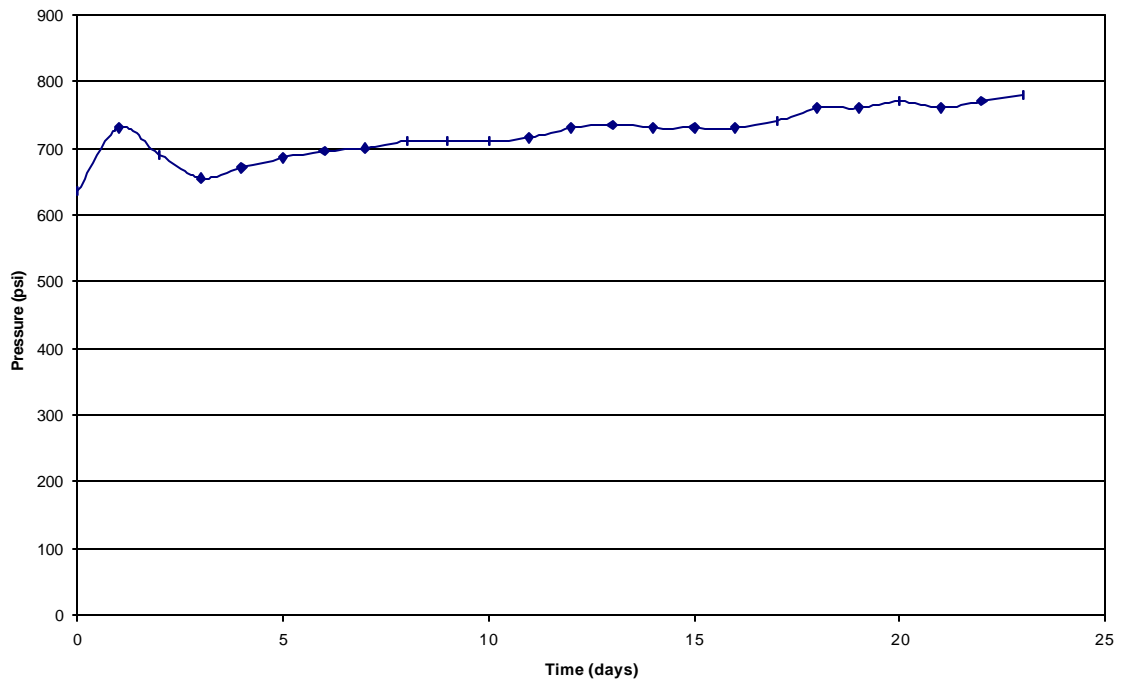**Fig.A-22-2   10 3/4" x 7 5/8" Annulus of Well A-3 - High Island A-557 in September**

ANALYTICAL MODEL OF SCP TRANSIENT IN ANNULUS CEMENTED TO SURFACE

Permeability of the cement column is calculated as

,
$$k_{avg} = \frac{\sum L_i}{\sum \dfrac{L_i}{k_i}}$$
(B1)

where,
k_{avg} = permeability of cement column (md),
L_t, k_t = cement column length (ft) with permeability k_t (md).
Boundary and initial conditions are depicted in Fig. B.1.
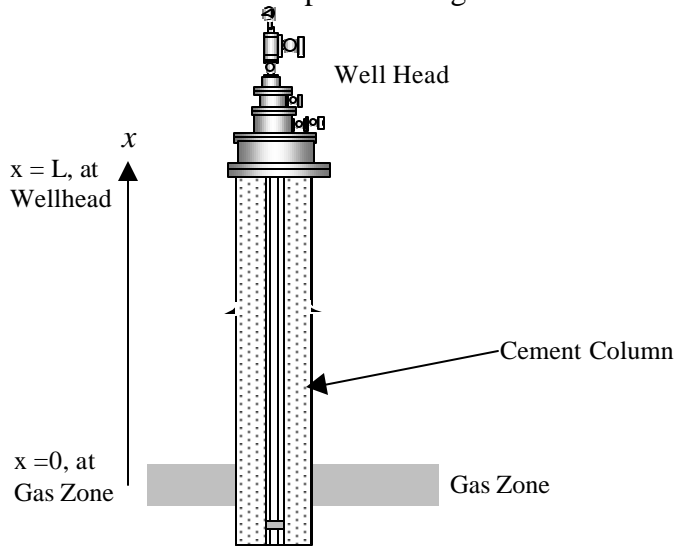
Figure B-1 Schematics of analytical model

The boundary conditions are as follows:
- the gas-zone pressure is constant (x = 0, P = Pe),
- the surface valve is closed (x = L, q = 0).

For the initial condition:
- a steady state flow described by Darcy's Law is assumed .so the pressure gradient is given by

$$\frac{dx}{dt} = 0.001127 \frac{k}{\mu} \frac{dp}{dx},$$
(B.2)

where
k = permeability (md),
μ = viscosity of gas (cp).
Diffusivity equation for compressible fluids in linear flow is given by

$$\frac{\partial^2 m}{\partial x^2} = \frac{f\mu c_t}{0.0002637k}\frac{\partial m}{\partial t},$$ (B.3)

where,

m = gas pseudo pressure (psia^2/cp).

Equation (B.3) can be expressed as,

$$\frac{\partial m}{\partial t} = c^2\frac{\partial^2 m}{\partial x^2},$$ (B.4)

where,

$$c^2 = \frac{0.0002637k}{f\mu c_t}.$$

The flow of gas is given by

$$qB_g = \frac{qP_{sc}T_z}{5.615T_{sc}p}.$$ (B.5)

Eqs. (B.2) and (B.5) give

$$\frac{qP_{sc}T_z}{5.615T_{sc}p} = 0.001127\frac{k}{\mu}\frac{dp}{dx}.$$ (B.6)

Converting pressure gradient to the pseudo gas pressure gradient gives

$$\frac{\partial m}{\partial x} = \frac{2p}{\mu}\frac{dp}{dx},$$ (B.7)

and,

$$\frac{dp}{dx} = \frac{qP_{sc}Tz}{5.615T_{sc}p}\frac{\mu}{0.001127k}.$$ (B.8)

or, after substitution,

$$\frac{\partial m}{\partial x} = \frac{2p}{\mu}\frac{dp}{dx} = \frac{2p}{\mu}\frac{qP_{sc}Tz}{5.615T_{sc}p}\frac{\mu}{0.001127k} = 316.05\frac{qP_{sc}T}{T_{sc}AK},$$

and

$$\partial m = 316.05\frac{qP_{sc}T}{T_{sc}AK}\partial x.$$ (B.9)

Integrating Eq. (B.9) gives

$$m(x) = 316.05\frac{qP_{sc}T}{T_{sc}AK}x.$$ (B.10)

To solve (B.4), we write pseudo gas pressure is a function of time and position as
$$m(x,t) = F(x)\cdot G(t).$$

The first derivative regarding position is

$$\frac{\partial m}{\partial x} = F'(x)G(t).$$

The second derivative with respect to position is

$$\frac{\partial m}{\partial x} = F''(x)G(t).$$

The first order derivative by time is

$$\frac{\partial m}{\partial t} = F(x)G'(t).$$

Substituting to (B.4) gives

$$F\dot{G} = c^2 F''G$$

or,

$$\frac{\dot{G}}{c^2 G} = \frac{F''}{F}.$$

The left-hand side of the above equation depends only on time and the right-hand side only on position, so that both sides must be equal to a constant. Only a negative constant gives a satisfied solution. Thus,

$$\frac{\dot{G}}{c^2 G} = \frac{F''}{F} = -\boldsymbol{a}^2,$$

$$F'' + \boldsymbol{a}^2 F = 0,$$ (B.11)

$$\dot{G} + c^2 \boldsymbol{a}^2 G = 0.$$ (B.12)

A general solution is given by

$$F(x) = A\cos\boldsymbol{a}x + B\sin\boldsymbol{a}x.$$

From the boundary condition (i), constant pressure at the gas zone is set as reference pressure, for the pseudo-gas pressure calculations. Thus, the pressure of the gas zone is set zero. It gives

$$F(0) = 0 = A\cos(0) + B\sin(0),$$

$$A = 0.$$

From boundary condition (ii), the first derivative is 0 at x = L, which gives

$$F'(x) = B\cos\boldsymbol{a}x,$$

$$F'(L) = B\cos\boldsymbol{a}L = 0.$$

Then, $\boldsymbol{a}$ is obtained as

$$\boldsymbol{a} = \left(n\boldsymbol{p} - \frac{\boldsymbol{p}}{2}\right)\frac{1}{L}.$$

From this result, $F(x)$ is given by

$$F(x) = B\sin\boldsymbol{a}x.$$

Setting B = 1 gives

$$F(x) = \sin\boldsymbol{a}x.$$

Eq. (B.12) is expressed as

$$\frac{dG}{dt} + c^2\boldsymbol{a}^2 G = 0,$$

or,

$$\frac{dG}{G} = -c^2\boldsymbol{a}^2 dt,$$

or,

$$\ln(G) = -c^2\boldsymbol{a}^2 dt$$

Thus, $G(x)$ is given by

$$G = B_n e^{-c^2 \mathbf{a}^2 t} \tag{B.13}$$

Finally, the pseudo gas pressure $m(x, t)$ is expressed as

$$m(x,t) = \sum_{n=1}^{\infty} B_n \sin[\mathbf{a}x] \cdot e^{-c^2[(\mathbf{a})^2 t]}$$

where,

$$B_n = \frac{2}{L} \int_0^L f(x) \sin[\mathbf{a}x] dx .$$

Eq. (B.10) gives

$$f(x) = 316.05 \frac{q P_{sc} T}{T_{sc} AK} x . \tag{B.14}$$

Integration of $(x\sin\mathbf{a}x)$ gives:

$$\int x \sin[\mathbf{a}x] dx = \frac{\sin[\mathbf{a}x]}{\mathbf{a}^2} - \frac{x \cos[\mathbf{a}x]}{\mathbf{a}} .$$

Also, the constant B_n is given by

$$B_n = \frac{2}{L} \int_0^L f(x) \sin[\mathbf{a}x] dx = \frac{316.05}{L} \frac{q P_{sc} T}{T_{sc} AK} \left(\frac{\sin[\mathbf{a}x]}{\mathbf{a}^2} - \frac{x \cos[\mathbf{a}x]}{\mathbf{a}} \right).$$

Thus, $m(x, t)$ is given as

$$m(x,t) = \sum_{n=1}^{\infty} \frac{316.05}{L} \cdot \frac{q P_{sc} T}{T_{sc} AK} \frac{(-1)^{n+1}}{\mathbf{a}^2} \sin[\mathbf{a}x] \cdot e^{-c^2 \mathbf{a}^2 t} .$$

Per the above assumption, the gas formation pseudo-pressure is set zero. Convertion from the reference level ($p = P_e$ at $x = 0$) to the actual pseudo pressure gives

$$m(x,t) = m(P_e) - \sum_{n=1}^{\infty} \frac{316.05}{L} \frac{q P_{sc} T}{T_{sc} AK} \frac{(-1)^{n+1}}{\mathbf{a}^2} \sin[\mathbf{a}x] \cdot e^{-c^2 \mathbf{a}^2 t} . \tag{B.15}$$

At the surface (x =L; sin("L)=1) the pseudo pressure is

$$m(t) = m(P_e) - \sum_{n=1}^{\infty} \frac{316.05}{L} \frac{q P_{sc} T}{T_{sc} AK} \frac{(-1)^{n+1}}{\mathbf{a}^2} \cdot e^{-c^2 \mathbf{a}^2 t} \tag{2}$$